The roles of suberin biopolymer and associated waxes in protecting plants against abiotic stresses

by

Nayana Dilini de Silva

A thesis submitted to the Faculty of Graduate and Postdoctoral Affairs in partial fulfillment of the requirements for the degree of

Doctor of Philosophy in Biology

Department of Biology
Carleton University
Ottawa, Ontario, Canada

ABSTRACT

Plants have various hydrophobic barriers that protect against environmental stresses. Suberin is one such extracellular lipid-based barrier that is deposited in various tissues in terrestrial plants. It is a complex aliphatic and aromatic heteropolymer that plays important roles in controlling water and ion movement. The precise roles of suberin in defending against abiotic stresses (e.g. drought, salinity and heavy metals) and the defensive mechanisms are currently unknown. A better understanding of these protective functions could provide information on novel genetic approaches to manipulate suberin for the development of stress tolerant crops. In this thesis, I explore some of the specific roles of root suberin and seed coat suberin in the model plant *Arabidopsis thaliana* in relation to abiotic stress tolerance.

Physio-chemical responses and stress tolerance as a result of alterations in suberin were investigated using several suberin-altered mutants of *Arabidopsis thaliana*. Drought-induced suberin reduced water loss through the root periderm. The amount of water loss in roots was inversely correlated to the amount of total suberin. Suberin lamellae structure was important in reducing water loss under drought stress. Salt stress responses in suberin-altered mutants indicate suberin composition or lamellae structure are essential in barrier function of root suberin against uncontrolled transport of Na into the shoot.

Mutants of Arabidopsis defective in various seed coat polymeric substances (suberin, cutin, mucilage, or proanthocyanidins) were tested for changes in germination and viability after stratification and imbibition in a range of mining environment-relevant chromium Cr(III) concentrations. Seeds reduced in total seed coat suberin were strongly affected by increasing Cr^{3+} concentrations, affecting both germination and embryo viability. This provides evidence for

the effective barrier function of seed coat suberin on the imposition of impermeability to Cr^{3+}. Although proanthocyanidin mutants displayed reduced germination in the presence of chromium, their embryo viability was only partially affected by higher levels of Cr^{3+}. Also, it was observed that decreases in germination (%) and embryo viability was not always associated with increased seed coat permeability to tetrazolium salt. Overall, these results reveal the risks associated with Cr^{3+} toxicity on the existence of plants with reduced seed coat suberin content in environments contaminated with high levels of chromium.

The findings presented in this thesis helps to clarify how suberin content, composition, and lamellae structure relate to tolerance against drought, salinity, and chromium (Cr^{3+}) toxicity. Further, these findings shed light on future directions in manipulating suberin genes for the development of stress-tolerant high-value crops.

PREFACE

This thesis follows the format of an integrated thesis. The data and text in Chapters 2 and 3 are nearly identical to manuscripts being prepared for publication, of which I am the primary author. Only minor modifications have been made to the text and figures, and this is just formatting.

Chapter 2 is derived from the manuscript titled **"Suberin composition and lamellae structure play important roles in reducing water loss in mature roots and reducing sodium transport to shoots in *Arabidopsis thaliana"*.** Authors: Nayana D G de Silva, Denise Chabot, Keith Hubbard, Peter Ryser, Isabel Molina, and Owen Rowland.

Declaration of the self-contribution and co-authors

The research work in the thesis was independently carried out by myself in the Department of Biology, Carleton University under the supervision of Dr. Owen Rowland. In Chapter 2, the research experiments were done by myself in addition to writing the manuscript. Revisions to the manuscript were made after discussing with the co-authors. The transmission electron microscopy was carried out at the Ottawa Research and Development Centre, Agriculture and Agri-Food Canada, Ottawa under the guidance of Denise Chabot.

Co-author Dr. Isabel Molina from Algoma University in Sault Ste. Marie, Ontario is the co-supervisor of my PhD thesis work. Throughout my study period, she provided guidance in lipid analysis, molecular biology, and biochemistry. She contributed to the suberin monomer identification using GC-MS. Dr. Peter Ryser is from Laurentian University, Sudbury, Ontario. He assisted in plant physiology and data interpretation using statistics. Co-authors Denise Chabot

and Keith Hubbard from the Ottawa Research and Development Centre, Agriculture and AgriFood Canada, Ottawa helped me with the processing of samples for TEM imaging.

Chapter 3 is derived from the manuscript , titled "**Seed coat suberin forms an effective barrier against chromium toxicity during early seed germination in *Arabidopsis thaliana*".** Authors: Nayana D G de Silva, Céline Boutin, Anna Lukina, Tamara L Western, Isabel Molina, and Owen Rowland.

Declaration of the self-contribution and co-authors

In Chapter 3, I carried out seed propagation and phenotypic analysis in the Department of Biology, Carleton University under the supervision of Dr. Owen Rowland. I drafted the manuscript and made revisions after discussing with the co-authors. The germination assays were set up at the National Wildlife Research Centre, Environment and Climate Change Canada, Science and Technology Branch, Carleton University Campus, Ottawa.

Co-author Dr. Celine Boutin is a collaborative partner from the National Wildlife Research Centre and she provided all the logistics related to the germination experiment. Co-author Dr. Tamara L Western is from Department of Biology at McGill University. She provided guidance in the phenotypic identification of mucilage mutants and contributed to revisions of the manuscript. Co-author Anna Lukina is a graduate student from Carleton University who assisted in setting up the germination assay and contributed to the reviews of the manuscript.

ACKNOWLEDGEMENTS

First of all, I would like to thank my thesis supervisor Dr. Owen Rowland for accepting me as a Ph.D. student in his lab and providing me with all the support, guidance and encouragement throughout this project. I would not have succeeded in accomplishing this goal without his understanding, thoughtfulness, and assistance given during the difficult times I had to face with the passing away of my beloved father. My sincere gratitude also goes to my co-supervisor Dr. Isabel Molina (Algoma University) for her guidance and help throughout the thesis during the entire study period. I am also grateful to Dr. Myron Smith and Dr. Linda Bonen for their timely advice as my committee advisors and the review of my thesis work. I would also like to thank Dr. Celine Boutin for the immense support given to carry out my research related to the third chapter of this thesis. A special thanks to Tamara Western (McGill University) for providing me the opportunity to visit her lab and get some hands-on practice on mucilage analysis and seed cross sectioning practice and reviewing the manuscript on the chromium project. I am also grateful to Dr. Peter Ryser (Laurentian University) for the guidance on plant stress physiology and thankful for reviewing the manuscript on drought and salt stress responses. His advice is highly appreciated.

I would also like to acknowledge David Carpenter at the National Wildlife and Research Center (Environment and Climate Change Canada) for all the support in numerous ways throughout my research at NWRC. Also, Anna Lukina in helping me set up the seed germination assay and reviewing the manuscript on the chromium project. I would also like to thank Dr. Ian Pulsifer for all the assistance with the GC-FID machines, as well as in genotyping of mutants on many occasions throughout the past years. Thank you to Denise Chabot and Keith Hubbard at the Ottawa Research and Development Centre (Agriculture and Agri-Food Canada) for their

microscopy expertise and Dr. Jhadeswar Murmu for guidance with molecular biology techniques. My sincere gratitude also goes to Dr. Nimal De Silva at the University of Ottawa for processing the leaf samples by ICP-MS and advice on data processing. I am grateful to my husband for making digital images of the seed and root cross sections in this thesis. Last, but not least, I would like to thank my family, brothers, and parents for their love, support, encouragement which kept me focused throughout my work at Carleton.

Table of Contents

ABSTRACT i

PREFACE iii

ACKNOWLEDGEMENTS v

List of Figures xi

List of Tables xiii

List of Abbreviations xiv

Chapter 1: General Introduction: suberin polymer and suberin-associated waxes 1

1.1 Chemical composition 2

1.2 Structure 6

1.3 Distribution in plant tissues 8

1.3 Functions 12

1.4 Biosynthesis and deposition of suberin 18

1.4.1 Biosynthesis of suberin monomers 20

1.4.2 Biosynthesis of suberin-associated waxes 24

1.4.3 Transport of monomers and polymerization 25

1.4.4 Regulation of deposition 26

1.5 Changes in suberin deposition under normal growth and stressful environmental conditions 27

1.6 Rationale and objectives of the thesis 30

1.6.1 The roles of root suberin and associated waxes in protecting plants against drought and salt stresses (presented in Chapter 2) 30

1.6.2 The roles of seed coat constituents in providing protection against chromium (Cr^{3+}) toxicity (presented in Chapter 3) 32

Chapter 2: Suberin composition and lamellae structure play important roles in reducing water loss in mature roots and reducing sodium transport to shoots in *Arabidopsis thaliana* 35

2.1 Abstract 35

2.2 Introduction 36

2.3 Materials and Methods 40

2.3.1 Plant growth conditions, drought and salt assays 40

2.3.2 Plant trait measurements 41

2.3.3 Root wax extraction 42

2.3.4 Root suberin analysis 42

2.3.5 Gas chromatography 43

2.3.6 Tissue elemental analysis 44

2.3.7 Measurement of root periderm segments for water loss 44

2.3.8 Transmission electron microscopy 45

2.3.9 Statistical analysis 46

2.4 Results 47

2.4.1 Suberin and suberin-associated wax deposition are altered by water availability 47

2.4.2 *Cyp86a1-1 cyp86b1-1* and *myb92-1 myb93-1* mutants have reduced total suberin content, but only *cyp86a1-1 cyp86b1-1* has altered lamellae structure 51

2.4.3 Drought stress did not affect the mutants more than wild-type 53

2.4.4 Drought increases suberin in wild-type and the suberin mutants tested, but does not alter the lamellae structure 56

2.4.5 Suberin deficiency and deformed ultra-structure increased water loss in root periderm 60

2.4.6 *Abcg2-1 abcg6-1 abcg20-1* mutant was very sensitive to NaCl treatment 64

2.4.7 Salt stress induced suberin biosynthesis in wild-type, but not in the suberin mutants ... 66

2.4.8 NaCl treatment caused ion imbalances (K/Na) in mutants with altered suberin composition and lamellae structure 71

2.5 Discussion 76

Chapter 3: Seed coat suberin forms an effective barrier against chromium (Cr^{3+}) during early seed germination in *Arabidopsis thaliana* 82

3.1 Abstract 82

3.2 Introduction 83

3.3 Materials and Methods 87

3.3.1 Plant materials and seed amplification 87

3.3.2 Preparation of chromium (Cr^{3+}) solutions and germination assay 88

3.3.3 Seed coat polyester analysis 89

3.3.4 Gas chromatography 91

3.3.5 Seed coat permeability assay 91

3.3.6 Analyses of seed coat mucilage by ruthenium red 92

3.3.7 Analysis of seed coat proanthocyanidins by vanillin 92

3.3.8 Seed viability test by tetrazolium salt 93

3.3.9 Statistical analysis 94

3.4 Results 94

3.4.1 Mutants used in this study and characterization of their seed coat phenotypes 95

3.4.2 Seed germination responses to chromium 105

3.5 Discussion 118

Chapter 4: Summary and Future Directions 125

4.1 Composition and ultra-structure of suberin play an important role in tolerance to drought and salinity in *Arabidopsis thaliana* 126

4.1.1 Summary of findings 127

4.1.2 Future directions 131

4.2 Seed coat suberin forms an effective barrier against chromium in *Arabidopsis thaliana* 133

4.2.1 Summary of findings 134

4.2.2 Future directions 134
References 137
Appendix I: 151
Appendix II: 152
Appendix III: 154
Appendix IV: 155
Appendix V: 156

List of Figures

Figure 1-1. Structure of the suberin lamellae…… 8
Figure 1-2. Development of suberin in Arabidopsis root…… 9
Figure 1-3. Schematic representation of root endodermal differentiation…….. 11
Figure 1-4. Suberized phellem (cork) in roots and shoots undergoing secondary growth…… 12
Figure 1-5. Schematic representation of three different pathways of water and solutes movement in roots……... 13
Figure 1-6. Water and solute movement across endodermis at stage I differentiation…….. 15
Figure 1-7. Water and solute movement across endodermis at stage II differentiation……16
Figure 1-8. Overview of the suberin biosynthetic pathway……..19
Figure 2-1. Time course analysis of Arabidopsis root suberin through development……... 48
Figure 2-2. Comparison of leaf dry biomass, root suberin content and root wax amount in wild-type (Col-0) plants……. 50
Figure 2-3. Comparison of root suberin monomer composition between wild-type (Col-0) and mutants *myb92-1 myb93-1* and *cyp86a1-1 cyp86b1-1*…….. 52
Figure 2-4. Comparison of drought stress responses between wild-type and mutants……... 55
Figure 2-5. Total suberin content and TEM images of *A. thaliana* root sections of wild-type and mutants showing suberin lamellae in the periderm under control and drought stress……...58
Figure 2-6. Suberin monomer composition under control and drought stress in wild-type and suberin mutants……. 59
Figure 2-7. Comparison of amount of water loss in wild-type and *cyp86a1-1 cyp86b1-1* root periderm segments…….. 61
Figure 2-8. Comparison of the amount of water loss, leaf relative water content (RWC) and total suberin content in wild-type and mutants……. 62
Figure 2-9. TEM images of *gpat5-1* root periderm sections under control and drought conditions……. 63
Figure 2-10. Comparison of genotypes grown at control (0 mM NaCl) and 2 weeks 100 mM NaCl treatment…… 65
Figure 2-11. Comparison of total dry mass and total suberin content in wild-type and mutants under control and 100 mM NaCl treatment…… 68

Figure 2-12. Comparison of root suberin monomer composition in mutants and wild-type under control and NaCl treatment…….. 69
Figure 2-13. Comparison of root-associated wax composition in wild-type plants under control conditions and after 3 weeks 100 mM NaCl treatment ……70
Figure 2-14. Segregation of leaf ionomic phenotypes in wild-type and mutants……. 72
Figure 2-15. Comparison of Na, K/Na and K in leaves of wild-type and mutants under control and NaCl treatment…… 75
Figure 3-1. Illustration of *A. thaliana* seed anatomy at the heart stage of embryogenesis…. 84
Figure 3-2. Characterization of the seed coats in wild-type and seed coat mutants……97
Figure 3-3. Seed coat polyester composition in wild-type and mutants…… 99
Figure 3-4. Comparison of germination responses to chromium treatment in wild-type and mutants altered in mucilage composition……. 106
Figure 3-5. Results of the seed viability test……... 108
Figure 3-6. Comparison of germination responses to chromium treatment in wild-type and mutants altered in seed coat suberin or cutin composition……. 111
Figure 3-7. Comparison of germination responses to chromium treatment in wild-type and mutants altered in seed coat flavonoids…… 114

List of Tables

Table 1-1. Chemical structures of common suberin monomers …… 4

Table 1-2. Comparison of the relative abundance of suberin monomers in three well characterized plant species…… 5

Table 2-1. ANOVA test results of the drought stress experiment……54

Table 2-2. Results of the salt stress experiment……67

Table 2-3. Analysis of elements in leaf tissues……..73

Table 3-1. Monomer composition of seed coat polyesters in wild-type and mucilage mutants..... 100

Table 3-2. Monomer composition of seed coat polyesters in wild-type and suberin- and cutin altered mutants……... 102

Table 3-3. Monomer composition of seed coat polyesters in wild-type and flavonoid altered mutants……..……..…….. 104

Table 3-4. Results of statistical analysis testing the effect of chromium dose on individual genotypes…… 116

List of Abbreviations

ABA : Abscisic acid
ABC : ATP-binding-cassette
ABRC : Arabidopsis Biological Resource Centre
AHC : Alkyl hydroxycinnamate
AHA10 : Autoinhibited H-ATPase isoform 10
ANOVA : Analysis of variance
ASFT : Aliphatic suberin feruloyl transferase
BAN : Banyuls
CB : Casparian band
CYP : Cytochrome P450 monooxygenase
DCA : Dicarboxylic acid
DFR : Dihydroflavonol 4-reductase
ER : Endoplasmic reticulum
FA **:** Fatty acid
FACT : Fatty alcohol caffeoyl-CoA transferase
FAE : Fatty acid elongation
FAME **:** Fatty acid methyl ester
FAR : Fatty acyl reductase
GC-FID : Gas chromatography-flame ionization detection
GC-MS : Gas chromatography-mass spectrometry
G3P : Glycerol-3-phosphate
GPAT : Glycerol 3-phosphate acyltransferase (GPAT)
ICP-MS : Inductively coupled plasma-mass spectrometry
KCS : Ketoacyl-CoA synthase
L*er* : Landsberg *erecta*
LDOX : Leucoanthocyanidin dioxygenase
ME : Methyl ester
MEN : Mucilage enhancer
OH-FA : Omega hydroxy fatty acid

PA : Proanthocyanidins

PS : Polyester synthase

RGI : Rhamnogalacturonan-I

ROL : Radial oxygen loss

ROS : Reactive oxygen species

RMR : Root mass ratio

RR : Ruthenium red

RWC : Relative water content

SPPD : Suberin poly-phenolic domain

SPAD : Suberin poly-aliphatic domain

TZ : Tetrazolium salt

TEM : Transmission electron microscopy

VLCFA : Very-long-chain fatty acid

WUE : Water use efficiency

WT : Wild-type

Chapter 1: General Introduction: suberin polymer and suberin-associated waxes

In recent years, increased environmental pollution has caused significant climatic changes. Plant growth and development are influenced by changing environmental conditions. If any of the environmental factors is not ideal, plant growth and development may be adversely affected. Plants being sessile organisms cannot move away from unfavorable environmental conditions. Therefore, they have many physical and physiological mechanisms to cope with different stresses. One such mechanism involves reinforcement of their cell walls with lipid-based polymers and other specialized (secondary) metabolites (Salminen *et al*., 2018).

Important first lines of defense are cell wall-associated lipid-based polymeric barriers that are deposited at the interface between the plant and its environment. These barriers are cuticle (cutin polymer and embedded waxes) that coats aerial surfaces, sporopollenin polymer with associated tryphine waxes on pollen grain surfaces, and suberin polymer with associated waxes present at various tissues such as root endodermis and periderm. Suberin with its associated waxes forms a physiologically important hydrophobic barrier affecting water and solute transport, as well as pathogen ingress (Graca, 2015). In this general introductory chapter, I will summarize the chemical composition, structure, functions, and biosynthesis of suberin and associated waxes, as well as what is known about suberization of tissues in different species as they respond to various environmental stimuli. The rationale leading to the present study is followed by thesis objectives.

1.1 Chemical composition

Suberin is a complex, lipophilic hetero-polyester made up of aliphatics, glycerol and aromatic components, and associated with soluble waxes (Kolattukudy, 1981; Bernards, 2002; Nawrath, 2002; Franke and Schreiber, 2007; Pollard *et al*., 2008). The aliphatic polyesters of suberin in various plant species have been extensively characterized by analytical methods. For quantification of suberin monomer composition, the polyester is subjected to base- or acid-catalyzed depolymerization / transesterification to yield methyl esters of the monomers. The monomers are then usually identified by gas chromatography-mass spectrometry (GC-MS) and quantified by GC-MS or GC-flame ionization detection (GC-FID) (Ranatunge *et al*., 2011). The main aliphatic suberin monomers are long-chain (C16 and C18) and very-long-chain (≥C20) monomers, especially α,ω-dicarboxylic acids (DCAs), ω-hydroxy fatty acids (OH-FAs), unsubstituted fatty acids (FAs), and primary fatty alcohols and diols (Table 1-1) (Schreiber *et al*., 1999; Graça and Santos, 2007). There is considerable variability in suberin composition between species and different tissues of the same species (Matzke and Reiderer, 1991; Zeier and Schreiber, 1998). Suberin monomer compositions in the three species studied the most to date, *Arabidopis thaliana*, *Solanum tuberosum* (potato), and *Quercus suber* (cork oak), are given in Table 1-2. Glycerol is also a main constituent of the poly-aliphatic component and functions to link different fatty acyl types with hydroxyl groups by esterification (Kolattukudy, 1984; Andersen *et al*., 2015). Glycerol may be present as monoacylglycerol esters of alkanoic acids, α,ω-dicarboxylic acids, and ferulic acid (Graça and Pereira 2000b), as well as diglycerol esters with an α,ω-dicarboxylic acid linking the glycerols (Graça and Pereira 2000c). Therefore, it has been proposed that glycerol - α,ω- dicarboxylic acid - glycerol trimers form the backbone of the suberin polymer and thus suberin is a poly-(acyl glycerol)-polyester (Graça and Pereira 2000c). Additionally, glycerol has been reported as a major component of cutin where "glycerol-DCA-

glycerol" is assumed to be the dominant motif in DCA-rich cutins, such as that found in Arabidopsis (Yang *et al*., 2016). Although the aliphatic components of suberin have been studied in detail, the overall organization of the inter-unit linkages, including those involving unsubstituted fatty acids and primary fatty alcohols, remains to be determined. The aromatic component of the polyaliphatic suberin consists of *p*-hydroxycinnamic acid derivatives, especially ferulate (Bernards *et al*., 1995; Franke *et al*., 2009; Kolattukudy, 2001).

Table 2-1 Chemical structures of common suberin monomers. (Adapted from Koattukudy, 2001).

Monomer type	Chemical structure
Unsubstituted fatty acids (C_{16}-C_{26})	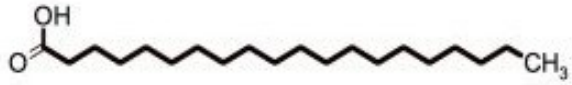
ω-hydroxy fatty acids (C_{16}-C_{26})	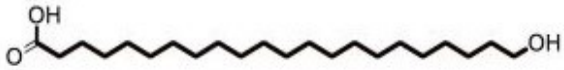
α,ω-dicarboxylic acids (C_{16}-C_{26})	
Fatty alcohols and diols (C_{18}-C_{22})	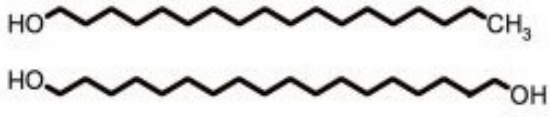
Glycerol	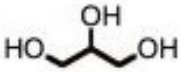
Ferulate	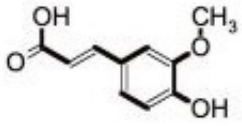

Table 1-2 Comparison of the relative abundance of suberin monomers in three well characterized plant species

Monomer type	*Arabidopsis thaliana* root tissue (Franke *et al.,* 2005)	*Solanum tuberosum* (potato) periderm (Kolattukudy and Agrawal, 1974)	*Quercus suber* cork tissue (Graça and Pereira, 1997; Marques and Pereira, 1994)
ω-hydroxy fatty acids	43%	16%	13.2%
α,ω-dicarboxylic acids	24%	24%	26.6%
Fatty acids	9%	8%	4%
Fatty alcohols	6%	6%	2.1%
Hydroxycinnamic acids	5%	<1%	1%
Glycerol	not included in quantification	20%	32.1%

Note: For Arabidopsis, % are for aliphatics, *i.e*. without glycerol.

The suberin polymer is thought to be embedded with waxes (Kosma *et al*., 2012; Delude *et al*., 2016). Suberin associated waxes are non-polymeric, solvent-soluble, lipophilic compounds believed to be a major contributor to the barrier function in roots (Ranathunge and Schreiber, 2011). The biosynthesis of the suberin polymer and associated waxes involves common pathways and occurs concomitantly, at least in Arabidopsis roots (Delude *et al*., 2016; Vishwanath *et al*., 2013). These waxes have been extracted by brief immersion of tissues in chloroform (Li *et al*., 2007; Vishwanath *et al*., 2013; Kosma *et al*., 2012), or by extensive solvent extraction methods (Delude *et al*., 2016). Suberin associated waxes are typically composed of alkyl hydroxycinnamates (AHCs – fatty alcohols esterified with coumaric, caffeic or ferulic acids), fatty acids (typically C16–C22), fatty alcohols (≥C18), and monoacylglycerols (Kosma *et al*., 2012). As in suberin, the abundance of different types of components detected in suberin associated waxes varies between species (Kosma *et al*., 2012). The main constituents of

Arabidopsis suberin-associated (or 'root waxes') are alkyl hydroxycinnamates (AHCs) where 80% of the total root waxes represent AHCs (Vishwanath *et al*., 2013). Alkyl coumarates and alkyl caffeates are the major components of Arabidopsis root waxes (Delude *et al*., 2016; Kosma *et al.*, 2012).

1.2 Structure

The macromolecular organizations of intact suberin polymers are currently unknown. Models for suberin structure has been proposed considering the chemical composition and conceptual ideas. Bernards (2002) proposed the following about suberin structure: 1) ferulic acids should be included as a component in suberin poly-aliphatic domain (SPAD) when they are esterified with fatty acids and fatty alcohols; 2) a poly-aromatic part made up of hydroxycinnamic acids and monolignols, which are located in primary cell walls, should be considered as a suberin polyphenolic domain (SPPD) and this polyphenolic domain of suberin is covalently linked with the suberin poly-aliphatic domain. Investigation of the TEM image reveals that suberin is typically layed down on the inner face of the primary cell wall adjacent to the plasma membrane (Figure 1-1). Suberin poly-phenolic domain (SPPD) and suberin poly-aliphatic domain (SPAD) correspond to respective electron-dense (dark) and electron-translucent (light) areas (Bernards, 2002). These are referred to as lamellae (Figure 1-1). In this proposed model, glycerol plays a main role in cross-linking aromatic components with aliphatic suberin components, while aliphatic and aromatic suberin monomers may only form a linear polymer on their own (Moire *et al*., 1999). However, according to a model proposed by Graça (2015), suberin is an "aliphatic polyester" that lacks a poly-phenolic domain. The main reason being the release of predominately aliphatic monomers, rather than aromatic monomers, during de-

polymerization with base- or acid-catalyzed trans-methylation (Graça and Pereira, 2000a). Althought some ferulate is released, it does not yield the polyaromatic monomers. Further, the polyaromatics are distinct chemically and structurally and also spatially separated from aliphatic suberin in suberized cell walls. Additionally, the aliphatic component of suberin has a defined macromolecular structure that is independent from polyaromatics by three main features: 1) glycerol molecules link in succession with α,ω-dicarboxylic acids to form the core backbone of the suberin polymer, 2) 18:1 ω-hydroxy fatty acids and α,ω-dicarboxylic acids are dominant components of suberins across many plant species, and 3) from de-polymerized suberin polymers, all ω-hydroxy fatty acid monomers are esterified with ferulic acids though their ω-hydroxyl groups (Graça and Pereira, 1998, 1999, 2000b). Graça (2015) further claimed that it is possible to consider the polyaromatic domain simply as lignin. Geldner (2013) also thinks that the polyphenolic domain should not be considered as part of suberin, but rather a separate lignin or lignin-like polymer.

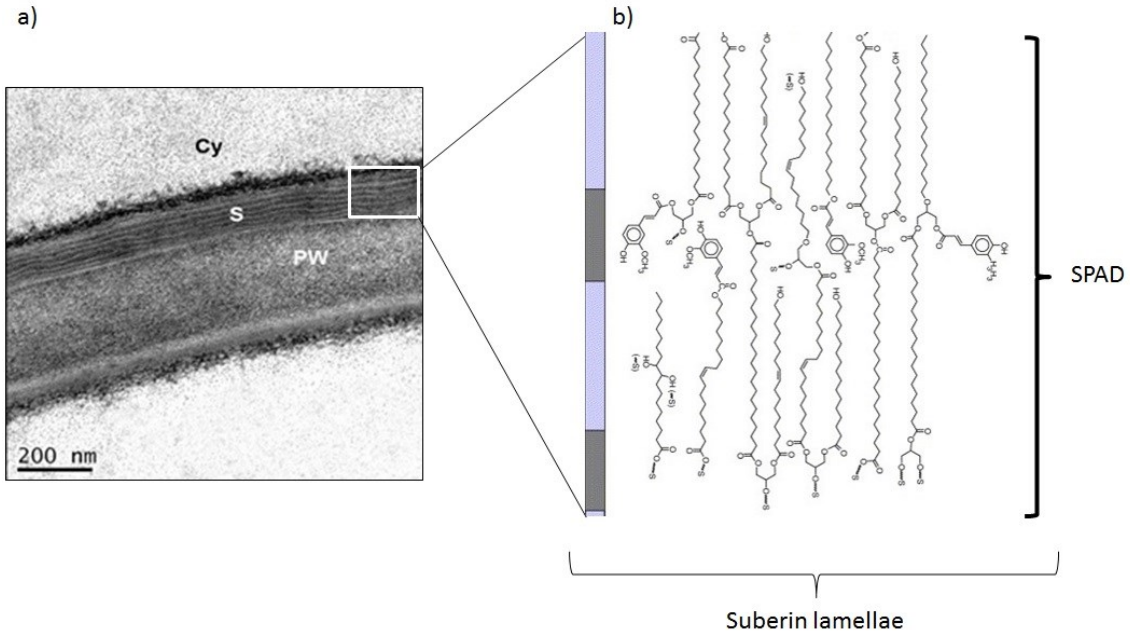

Figure 1-1. Structure of the suberin lamellae. a) TEM micrograph of a 4-weeks old *Arabidopsis thaliana* (Ecotype Columbia-0) root periderm section; b) Ultra-structure of the lamellae (inset), and corresponding model proposed by Bernards, 2002. SPAD: suberin poly-aliphatic domain (suberin); S: Dark and light banding pattern of suberin lamellae; Cy: cytoplasm; PW: Primary cell wall (TEM image by Nayana de Silva, suberin model adapted from Bernard, 2002).

In addition to suberin lamellae deposited in cell walls, suberin can also be deposited as "diffuse suberin" or in the form of non-lamellar structure, mainly in the epidermal cell walls of some species to provide defense against pathogen attack (Thomas *et al*., 2007). When observed under TEM, the epidermal cells of onion (*Allium cepa*) contained suberin distributed in faint bands within the cell walls and that was termed as "diffused suberin" (Peterson *et al*., 1978).

1.3 Distribution in plant tissues

Suberin is deposited in the cell walls of a variety of border tissues. The commonly known example is the suberized periderm of phellem tissue (cork) of shoots and roots undergoing secondary growth or thickening (Esau, 1977). Suberin is also present in the endodermis cell wall of primary roots. In some monocotyledonous species (e.g. *Zea mays* and *Oryza sativa)*, suberin is deposited in exodermis, the cell layer beneath the epidermis. In perennial species that undergo secondary growth in shoots, i.e. trees, suberin is deposited in the bark (Figure 1-4b). A well-known example of suberin found in the bark of a tree is "cork oak" (*Quercus suber).* Suberin in cork oak is commonly used in industry as an insulation or sealing material (Graça and Pereira, 1997; Silva *et al.,* 2005). Further, the impermeability, buoyancy, and elasticity of cork makes it an effective bottle stopper, which finds most use in the wine industry. Additionally, the thick

cork layer in the bark of *Sequoiadendron giganteum* (giant sequoia trees) allows these trees, which can live thousands of years, to survive wild fires (Bellows *et al.,* 2016). Suberin is also present in high amounts in the tuber periderm (skin) of *Solanum tuberosum* (potato) (Kolattukudy and Agrawal, 1974). Induction of suberin has also been detected after wounding of potato periderm (Schreiber *et al*., 2005b). Suberin is also deposited in bundle sheath cells of grass leaves (Mertz and Brutnell, 2014; Griffith *et al*., 1985) and conifer needles (Wu *et al*., 2003). The model plant *Arabidopsis thaliana* deposits suberin in endodermis of young roots (Figure 1-2) and in periderm of mature roots (Figure 1-4a) (Kresziesa *et al*., 2018). Suberin is also deposited in the Arabidopsis seed coat including the micropyle region (Molina *et al*., 2008).

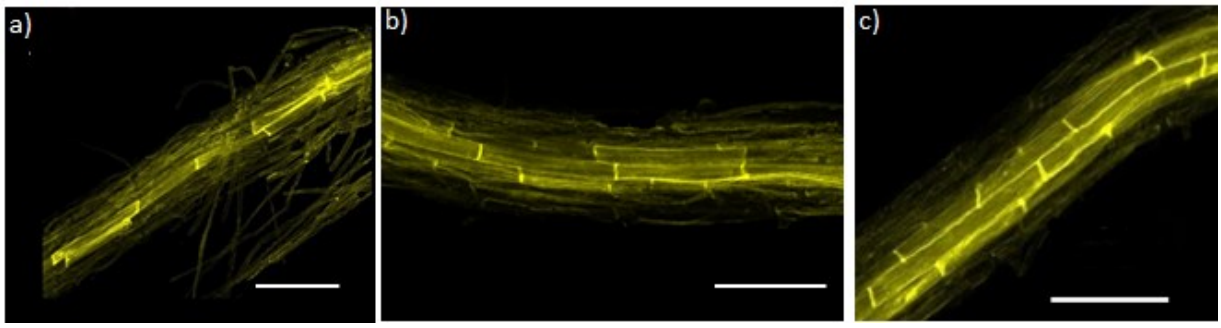

Figure 1-2. Development of suberin in Arabidopsis root. Whole mounts of 3 day (a), 4 day (b) and 5 day (c) old wild-type (Col-0) endodermis. Stained with flourol yellow 088 (Appendix I). Scale bar = 100µm. Microscopy by Nayana de Silva

Suberization of root endodermis passes through different stages of differentiation. As reported by Martinka *et al*. (2012), root endodermal cells of vascular plants undergo three developmental stages: primary, secondary and tertiary. During primary stage (Stage I), Casparian bands (CBs) are formed continually along the inner surface of anticlinal cell walls (Figure 1-3; Ma and Peterson, 2003). The CBs are primary cell wall modifications, consisting of lignin as a

major component (Naseer *et al*., 2012). As CBs are the first to develop, this stage is usually initiated close to the root tip. In the secondary stage (Stage II), suberin lamellae are laid down in both anticlinal and tangential walls (Figure 1-3). A qualitative investigation by Martinka *et al.* (2012) demonstrated that suberin lamellae contains more suberin than lignin. Transition from Stage I to Stage II starts with the appearance of suberin lamellae as patches (Figure 1-2 a-b), eventually becoming a zone of continuous suberin deposition in the endodermis (Figure 1-2c). The continuous suberin deposition zone can also contain un-suberized cells called passage cells (Andersen *et al*., 2018). Passage cells allow movement of water and solutes across the endodermal barrier (Kresziesa *et al.,* 2018). The function of the endodermal barrier can change when environmental conditions change (Doblas *et al.*, 2017). A recent study highlighted that suberin deposition in Arabidopsis roots is a reversible process controlled by plant hormones in response to nutrient stresses (Barberon *et al*., 2016). In some species, such as *Zea mays* (maize), endodermal cells show an additional stage of differentiation (stage III) having U- shaped thick secondary cell wall deposition (Enstone *et al*., 2003). In these cells, cellulosic walls may contain additional poly(phenolics) and/or multiple suberin lamellae deposited on the inner face of the endodermal cell walls (Thomas *et al*., 2007). In *Iris germanica* roots,the endodermal cells appear as U-shaped when the inner tangential walls depost extensive amounts of lignin (Meyer *et al*., 2009).

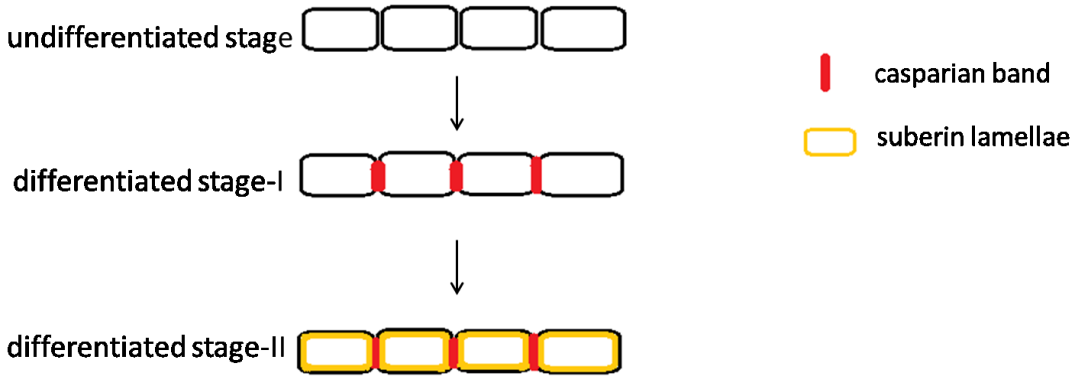

Figure 1-3. Schematic representation of root endodermal differentiation. Stage I is characterized by deposition of localized lignin at the junction between adjacent endodermal cells that fuse to form a ring, sealing the apoplastic space (Casparian Bands or Strips). Stage II is marked by presence of suberin lamellae at the inner surface of primary cell walls covering the entire surface of endodermal cells.

Unlike in monocotyledonous roots, dicotyledonous roots and stems undergo secondary growth. The secondary growth starts with the division of vascular cambium, which gives rise to secondary xylem and phloem. With the formation of new secondary vascular tissues, the middle part of the root expands and pushes the primary tissues outwards. Therefore, epidermis, cortex and endodermis get sloughed off at the outermost surface of the root. Then, in order to form a protective tissue at the plant-soil interface, pericycle cells located inside of the endodermis cell layer resume their meristematic activity and gives rise to a periderm. These dividing pericyclic cells are termed phellogen (cork cambium). Cork cambium forms phellem cells (cork cells) outwards and phelloderm inwards. The cork cells are dead at maturity with suberized cell walls that are impermeable to water. All three tissues, phellem, phellogen, and phelloderm, are collectively called periderm. In most species, phellem is the most prominent tissue in the

periderm (Graça, 2015). Phellem in Arabidopsis roots consists of several layers of cells (Figure 1-4a). A periderm is also found in the bark of trees that undergo secondary growth, which is also known to protect plants against water loss and pathogen attack (Figure 1-4b).

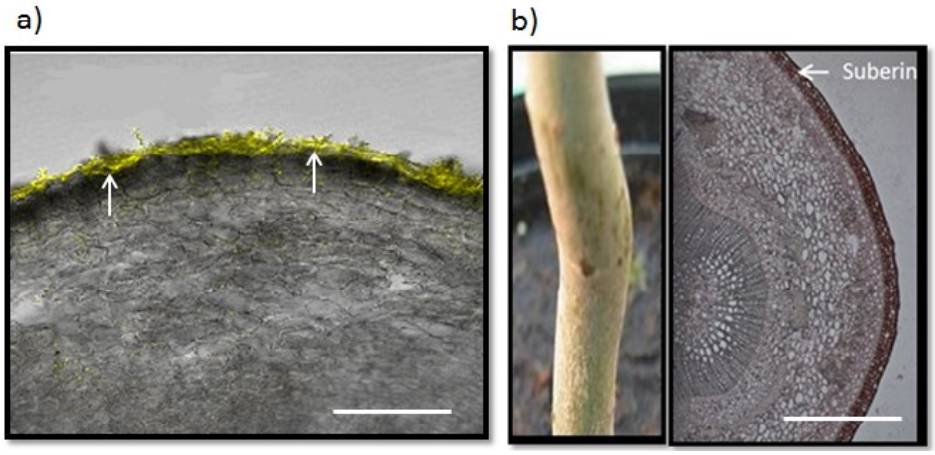

Figure 1-4. Suberized phellem (cork) in roots and shoots undergoing secondary growth. a): Cross-section of a 4-week old *Arabidopsis thalina* wild-type (Col-0) root stained with fluorol yellow 088; Scale bar = 100µm. b): External appearance of suberin on the bark and a cross section of a *Populus trichocarpa* (poplar) tree bark stained with Sudan red. Arrows indicate suberized periderm cells. Scale bar = 250 µm. Images by Nayana de Silva.

1.3 Functions

Plants deposit suberin in specialized tissues to create a protective barrier at different tissues above- or below-ground. Since suberin is hydrophobic, it can impart barrier functions to water diffusion. It also can control the selective uptake of solutes from the soil environment (Baxter *et al*., 2009). The function of suberin as a transport barrier is thought to be mostly determined by the aliphatic portion (Franke and Schreiber, 2007). Plants take up water from soil through roots. In this journey, water passes from the cortex into the vascular tissues. There are three routes that

water and solutes flow in roots, known as the apoplastic, symplastic and transcellular pathways (Figure 1-5).

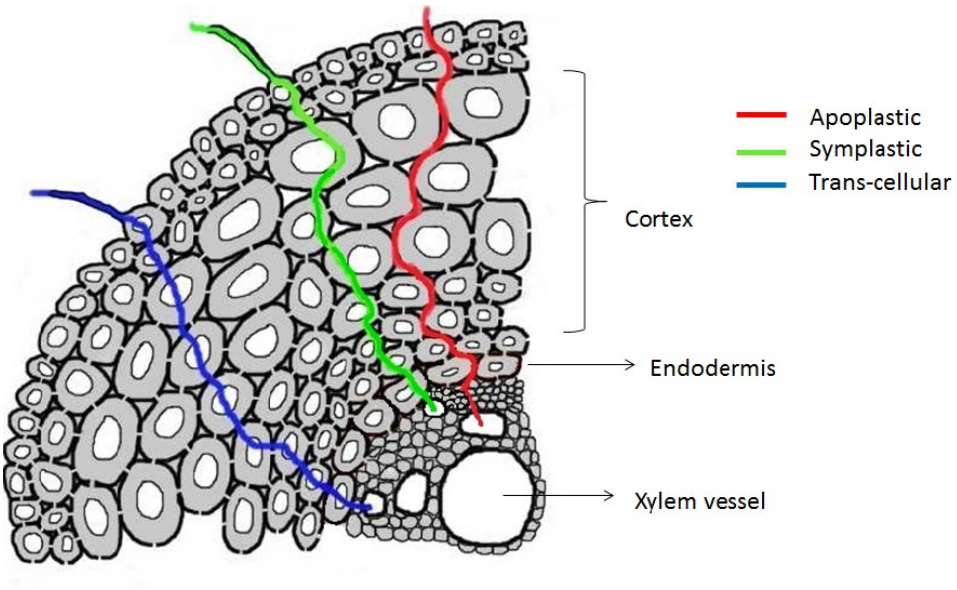

Figure 1-5. Schematic representation of three different pathways of water and solutes movement in roots. The apoplast provides a porous path through the cell walls and intercellular spaces. The symplastic path is through plasmodesmata and the cytosol of cells. Along the transcellular path, water and solutes have to cross many membranes facilitated by aquaporins or channels/transporters, respectively. (Figure modified from Ph.D. dissertation, Ranathunge 2005).

Roots absorb water from soil by two different mechanisms: active and passive absorption (Kramer, 1949). Active absorption occurs when the transpiration rate of the plant is low. In the active transport mechanism, water moves through the symplastic pathway and follows the cell protoplasm, moving from one cell to the other through plasmodesmata (Figure 1-5, green line). Passive transport, occurs through the apoplastic pathway when the transpiration rate of the plant is high. In passive transport, water moves through permeable cell walls and intercellular spaces (Figure 1-5, red line). Water molecules can travel faster via the apoplastic pathway than the

symplastic pathway. In the transcellular pathway (also called transmembrane pathway), water and solutes move through cell walls and aquaporins/transporters in the plasma cell membrane (Peterson and Cholewa, 1998; Steudle and Peterson, 1998) (Figure 1-5, blue line). In the trans-cellular pathway, water movement takes place via aquaporin channels located inside plasmadesmata (Figure 1-6, upper panel blue dotted line), whereas the solutes move via polarized influx and efflux transporters of the plasma membrane (Figure 1-6, upper panel green dotted line). Therefore the transcellular pathway involves transport of water across the plasma membrane and vacuolar membrane (Johansson *et al*., 2000). Experimentally, symplastic and transcellular pathways are difficult to separate as water molecules can move through both pathways (Steudle, 2000). For this reason, symplastic and transcellular pathways are sometimes considered together as the "cell-to-cell" pathway (Figure 1-6), (Kresziesa *et al*., 2018; Steudle and Peterson, 1998).

Depending on the stage of differentiation, endodermis can deposit Casparian bands (Stage I) or both Casparian bands and suberin lamellae (Stage II). It is thought that these barriers play a major role in controlling water and nutrient uptake in plants (Barberon, 2017). The control can occur at varying distances from the root tip depending on where the apoplastic barriers are formed. Thus, this barrier can only be bypassed close to the primary or lateral root tips, where endodermis is in an undifferentiated state (Steudle and Peterson, 1998).

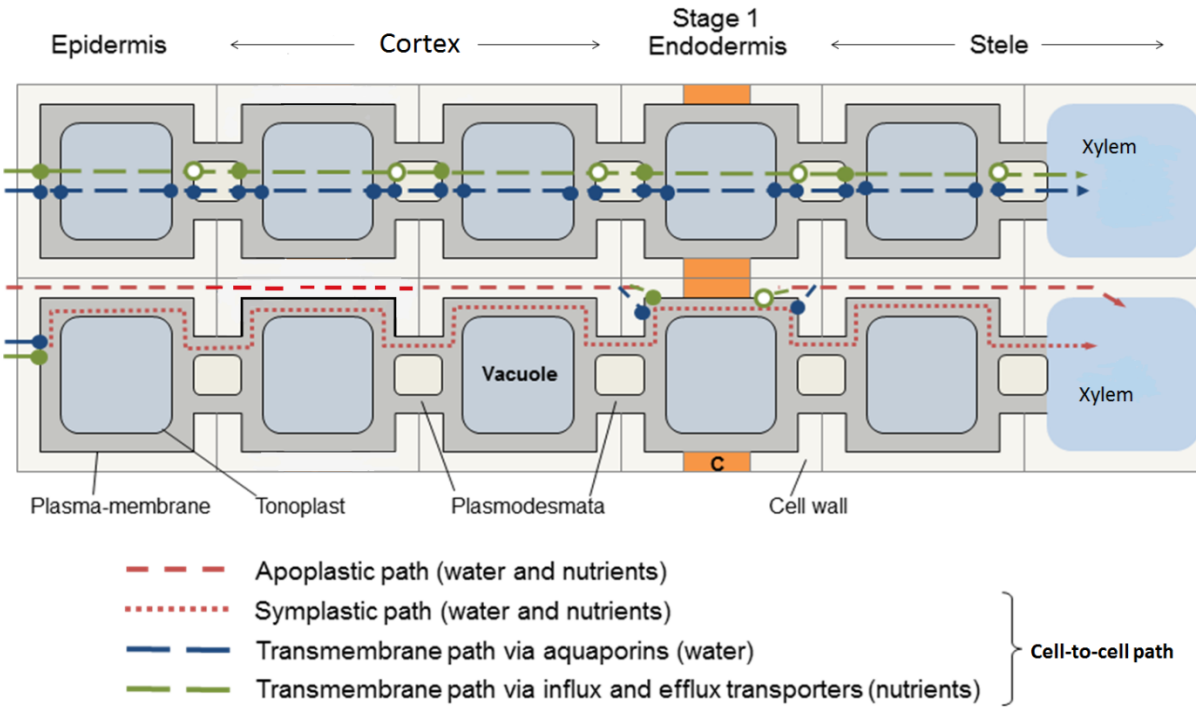

Figure 1-6. Water and solute movement across endodermis at Stage I differentiation. C: Casparin band. Diagram modified from the e-book, http://plantsinaction.science.uq.edu.au/

In Stage I endodermal differentiation, water movement via the apoplastic pathway can occur only up to the endodermis as the Casparian band blocks further passage towards the xylem tissue (Figure 1-6, lower panel). Therefore, it was suggested that the role of Casparian band is to control the water movement through the apoplastic pathway (Hosmani *et al*., 2013; Naseer *et al*., 2012). Suberin lamellae would not affect apoplastic transport since suberin lamellae is deposited on the inner surface of the primary wall and would not seal the spaces between cells. Mutants with ectopic suberization or mutants with no suberin lamellae demonstrated no effect on the movement of propodium iodide (PI), an apoplastic tracer (Naseer *et al*., 2012; Hosmani *et al*., 2013). However, the presence of suberin lamellae could affect uptake of nutrients and water from

the transcellular pathway into endodermal cells which eventually impacts the "cell-to-cell" path at the endodermis (Geldner, 2013; Robbins *et al*., 2014; Figure 1-7 upper panel). Therefore, when endodermis is in Stage II differentiation, water and solutes can enter the endodermal cell from neighbouring cortical cells only through plasmodesmata /symplastic pathway (Andersen *et al*., 2015; Figure 1-7 lower panel). On the other hand, suberin lamellae may function as an apoplastic diffusion barrier at sites of lateral root emergence when Casparian bands are disrupted (Li *et al*., 2017).

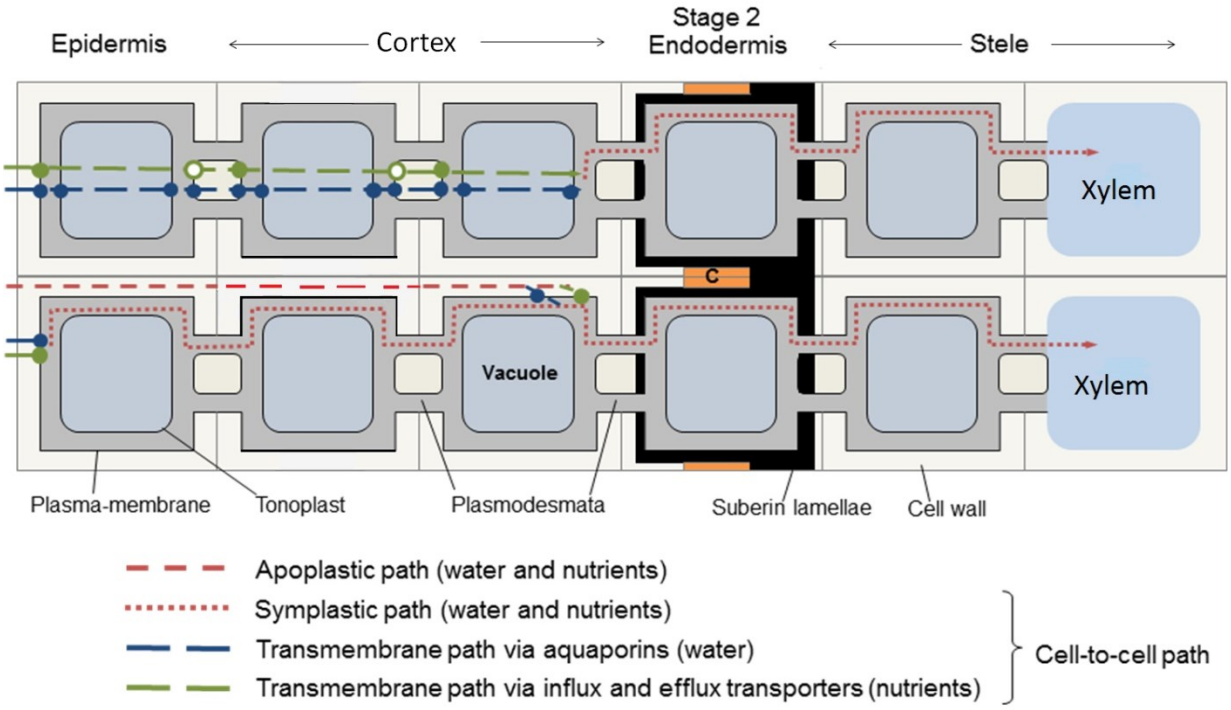

Figure 1-7. Water and solute movement across endodermis at Stage II differentiation. C: Casparin band. Diagram modified from the ebook, http://plantsinaction.science.uq.edu.au/

With regards to plant nutrition, the function of suberin is well documented in various plant species with differences in suberin content (Doblas *et al*., 2017). Ionomic analysis of the *esb1*

mutant with disrupted Casparian band and ectopic suberization showed a decrease in the accumulation of calcium, manganese, and zinc and an increase in the accumulation of sodium, sulfur, potassium, arsenic, molybdenum, and selenium (Baxter *et al*., 2009; Hosmani *et al*., 2013). Moreover, characterization of the *lotr1* mutant revealed that ectopic suberization inhibits calcium transport from root to shoots (Li *et al*., 2017). These results demonstrate that suberin plays different roles in plant nutrition, depending on the solute that passes through the suberin barrier. For example, suberin plays a role as a barrier to the entry of some elements such as calcium and manganese, and might rather act to retain other minerals such as sulfur and potassium within the stele (Doblas *et al*., 2017).

In some species, suberin is deposited in the exodermis to prevent water loss from roots to the soil in dry conditions This mechanism can enhance the water retention capacity in roots as observed in maize, onion, sunflower, rhodes grass and sorghum that form an exodermis with suberization (Taleisnik *et al*., 1999). Suberin also plays an important role in limiting radial oxygen loss (ROL) from roots growing in marshy environments (deoxygenated condition). In rice (*Oryza sativa* L.), early development of Casparian bands and suberin lamellae in the exodermis was associated with a decrease in ROL in roots (Kotula *et al*., 2009). Suberin and associated waxes also play a major function against water loss during post-harvest storage of tubers (eg. potato) and during induction of periderm by wounding (Schreiber *et al*., 2005b).

Aliphatic suberin and associated polyaromatics may also function in pathogen defenses. Although suberin deposition cannot completely stop pathogen invasion, it has been shown to reduce colonization by pathogens. A soybean (*Glycine max*) line with highly suberized cell walls demonstrated partial resistance to the oomycete *Phytophthora sojae* and induced aliphatic suberin deposition up to 4 days earlier than a susceptible soybean line (Ranathunga *et al*., 2008).

Studies on potato wound periderm revealed that the polyaromatic domain is important for resistance against *Erwinia carotovora* subsp. *carotovora* (a bacterium), while the polyaliphatic domain is important for resistance against the fungus *Fusarium sambucinum* (Lulai and Corsini, 1998; Lulai and Freeman, 2001).

1.4 Biosynthesis and deposition of suberin

The biosynthetic machinery of suberin production is complex. It consists of a network of many sequential and parallel enzymatic reactions (Figure 1-8). The enzymology of suberin monomer biosynthesis has been extensively characterized (Vishwanath *et al.*, 2015). Most of the present knowledge of suberin biosynthesis arises from genetic studies in *Arabidopsis thaliana.*

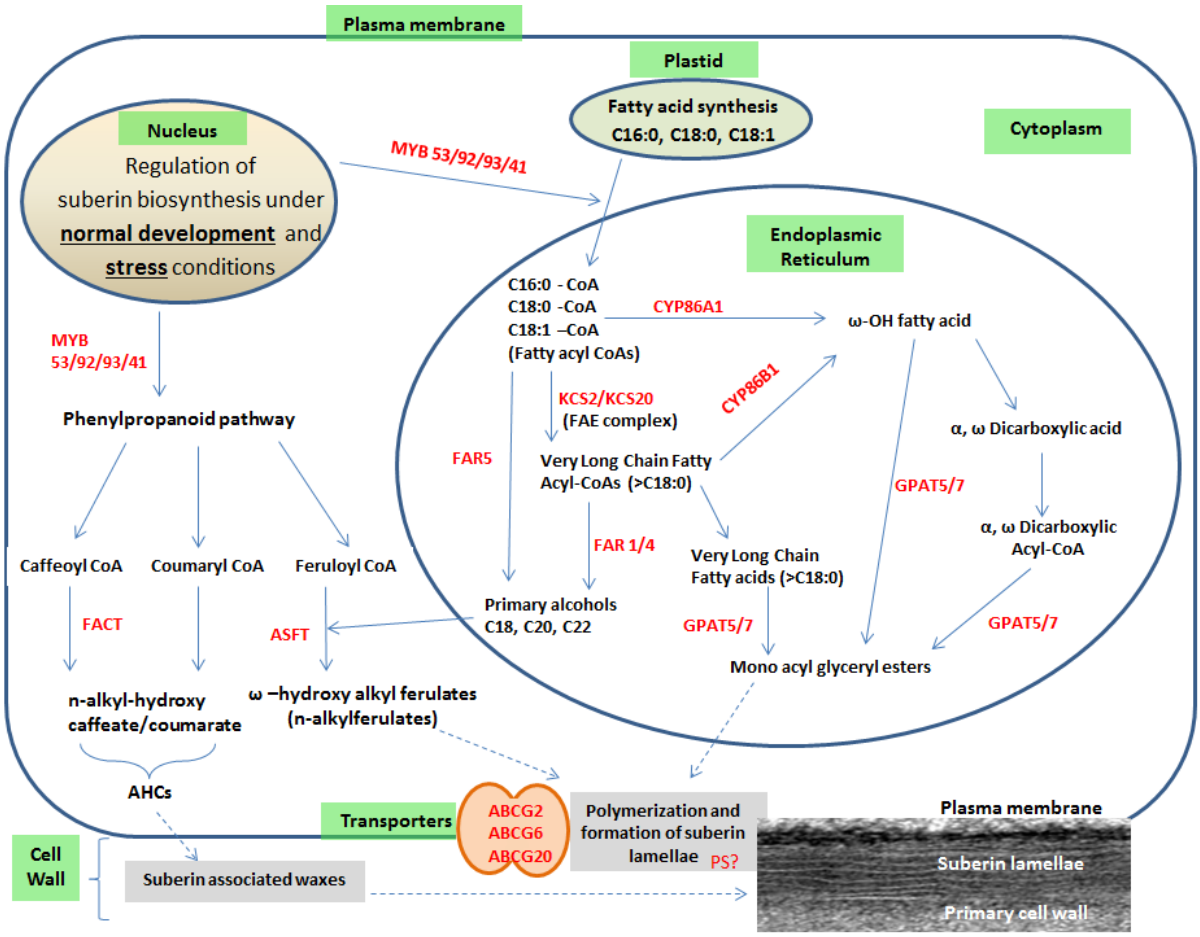

Figure 1-8. Overview of the suberin biosynthetic pathway. Specific protein names in red are those discovered in *Arabidopsis thaliana*. Fatty acid synthesis occurs in the plastid giving rise to predominately 16:0 and 18:1 acyl chains. Fatty acyl elongation occurs via the endoplasmic reticulum (ER)-associated fatty acid elongation (FAE) complex producing very long chain fatty acyl chains. Acyl reduction by fatty acyl reductases (FARs) producing primary alcohols, fatty acyl oxidation by cytochrome P450 enzymes (CYPs) producing ω-hydroxy fatty acids (ω-OHs) and α,ω -dicarboxylic acids (DCAs), and esterification of ω-OHs and DCAs to glycerol-3-phosphate (G3P) by glycerol 3-phosphate acyltransferases (GPATs) producing monoacylglycerols also all occur at the ER membrane. The intracellular transport mechanisms

and polymerization steps of suberin building blocks are not yet known. ATP-binding-cassette (ABC) transporters are thought to be involved in the transport of suberin monomers across the plasma membrane. Cell wall associated polyester synthase(s) (PS) likely produce high molecular weight polyesters. Coumaric, caffeic, and ferulic acids, products of the phenylpropanoid pathway, are linked to fatty alcohols by BAHD-type acyltransferases to produce alkyl hydroxycinnamates (AHCs) found in suberin-associated waxes. ASFT, Aliphatic Suberin Feruloyl Transferase; FACT, Fatty Alcohol Caffeoyl-CoA Transferase. MYB-type transcription factors are important for controlling the specific developmental and stress-induced gene expression patterns of the suberin biosynthetic genes.

1.4.1 Biosynthesis of suberin monomers

Suberin deposition requires biosynthesis of aliphatic, phenolic and glycerolipid monomers, and then transportation to the cell walls to form the hydrophobic macromolecular polymer. Suberin aliphatic monomers are mostly derived from 16:0 and 18:1 fatty acyl-CoAs that are produced *de novo* in plastids and then exported to the cytosol. They are then modified by suberin biosynthetic enzymes localized at the endoplasmic reticulum (ER) (Figure 1-8). The major steps involved in enzymatic reactions in the synthesis of suberin polyesters are discussed below.

KCS (ß-ketoacyl-CoA Synthases):

Very-long-chain fatty acids (VLCFAs) are synthesized at the endoplasmic reticulum by sequential additions of C2 moieties from malonyl-CoA to preformed C16 or C18 acyl groups derived from the *de novo* fatty acid synthesis pathway of the plastid. Four enzymatic reactions are involved in the ER fatty acid elongation process: condensation of C16/C18-CoA with

malonyl-CoA to form a 3-ketoacyl-CoA, reduction of 3-ketoacyl-CoA to 3-hydroxy-CoA, dehydration to an enoyl-CoA, and reduction of the enoyl-CoA to the fully reduced acyl chain (Fehling and Mukherjee, 1991). This cycle can be repeated (e.g. C20 to C22). Ketoacyl-CoA synthases (KCS), which are present as part of the endoplasmic reticulum-localized fatty acid elongase complex (FAE), are responsible for the first enzymatic step in the elongation of C16/C18 fatty acyl chains into very long-chain (≥C20) fatty acid derivatives (Millar and Kunst, 1997). The non-elongated and elongated acyl chains are either reduced into primary alcohols, oxidized into ω-hydroxy fatty acids, or released as fatty acids (Figure 1-8). The condensing enzyme DAISY/AtKCS2 was reported to be involved in suberin biosynthesis (Franke *et al*., 2009). Loss-of-function *daisy/kcs2* mutants have reductions in C22 and C24 very-long-chain fatty acid derivatives in root suberin (Franke *et al*., 2009). The double *kcs2 kcs20* mutant is further reduced in C22 and C24 very long-chain fatty acid derivatives in roots, compared with either single mutant, indicating that the two KCS enzymes function in a partially redundant manner (Lee *et al*., 2009). The total amount of suberin in these mutants is similar to that of wild-type, perhaps due to compensatory increases of shorter chain (≤C20) fatty acid derivatives.

CYP (Cytochrome P450 monooxygenases):

The two major monomer classes found in the suberin polymer are ω-hydroxy acids and α,ω-dicarboxylic acids. Hydroxylation of the terminal methyl group of aliphatics (ω-position) is catalyzed by enzymes belonging to the CYP86 subfamily of cytochrome P450 monooxygenases (Molina, 2010). The fatty acids are hydroxylated to 16:0 and 18:1 ω-hydroxy fatty acids, and then further oxidized into α,ω-dicarboxylic acids by an ω-hydroxy fatty acid dehydrogenase (Agrawal and Kolattukudy, 1978), which is possibly the same P450 enzyme. The *CYP86A1* gene

is expressed in root endodermis (Hofer *et al*., 2008) . *CYP86A1* knock-out mutants have about 60% of the aliphatic suberin than that of wild-type roots (Hofer *et al*., 2008). This is mainly resulting from strong reductions in C16 and C18 ω-hydroxy acids and α,ω-dicarboxylic acids compared to wild-type (Hofer *et al*., 2008). This chemical phenotype suggests that CYP86A1 is a C16/C18 fatty acid ω-hydroxylase, and it may further oxidize the ω-hydroxy acids to yield α,ω-dicarboxylic acids.

CYP86B1 produces very-long-chain C22 to C24 ω-hydroxy acids from fatty acids (Compagnon *et al*., 2009). Transgenic lines containing the *CYP86B1* promoter fused to the β-glucuronidase (GUS) reporter gene have strong expression of the reporter gene in the root endodermis (Compagnon *et al*., 2009). Loss-of-function *cyb86b1* mutants have almost complete loss of C22-C24 ω-hydroxy fatty acids and α,ω- dicarboxylic fatty acids, which are accompanied by increased amounts of C22-C24 fatty acids in the polymer (Molina *et al.*, 2009; Compagnon *et al*., 2009)

FAR (Fatty Acyl Reductases)

Saturated fatty alcohols of chain lengths C18, C20 and C22 are components of Arabidopsis root suberin and its associated waxes (Domergue *et al*., 2010; Vishwanath *et al*., 2013; Delude *et al*., 2016). Fatty acyl reductases catalyze the reduction of fatty acyl-CoAs to primary fatty alcohols via an unreleased fatty aldehyde intermediate (Rowland and Domergue, 2012). Out of the eight-member *FAR* gene family in Arabidopsis, the gene expression patterns of *FAR1, FAR4* and *FAR5* coincide with known sites of suberin deposition (Domergue *et al*., 2010). Reduced contents of 18:0-OH, 20:0-OH and 22:0-OH were found in *far5, far4,* and *far1* mutants, respectively. Consistent with these genetic results, heterologous expression of these FARs in

yeast revealed that FAR1, FAR4 and FAR5 primarily produce 22:0, 20:0 and 18:0 chain length primary fatty alcohols, respectively (Domergue *et al*., 2010). Also, *far* double and triple mutants were studied to further examine the effects on suberin-associated 18:0-22:0 primary fatty alcohols in root and seed coats (Vishwanath *et al*., 2013). The *far* triple mutants have 70% and 80% reduction in fatty alcohol load in roots and seed coats, respectively. Primary alcohols are also found in a combined state in root waxes, specifically as 18:0, 20:0, and 22:0 alkyl hydroxycinnamates (AHCs) (Li *et al*., 2007; Kosma *et al*., 2012). The *far* double and triple mutants have chain-length specific reductions in AHCs in suberin-associated root waxes, with *far1 far4* and *far1 far4 far5* mutants nearly completely lacking AHCs (Vishwanath *et al*., 2013).

GPAT5 (Glycerol 3-Phosphate Acyl Transferases):

The suberin biosynthetic pathway includes acyl transfer reactions (Figure 1-8). *GPAT5* encodes a protein with acyl-CoA: glycerol-3-phosphate acyltransferase activity and the gene is expressed in Arabidopsis root endodermis and seed coat (Beisson *et al.,* 2007). GPATs are responsible for acyl transfer reactions to produce *sn2*-monoacylglycerols that function as core suberin building blocks (Vishwanath *et al*., 2015). Knock-out *gpat5* mutants have several-fold reductions in very-long-chain (C22 and C24) ω-hydroxy fatty acids and α,ω-dicarboxylic acids. These alterations are correlated with increases in root and seed coat permeabilities (Beisson, *et al.*, 2007).

ASFT (Aliphatic Suberin Feruloyl Transferase):

Arabidopsis ASFT (Aliphatic Suberin Feruloyl Transferase) is a member of the BAHD family of acyltransferases. It catalyzes the acyl transfer of feruloyl-CoA to ω-hydroxy acids and fatty alcohols to produce alkyl hydroxycinnamates (AHCs) (Molina *et al*., 2009), incorporating

ferulate into aliphatic suberin. ASFT is predicted to be a cytosol-localized enzyme, which is different from the other suberin-related enzymes described above that are localized to the endoplasmic reticulum (Figure 1-8) (Serra *et al*., 2010). Loss-of-function mutants of *ASFT* almost completely lack ferulate in Arabidopsis root and seed coat suberin (Gou *et al*., 2009; Molina *et al*., 2009). The reduction in ferulate in mutant seeds is associated with an approximate stoichiometric decrease in aliphatic monomers containing ω-hydroxy groups. The changes in monomer composition are correlated with increased seed coat permeability to tetrazolium salts in comparison to wild-type (Molina *et al*., 2009). Nevertheless, an absence of ferulate does not lead to a reduction in suberin aliphatic components or any structural alterations in the suberin lamellae, which would be expected if ferulate is crucial to link the polyphenolic domain as suggested previously (Molina *et al*., 2009).

1.4.2 Biosynthesis of suberin-associated waxes

In Arabidopsis, suberin-associated waxes are found in root endodermis and mature root periderm and are mostly composed of alkyl hydroxycinnamates (AHCs), representing about 90% of the total waxes in Arabidopsis. Among them, 18:0-22:0 alkyl caffeates are the most abundant components (Kosma *et al*., 2015; Delude *et al*., 2016). The other components are a combination of alkyl coumarate and alkyl ferulate esters, fatty acids, fatty alcohols, 29:0 alkanes and their mid-chain oxidized derivatives, sterols and *sn2*-monoacylglycerols (Li *et al*., 2007; Molina *et al*., 2009; Kosma *et al*., 2012). FATTY ALCOHOL:CAFFEOYL-CoA CAFFEOYL TRANSFERASE (FACT) is another member of the BAHD family of acyltransferases responsible for the synthesis of the alkyl caffeates present in Arabidopsis root waxes (Kosma *et al*., 2012). Arabidopsis root waxes have chemical characteristics in common with monomers

released upon depolymerisation of root suberin (Li *et al*., 2007; Vishwanath *et al*., 2013). Further, FARs are responsible for the synthesis of the C18–C22 fatty alcohols present in the suberin polymer and those found in root waxes (Kosma *et al.,* 2012; Vishwanath *et al*., 2013). This suggests the presence of a common biosynthetic pathway for production of polymerized and non-covalently linked waxes associated with suberin (Li *et al*., 2007; Delude *et al.,* 2016).

1.4.3 Transport of monomers and polymerization

Suberin monomers or partially formed oligomers need to be transported from the ER to and across the plasma membrane. Then, they need to be polymerized in the apoplasm before deposition in the form of suberin lamellae or "diffuse suberin" (Vishwanath *et al*., 2015). Even though the synthesis of aliphatic suberin monomers is fairly well known, the transportation and polymerization mechanisms remain unknown. Polyester synthases responsible for lipid polymer assembly have been identified for cutin in tomato (Yeats *et al*., 2012), but no candidates have yet been reported for suberin polymerization. Nevertheless, Yadev *et al*. (2014) reported three genes involved in suberin transport: ATP binding cassette (ABC)-type transporters, ABCG2, ABCG6, and ABCG20. Investigation of the triple mutant, *abcg2 abcg6 abcg20*, revealed incomplete suberin barrier formation in roots and seed coats. Further, the suberin lamellae structure of the triple *abcg2 abcg6 abcg20* mutant is distorted and seeds are highly permeable to tetrazolium salts relative to wild-type, indicating reduced suberin barrier function (Yadav *et al*., 2014). The total suberin polyester monomer in the seed coat is less than that of wild-type seeds (Yadav *et al*., 2014). However, compared to wild-type, higher suberin monomer content was found in the *abcg2 abcg6 abcg20* triple mutant roots (Yadav *et al*., 2014). Mutant roots had higher transcript levels of *GPAT5*, *CYP86A1*, *CYP86B1*, and *ASFT* than did wild-type roots which explains the

increase in suberin monomer content (Yadav *et al*., 2014). Although mutant roots did make suberin, it was structurally altered, perhaps due to monomer transport defects.

1.4.4 Regulation of deposition

Suberization is a structural phenomenon that takes place in specialized tissues and under different stress conditions. Although the enzymology and chemical composition of suberin are relatively well known, little is known regarding the regulatory mechanisms governing suberin deposition. Suberin deposition is controlled to a large degree at the level of transcription, which is supported by gene expression studies of suberin biosynthetic genes (Ranathunge *et al*., 2011; Vishwanath *et al*., 2015). The expression of suberin biosynthetic genes is tightly controlled spatially and in response to environmental cues. Suberin occurrence under non-stress conditions in various tissues as well as under stress conditions suggests complexity in its regulated deposition (Bernards and Lewis, 1998). The transcription factor AtMYB41, when overexpressed, is able to activate all steps necessary for aliphatic suberin synthesis and deposition of cell wall-associated suberin-like lamellae in both *Arabidopsis thaliana* and *Nicotiana benthamiana* leaves (Kosma *et al*., 2014). Overexpression of *AtMYB41* results in the accumulation of suberin-type aliphatic monomers, monolignols, and phenylpropanoids in *N. benthamiana* and *A. thaliana* leaves. Furthermore, the *AtMYB41* promoter is activated in root endodermal cells by ABA and NaCl stress, but not under non-stress conditions (Kosma *et al*., 2014). Under non-stressed conditions, *AtMYB53*, *AtMYB92* and *AtMYB93* are responsible for regulating suberin biosynthesis in root endodermis (Murmu and Hu *et al*., manuscript in preparation). Also, apple MYB93 is thought to play a major role in the regulation of suberin deposition in russeted apple skins (Legay *et al*., 2016). Two genes, AtMYB9 and AtMYB107, are responsible for regulating

suberin assembly in *Arabidopsis thaliana* seed coats, and the knock-out mutations of these genes result in significant reductions in seed coat suberin and low germination rates under stress (Lashbrooke *et al*., 2016; Gou *et al*., 2017). *Myb107* loss-of-function mutants display significant (50%-60%) decreases in seed coat suberin (Gou *et al.,* 2017). The *myb107* mutants also have higher permeability to tetrazolium salts than wild-type seeds (Gou *et al*., 2017).

1.5 Changes in suberin deposition under normal growth and stressful environmental conditions

Hofer *et al.* (2008) reported suberin composition during tissue maturation in Arabidopsis roots. The total suberin content in Arabidopsis roots increased with distance from root tip to the base. In this study, aliphatic monomers at three locations along the length (apical, middle, and basal) of *Arabidopsis thaliana* roots were quantified. Another compositional analysis study during the early developmental stages of Arabidopsis wild-type plants (Col-0) grown in tissue culture revealed an increase in root suberin and associated waxes during the first week of growth followed by a steady state with no further increase (Delude *et al.* 2016). A significant difference in the abundance of aliphatic monomers in wound-induced periderm in *S. tuberosum* over the course of seven days of development was also recorded by Yang and Bernards (2007).

Although suberin is constitutively deposited in certain tissues, plants also respond to environmental stimuli by modifying the degree of suberization in cell walls (Franke *et al*., 2012). A number of studies have shown changes in suberin deposition by various stress factors in different species. Franke *et al*. (2009) reported an increase in Arabidopsis *DAISY/KCS2* transcript levels under polyethylene glycol-induced osmotic stress and under high concentrations of NaCl. Concomitantly, root suberin quantities in 5-week-old Arabidopsis plants were increased compared to unstressed plants. In hydroponically grown rice (*Oriza sativa* L.) cultivars, the salt

tolerant cultivar (Pokkali) exhibited extensive suberization in roots compared to salt sensitive cultivars (IR20 and Jaya). Furthermore, the lowest amount of Na^+ in the shoot was recorded in Pokkali cultivar (Krishnamurthy *et al*., 2009). Compared to aerated grown conditions, suberized exodermis was detected in rice (*Oriza sativa* L.) grown under stagnant (oxygen deficient) conditions (Kotula *et al*., 2009). These changes in suberin accumulation have been suggested to increase resistance to radial oxygen loss (Watanabe *et al*., 2013). Suberin biosynthesis was up-regulated by salt treatment in *Avicennia officinalis* roots and leaves (Krishnamurthy *et al*., 2014) and by waterlogged conditions in rice (Watanabe *et al*., 2013) and maize (Enstone and Peterson, 2005). Suberin amounts were significantly increased in endodermal, rhizodermal and hypodermal cell walls of hydroponically cultivated Castor bean (*Ricinus communis* L.) under salt stress (100 mM NaCl) (Schreiber *et al.*, 2005). In contrast, under nitrogen deficient conditions the opposite was observed and plants reduced suberization of their apoplastic transport barriers to facilitate nutrient uptake from the soil (Schreiber *et al*., 2005a; Barberon *et al*., 2016). Abscisic acid stimulated deposition of suberin and associated waxes in potato tuber (Cottle and Kolattukudy, 1982). Recently, Barberon *et al*. (2016) reported that endodermal suberization of Arabidopsis could respond to a wide range of nutrient stresses due to the involvement of stress hormones, and this was shown to be via abscisic acid- and ethylene-mediated regulation. Suberization was delayed under Fe, Mn or Zn deficient conditions compared to the control condition. On the other hand, suberization was enhanced under K or S deficient conditions (Barberon *et al.,* 2016). These authors claimed that roots can increase suberin but also decrease pre-formed suberin to allow plants to adapt to rapidly changing soil environments (Doblas *et al*., 2017; Barberon *et al*., 2016).

As described earlier (Section 1.3), it was shown that resistance of potato tubers to bacterial (*Erwinia spp.*) and fungal (*Fusarium* spp.) infection was related to the differential deposition of the two major suberin components (phenolics and aliphatics). Although polyphenolic and polyaliphatic domains are parts of the suberin polymer, polyphenolic deposition occurs before polyaliphatic suberin deposition (Lulai and Corsini, 1998). Resistance to infection by *E. carotovora* occurred after completion of polyphenolic deposition on the outer tangential wall of the first layer of cells (2-3 days), while resistance to fungal infection was attained only after completion of aliphatic deposition within the first layer of suberizing cells (5-7 days). This indicates distinct control of the polyphenolic and polyaliphatic branches of the suberin biosynthetic machinery (Lulai and Corsini, 1998). A description of the suberin model by Graça, (2015) also supports the polyphenolic and polyaliphatic domains of suberin having functional differences.

Several studies also provide evidence that changes in suberin deposition are associated with alterations in physiological parameters. North and Nobel (1994) reported a decrease in radial conductivity and root hydraulic conductivity primarily because of increased suberization of the periderm in tropical epiphytic cacti under drought stress. Similarly, an increase in root hydraulic conductivity in the Arabidopsis mutant *cyp86a1* is associated with reduced root suberin content relative to wild-type (Ranathunge and Schreiber, 2011). Perhaps the increase in root hydraulic conductivity is associated with increasesd uptake of water by root endodermis. Also, increased root suberin under high ammonium levels is associated with decreased solute permeability through roots (Ranathunge *et al*., 2015). Furthermore, an increase in root suberization in rice is correlated with a decrease in shoot Na^+ content under salt stress (Krishnamurthy *et al*., 2011). After 3-5 days of organic acid treatment, radial oxygen loss (ROL)

from apical regions of rice adventitious roots and from lateral roots of *Phragmites australis* (perennial grass) was reduced to very low values and associated with higher cell wall lignification as well as higher suberization in the root outer cell layers (Armstrong and Armstrong, 2001). Although the Casparian bands in Arabidopsis *esb1* loss-of-function mutants are deformed, the increased root suberin in the Arabidopsis *esb1* mutant is associated with increased water use efficiency (WUE) and reduced day time transpiration rates during vegetative growth (Baxter *et al*., 2009). Wetland plants form an outer apoplastic barrier containing suberin to limit diffusion of ROL under waterlogging conditions (Watanabe *et al*. 2013). Under stagnant deoxygenated conditions, suberin and esterified phenolics (coumaric and ferulic acid) are significantly increased in rice roots compared to non-hypoxic control conditions (Ranathunge *et al*., 2011). The species chosen in this study is *Arabidopsis thaliana*, which is a eudicot. However, most of the literature cited in this thesis providing evidence for the relationship between suberin and various stresses are monocots (e.g. rice and maize) and therefore those findings may not be applicable to eudicots. Nonetheless, an endodermis is present in young roots of both eudicots and monocots. A root periderm is formed in dicots after initiation of secondary growth, which resembles the exodermis formed in monocots and may have a similar function.

1.6 Rationale and objectives of the thesis

1.6.1 The roles of root suberin and associated waxes in protecting plants against drought and salt stresses (presented in Chapter 2)

Rapid human-caused climate change is becoming a great challenge for crop production world-wide. Drought and salinity are some of the leading environmental problems faced by farmers. Plant research, leading to the development of improved crop varieties, has become

important in addressing these challenges. As discussed in the previous section, besides its constitutive synthesis in certain tissues, the degree of suberization in cell walls can be modified by various environmental stresses. These changes suggest a physiological importance of suberin in plants for protection against unfavorable environmental stresses. To date, the precise roles and mechanisms of suberin and associated waxes for plant protection against drought and salinity are unknown.

In recent years, mutants of various genes of *Arabidopsis thaliana* have been identified that each harbour unique alterations in root suberin amount and/or composition. They provide a great resource to examine the mechanistic roles of suberin in protecting plants against various stresses. In the present study, suberin mutants of *Arabidopsis thaliana* with specific defects in suberin composition, in comparison to Columbia (Col-0) wild type as the genetically unaltered genotype, were analyzed. There have been no experimental data reported previously to show how whole plant physiology of Arabidopsis suberin mutants is affected by drought and salt stresses. Additionally, no physio-chemical data are available to provide insights for the possible mechanistic roles of suberin in drought and salt tolerance. I provide some insights into how different mutants are altered in their response to drought or salt stresses. The knowledge on physiological and morphological responses in plants in relation to different root suberin compositions, amounts, and their effects on water and solute transport will provide important information for the development of stress tolerant plants.

I present the following hypotheses:

Suberin polymer and its associated waxes play important roles in reducing:

1. Water loss through roots to the soil during severe drought stress.

2. Uncontrolled transport of Na into the vasculature under high salinity (NaCl) conditions.

My prediction is that different suberin mutants with deficient or altered monomer levels in their suberin composition would differ in their tolerance to drought or salinity in comparison to wild-type. These differences in stress tolerance should be detected by whole plant performance and physiological changes. Additionally, mutants are predicted to display compromised adaptive responses to these two stresses.

The following were the specific objectives to test these hypotheses:

a) Examine alterations in suberin deposition under chronic drought stress and under high salt conditions in wild-type and suberin-altered mutants
b) To investigate the physiological responses of wild-type and suberin mutants under chronic drought stress and salt stress conditions
c) To investigate the relationship between suberin lamellae structure and drought or salinity tolerance
d) To investigate the roles of individual suberin monomers in the protective functions of suberin

1.6.2 The roles of seed coat constituents in providing protection against chromium (Cr^{3+}) toxicity (presented in Chapter 3)

Heavy metal contamination is one of the major environmental issues in the mining industry. Extensive chromite ore deposits have been discovered in Northern Ontario (Ring of Fire region). Therefore, chromium mining may increase in this area in the future. Even though several mutants altered in the different chemical constituents of the seed coat in the model plant *Arabidopsis thaliana* have been characterized, the roles of these constituents in protecting

embryos against heavy metal stresses are poorly understood. This study represents the first step in understanding deleterious effects of chromium toxicity (Cr^{3+}) on Arabidopsis seed viability and germination. My specific focus was to investigate the role of seed coat suberin in protecting embryos from chromium toxicity in relation to other polymers present in the seed coat (mucilage, cutin, and proanthocyanidins). This study may provide insights into the protective functions of different seed coat chemical constituents against chromium toxicity. These findings may also help us to understand the reason for selective chromium toxicity in terms of seed germination among different plant species (Lukina *et al*., 2016).

Hypothesis

Suberin mutants deficient in seed coat suberin are permeable to tetrazolium (TZ) salt (Besson *et al*., 2007) . Therefore, I hypothesize that out of the four major polymeric constituents of Arabidopsis seed coat (mucilage, suberin, cutin, and proanthocyanidins), suberin functions as the main barrier against chromium uptake.

The prediction is that seeds of mutants with altered seed coat suberin contents would have reduced germination percentage when exposed to different chromium concentrations in comparison to wild-type and the other mutant classes.

The following were the specific objectives to test this hypothesis:

a) Investigate the specific constituents of seed coat that confer protection of embryos against high chromium (Cr^{3+}) levels.

b) Investigate the seed coat permeability characteristics of mutants that are altered in mucilage, suberin, cutin, or proanthocyanidins.

c) Investigate the corelationship between seed coat permeability to chromium (Cr^{3+}) and embryo damage.

d) Investigate the effect of chromium (Cr^{3+}) toxicity on seed dormancy.

Chapter 2: Suberin composition and lamellae structure play important roles in reducing water loss in mature roots and reducing sodium transport to shoots in *Arabidopsis thaliana*

2.1 Abstract

Suberin is a cell-wall-associated heteropolymer that is deposited in root endodermis and root periderm. Although links between suberin and drought and salt stress are known, the precise role of suberin and its associated waxes in protecting plants against these conditions is unclear. Using the model plant *Arabidopsis thaliana*, I tested the biochemical and physiological responses to drought in various mutants that are differentially affected in suberin composition and ultra-structure. Mutants tested were altered in suberin monomer biosynthesis (*cyp86a1-1 cyp86b1-1* and *far1-2 far4-1 far5-1*), transport (*abcg2-1 abcg6-1 abcg20-1*), or regulation (*myb92-1 myb93-1*). Drought increased suberin and suberin-associated waxes in wild-type, and also in suberin mutants but to varying degrees and with differences in the suberin chemical compositions. Suprisingly, compared to wild-type, mutants were not more susceptible to the chronic drought stress imposed in this study. However, the *cyp86a1-1 cyp86b1-1* mutant, which had severely altered suberin composition and structure, had an increased amount of water loss through the root periderm. *Cyp86a1-1 cyp86b1-1* acclimatized to drought stress more than wild-type, likely explaining the lack of drought susceptibility in terms of relative water content and biomass allocation to roots. The *abcg2-1 abcg6-1 abcg20-1* mutant was highly sensitive to NaCl treatment and caused mortality at 100 mM NaCl, suggesting a major role for suberin in salt tolerence. Under high salt conditions, compared to wild-type, suberin mutants with highly altered suberin composition and content had increased sodium accumulation and a reduced K/Na ratio in leaves. Altogether, these results provide evidence for the importance of chemical composition and lamellae structure for the suberin barrier function in reducing water loss and reducing uptake

of sodium, which allow for improved physiological performance of plants under drought and salt stress conditions.

2.2 Introduction

Over the last decade, due to limitations in crop productivity caused by climate change, drought and salinity have been the primary focus in crop improvement efforts (Cominelli *et al.,* 2013). Drought can be chronic in climatic regions with overall low water availability or random and unpredictable due to rapid changes in weather conditions (Pereira, 2016). Water deficiency in soil is often linked to high salinity, which is also symptomatic of general soil degradation. Salinity is commonly dominated by sodium chloride (NaCl) toxicity (Flowers and Colmer, 2008). Thus, an understanding of chronic drought stress and salinity in relation to plant growth is of great importance for sustainable agriculture.

Plants, being sessile, have evolved specific acclimation and adaptation mechanisms to respond to abiotic stresses. Analysis of these protective mechanisms will contribute to our knowledge of tolerance and resistance to stresses. Plants have various hydrophobic barriers that provide protection against adverse environmental conditions. Suberin is one such cell-wall-associated barrier located in various specialized tissues, such as root endodermis and periderm. Suberin consists of poly-aliphatic and poly-aromatic domains (Bernards, 2002). The polyaliphatic domain contains long-chain and very-long-chain fatty acids, ω-hydroxy fatty acids, α,ω-dicarboxylic acids, and primary alcohols, as well as glycerol and ferulic acid (Graça, 2015). The most abundant monomer groups are α,ω-dicarboxylic acids (DCAs) and ω-hydroxy fatty acids (OH-FAs), which represent 24% and 43% of the aliphatic monomer content, respectively, in Arabidopsis roots (Franke *et al*., 2005).

Root suberin deposition occurs during normal growth conditions, but is subject to changes through development. Hofer *et al*. (2008) provided evidence for increasing suberin amount from the tip to the base of the root in Arabidopsis, as well as variability in suberin composition along the root axis. Another study with Arabidopsis grown in tissue culture showed that the deposition of suberin in roots occurs mainly within the first 3 weeks. The composition of the suberized layers as well as the partition of acyl chains between the soluble and polymerized fractions remain about the same within the 4-week period (Delude *et al*., 2016). Although these studies examined suberin biosynthesis under non-stress conditions, regulation of suberin biosynthesis under stress conditions was not addressed.

There is evidence in various plants for changes in suberin biosynthesis in response to different environmental stresses. North and Nobel (1994) reported a decrease in root hydraulic conductivity caused by increased suberization in tropical epiphytic cacti roots under drought stress. Studies in rice (*Oriza sativa*) revealed induction of suberin biosynthesis under salt stress (Krishnamurthy *et al*., 2009) and oxygen deficiency (Kotula *et al*., 2009). Also, in rice, high ammonium levels increases root suberin content and decreases solute permeability in roots (Ranathunge *et al*., 2016). The opposite was observed for lower ammonium levels. Furthermore, an increase in root suberization in rice was correlated with a decrease in shoot Na content under salt stress (Krishnamurthy *et al*., 2011). Suberin biosynthesis is increased by salt treatment in *Avicennia officinalis* roots (Krishnamurthy *et al*., 2014), by waterlogged conditions in rice (Watanabe *et al*., 2013) and maize (Enstone and Peterson, 2005), and under soil nutrient deficiency in castor bean (Schreiber *et al*., 2005a) and Arabidopsis (Barberon *et al*., 2016). Franke *et al*. (2009) reported an increase in *DAISY/KCS2* mRNA levels under polyethylene glycol-induced osmotic stress and under high concentrations of NaCl in Arabidopsis.

Concomitantly, root suberin in 5-week-old plants were increased by 100 mM NaCl salt stress compared to unstressed plants. The mutant *esb1* has deformed Casparian bands and ectopic suberin deposition in roots. In *esb,* compared to wild-type, water use efficiency is improved and transpiration rate isreduced with the increase in root suberin content (Baxter *et al*., 2009).

Although the above described studies imply a relationship between suberization and physiological parameters that relate to water movement and solute uptake, there is a gap in our understanding of the role of suberin composition and ultrastructure in tolerance to drought and salinity. The knock-out mutation in *CYP86A1,* which encodes a fatty acid ω-hydroxylase involved in suberin monomer biosynthesis, results in higher root hydraulic conductivity than wild-type (Ranathunge and Schreiber, 2011). I therefore speculated that mutant Arabidopsis lines with more severe or different alterations in suberin would cause severe impacts on root water transport. The mutants chosen in this study were affected in suberin transport (*abcg2-1 abcg6-1 abcg20-1*), suberin biosynthesis (*far1-2 far4-1 far5-1* and *cyp86a1-1 cyp86b1-1*), or regulation of suberin deposition (*myb92-1 myb93-1*). Compared to wild-type, *abcg2-1 abcg6-1 abcg20-1* roots have distorted suberin lamellae structure and major reductions in alkylhydroxycinnmates of suberin associated waxes (Yadav *et al.,* 2014). However, the total suberin aliphatic monomer content of *abcg2-1 abcg6-1 abcg20-1* is 70% higher than wild-type in roots of 10-day-old seedlings and three times higher than wild-type in roots from 7-week-old plants. The mature root periderm of *abcg2-1 abcg6-1 abcg20-1* is reduced in 20:0 and 22:0 fatty acids and 22:0 fatty alcohol. Further, it has a 33% decrease in 18:1 ω-hydroxy fatty acid compared to wild-type (Yadav *et al*., 2014). Additionally, the root system of the *ABCG* triple mutant was previously reported to be more permeable to water and salts (Yadav *et al*., 2014). Mutations in *FAR1*, *FAR4* and *FAR5* cause reductions in 22:0-OH, 20:0-OH and 18:0-OH, respectively, and triple *far1 far4*

far5 knock-out mutants have a 70% overall reduction in primary alcohol content in the suberin polymer (all chain lengths affected) and a greater than 90% reduction in alkyhydroxycinnamates in the suberin associated waxes (Vishwanath *et al.,* 2013). Despite the changes in monomer composition, the total suberin content of *far1-2 far4-1 far5-1* is not less than wild-type. Two previously uncharacterized mutants, *cyp86a1-1 cyp86b1-1* and *myb92-1 myb93-1*, which each have reduced amounts of suberin content than wild-type were also tested here. Individual knock-out mutations in *CYP86A1* and *CYP86B1* result in strong reductions in C16 and C18 (Hofer *et al.,* 2008) and C22 and C24 (Compagnon *et al.,* 2009) chain-length OH-FAs and DCAs, respectively. I examined double *cyp86a1 cyp86b1* mutants because they are affected in all chain-lengths of OH-FAs and DCAs and thus are expected to have a major suberin perturbation of structure and function. I also examined the double *myb92-1 myb93-1* mutant because previous work in the Rowland lab revealed that *MYB92* and *MYB93* function in a partially redundant manner and in the double mutant all suberin monomers are reduced in comparison to wild-type (Murmu *et al.,* unpublished; Appendix III).

The findings presented here provide evidance for the importance of suberin content and structure to sustaning plant water balance and performance under drought and high salinity.

2.3 Materials and Methods

2.3.1 Plant growth conditions, drought and salt assays

Arabidopsis thaliana wild-type (WT) (Col-0 ecotype) and double and triple T-DNA insertion lines of suberin mutants were either generated by the authors or obtained from the Arabidopsis Biological Resource Center (ABRC). Homozygous T-DNA insertion lines were confirmed by PCR genotyping using primers listed in Appendix II. Seeds of WT and mutants were surface sterilized and stratified for 3 to 4 days at 4°C. Commercial play sand (pH 6.3; KING's brand, ON, Canada) was used as growth medium as it helps to easily control water content gravimetrically. The sand consisted of a low percentage of silt particles (5-10%) and a high percentage of sand particles (80-90%). Sand was completely dried in an oven at 100°C for 48h and passed through a 2 mm-sieve. Plastic cups of 250 ml were used with two holes (~ 1 cm^2 size) on the bottom lined with a piece of fabric to avoid sand particles passing through the holes. Fifty ml of 20-20-20 NPK fertilizer (1 g/L) (Plant-Prod, Brampton, ON) was added to each pot. The amount of water need to be added for 20% (V/V) was calculated based on the volume of the cup. All pots were kept at 20% (V/V) water content in a controlled growth chamber at 21-22°C, 40-60% humidity, under long-day conditions (16 h light/8 h dark cycle). Two to three seeds were sown initially and kept covered with transparent plastic domes for one week and thinned out to one seedling after 1 week. The water content was maintained by daily monitoring the weights of pots and adding the required amount of water. To induce the drought stress, watering was withdrawn in 2/3 of the plants on the 10^{th} day after sowing. Three days after water withdrawal, the soil moisture level reached 5% (V/V) and was maintained at that level throughout the experiment for the drought-stressed plants. To analyse regulation of suberin production under re-watering condition, two weeks after drought stress was introduced, half of the plants under

drought stress were watered again to reach 20% (V/V). For the salt stress assay, another set of plants were maintained at 20% water. To induce the salt stress, 0.1 g of NaCl was added on each of three consecutive days starting on the 10th day after sowing. The salt concentration in the soil reached 100 mM on the 14th day (2 weeks after sowing).

2.3.2 Plant trait measurements

At the required time, the root system was carefully harvested by rinsing off the sand and gently drying with paper wipes. Plant tissues were dried in an oven for 48 h at 80°C. The shoot dry mass includes all plant parts above ground (flowering stalk, leaves on the flowering stalk, and rosette leaves). The root biomass included the entire intact root system. A separate set of fresh root tissues from each genotype and treatment was processed for suberin analysis. At 4 weeks of age, a fully developed young leaf from each plant was collected from drought-stressed and control treatment to determine the leaf relative water content (RWC). The leaves were stored in a re-sealable plastic zipper bag, and the fresh masses (FM) were determined immediately. These leaves were then hydrated overnight according to the protocol described in Ryser *et al.,* (2008) by placing them between moist paper towels for 24h, after which the saturated mass of the fully turgid leaves (SM) was measured. Leaves were then dried for 48 h at 80°C, and their dry mass (DM) was recorded. The relative water content was calculated as the ratio (FM–DM)/(SM–DM) (Turner, 1981).

2.3.3 Root wax extraction

Five-week old wild-type tap roots were used in this study because it has been found that suberin associated wax deposition mostly takes place after 4 weeks age (Kosma *et al.,* 2015). Three individual plants were pooled for a single replicate under control condition and for drought condition (3 weeks of drought stress). Root fresh weights were recorded and dipped in chloroform for 1 min. The solution contained 5 µg each of *n*-tetracosane (24:0 alkane), 1-pentadecanol (15:0-OH), heptadecanoic acid (17:0), and tridecyl (13:0)-ferulate, which served as internal standards. Extracts were evaporated under nitrogen and derivatized with 100 µl of *N,O-bis*-(trimethylsilyl)-trifluoroacetamide (BSTFA) plus 100 µl of pyridine at 110^{o}C. The derivatized samples were allowed to cool down and the solvent evaporated under nitrogen. The samples were re-suspended in heptane:toluene (1:1 v/v) for analysis by gas chromatography (GC).

2.3.4 Root suberin analysis

Roots were immersed in 4 ml hot isopropanol and incubated for 30 min at 85^{o}C. Then samples were delipidated for 24 h each with chloroform: methanol (2:1, v/v), chloroform: methanol (1:1, v/v), chloroform: methanol (1:2, v/v), and 100% methanol as described in Vishwanath *et al.* (2013). Sodium methoxide catalyzed depolymerization and GC-mass spectrometry (MS) or GC-flame ionization detector (FID) analyses were performed following the protocol detailed in Molina *et al.* (2006). The solvent extracted dried residues were weighed and 20 µg each of 17:0 methyl ester (ME) and ω-pentadecanolactone (OPL) were added as internal standards. Samples were depolymerized by transmethylation at 60^{o}C for 2 h using 0.9 ml

methanol, 0.225 ml methyl acetate, 0.375 ml sodium methoxide for each sample. After cooling down to room temperature, the mixture was acidified with 1 ml of glacial acetic acid to pH 4-5. Then, 2.5 ml of dichloromethane was added to extract fatty acid methyl esters followed by 2 ml of 0.5 M NaCl to separate phases. After centrifugation for 5 min at 2000 rpm, the organic phase was transferred to a clean tube, washed two times with 2 ml of 0.5 M NaCl, and then about 0.5 volume of anhydrous sodium sulfate was added to remove residual water. The organic phase was transferred to a clean tube again and the solvent evaporated to dryness under nitrogen. To obtain the acetyl derivatives, the residues were dissolved in 100 µl pyridine plus 100 µL acetic anhydride and incubated 1 h at 60^{o}C. The reagents were then evaporated under nitrogen gas, and the dry samples were dissolved in 100 µl hexane for GC analysis.

2.3.5 Gas chromatography

Polymeric fractions and suberin-associated waxes were quantified with a Varian-3900 gas chromatograph equipped with a flame ionization detector (GC-FID) and a HP-5MS capillary column (30 m length, 0.25 mm inner diameter, 0.25 µm film thickness). A 1 µl aliquot of the sample was injected in splitless mode, and high purity helium was used as the carrier gas at a flow rate of 1.5 ml per min. For suberin analysis, the temperature of the injector was at 250°C, and the column oven temperature was held at 50°C for 1 min and then increased from 50°C to 200°C at a rate of 25°C per min, followed by a 1 min hold, and then it was ramped up again at the rate of 10°C per min to a final temperature of 320°C, which was held for 8 min. The detector was at 350°C. Quantification of monomers was based on peak areas in the GC-FID chromatograms, identified using their retention time, and using the peak area of the respective internal standard. The identities of the peaks were verified by GC mass spectrometry. For root

waxes, temperature settings were as follows: inlet 350°C, detector 320°C, oven temperature program was set to 130°C for 2 min and increased to 325°C at a rate of 5°C per min, and held at 325°C for 17 min.

2.3.6 Tissue elemental analysis

Leaf tissue samples were oven dried at 85°C for 48 h in 7 ml perfluoroalkoxy (PFA) vials until the sample weight reached a constant weight such that the samples were completely dehydrated. Dried leaves were homogenized by gently crushing into a fine powder with an agate mortar and pestle. Approximately, 10 mg sample was weighed into a PFA vial, lightly closed and digested with 0.5 ml 15 M HNO_3 on a hotplate at 110°C for 8 h. The solution was diluted gravimetrically to 10 g and measured by microwave plasma spectrometry (MP-MS) (Agilent 4200 MPES) and inductively coupled plasma mass spectrometry (ICP-MS) (Agilent 8800QQQ Triple Quadrupole ICP-MS). The elements Ca, K, Mg and Na were measured by MP-ES, and the elements Li, B, Al, Si, Cr, Mn, Fe, Co, Ni, Cu, Zn, As, Se, Mo, and Cd were measured by ICP-MS. Reproducibility due to sample heterogeneity and measurement uncertainty was evaluated using 10 mg replicate portions corresponding to the same homogenized plant specimen.

2.3.7 Measurement of root periderm segments for water loss

The method described in Bu *et al*., (2014) was used to measure water loss. A ~1 cm tap root segment at the base of the root system was excised from individual 4-week-old plants (2 weeks after drought stress for drought treatment samples). A thin layer of Paraplast wax was applied to the cut surfaces, and the weight was recorded immediately. The root segments were

then placed on a bench and weights were recorded at 15 min intervals. The loss of fresh mass was calculated as percentage of the initial mass.

2.3.8 Transmission electron microscopy

Microwave processing of the samples was adapted from Levesque-Lemay *et al*. (2016) and Russin and Trivett (2001). Samples were processed using a Pelco Biowave 34700 microwave (TedPella, Redding, CA, USA). All microwave steps were performed under vacuum (> 20 mm Hg), except dehydration and polymerization. Tap roots from 4-week-old Arabidopsis wild-type and mutant plants grown in 20% moisture (control) or 5% moisture (drought) levels were submerged in 0.1 M Na cacodylate buffer (pH 7.2) in petri dishes and cut into ~1 mm pieces using a clean, sharp razor blade. The samples were transferred to 1.5 ml centrifuge tubes containing 600 µl of 2.4% glutaraldehyde and 2.0 % paraformaldehyde in 0.1 M sodium cacodylate buffer (pH 7.2), de-gassed under vacuum (> 20 mm Hg) for 20 min, and then put in the microwave, held under vacuum for 1 min, microwaved at 250 W with a 37°C restrictive temp for 40 s at 100% power, held under vacuum for another 3 min and then removed from the microwave. The samples were rinsed with sodium cacodylate buffer and then washed twice in the same buffer in the microwave under vacuum (> 20 mm Hg) at 450 W at ≤ 40°C, then held under vacuum for 1 min and 40 s at 100% power. The samples were post-fixed in 1% OsO_4 in 0.1 M sodium cacodylate buffer in the microwave under vacuum (> 20 mm Hg) at 450 W at ≤ 37°C, then held under vacuum for 1 min, 40s at 100% power, and 3 min under vacuum. Samples were rinsed with water and then washed in the microwave under vacuum (> 20 mm Hg) at 250 W at ≤ 40°C for 1 min under vacuum and 40 s at 100% power. Samples were then dehydrated via an ethanol series of 30, 50, 70, 80, 90, 95%, and twice with 100%, followed by two times in

acetone. At each dehydration step, the samples were microwaved at 250 W at ≤ 37°C for 40 s at 100% power. Infiltration was performed three times in Spurr's low viscosity resin (Electron Microscopy Sciences, Hatfield, PA, USA) in the microwave at 450 W at ≤ 43°C for 2 min at 100% power. Samples were polymerized in capsules in the microwave at 750 W at ≤ 60°C for 19 min at 100% power, at ≤ 70°C for 12 min at 100% power, at ≤ 80°C for 12 min at 100% power, and at ≤100°C for 45 min at 100% power. Embedded tissues were sectioned at 100 nm thickness using a diamond knife and a Reichert Ultracut E ultramicrotome (Leica Microsystems, Vienna, Austria) and collected onto copper grids that were coated with formvar and carbon (Electron Microscopy Sciences, Hatfield, PA, USA). Grids were treated with 10% hydrogen peroxide for 10 min and stained with 10% uranyl acetate in methanol for 8 min, and Reynold's lead citrate for 10 min (Molina *et al*., 2009). The samples were analyzed with a Hitachi H-7000 TEM (Hitachi, Tokyo, Japan) equipped with an ORIUS SC200 digital camera using Digital Micrograph software version 1.8.3 (Gatan Inc., Pleasanton, CA, USA). Images were processed with Adobe Photoshop CS6.

2.3.9 Statistical analysis

Statistical analyses were performed using SYSTAT 13 (Systat Software Inc., Chicago, IL, USA). Prior to analyses, log transformation of data was done, if necessary, to attain normal distribution. To evaluate if drought and salinity had any effect on measured traits, ANOVA tests were performed. Kruskal-Wallis test was conducted when assumptions of normality were not met. Tukey multiple comparisons were performed when there was a significant genotypic and treatment interaction and comparisons were made for each treatment separately.

2.4 Results

2.4.1 Suberin and suberin-associated wax deposition are altered by water availability

To better understand how suberin biosynthesis is regulated under normal growth conditions, I analyzed root suberin production in WT (Col-0) over a time-course. There was an increase in total suberin content from 4 to 6 weeks. Suberin production reached a plateau at 6 weeks (Figure 2-1a). The highest increase in the rate of suberin production was observed between weeks 4 and 5, when it nearly doubled in one week (Figure 2-1a). This coincided with increases in the most abundant suberin monomers, α,ω-dicarboxylic acids and ω-hydroxy fatty acids (Figure 2-1b). With a few exceptions, all suberin monomers increased in a similar proportion over time (Figure 2-1b-d), comparable to the trend observed for total suberin content (Figure 2-1a). During the 4-7 week time course, ferulate and 16:0 FA reached the highest level of suberin at at 5 weeks of age and all other aliphatic monomers at 6 weeks of age (Figure 2-1d).

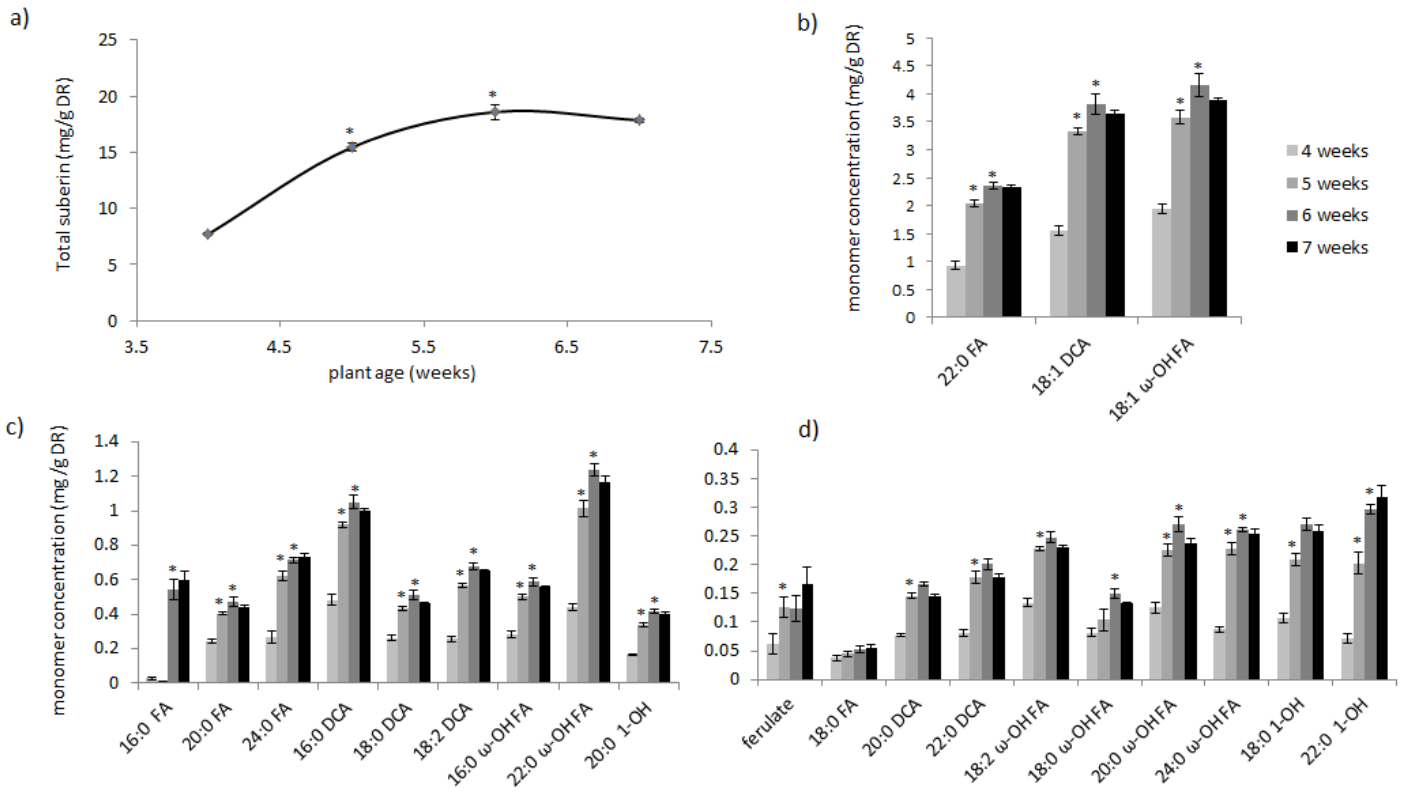

Figure 2-1. Time course analysis of Arabidopsis root suberin through development.

a) Total suberin content, b) most abundant suberin monomers, c) moderately abundant suberin monomers, and d) least abundant suberin monomers in roots of wild-type (Col-0) plants at different ages (4 -7 weeks) grown at a constant, non-stress (20% water level). Data points are mean values in milligrams per gram of delipidated dry residue (DR) from five replicate samples ± SE. Each replicate represented a pool of 4-5 plants. FA, fatty acid; DCA, dicarboxylic acid; ω-OH FA, omega hydroxy fatty acid; 1-OH, primary alcohol. Asterisks indicate significance at $p<0.05$ by student's t-test comparing the suberin content of previous week.

Drought as a stress in the field is subject to a combination of stresses, such as excess heat and low nutrient availability (Pereira, 2016). Implementation of an acute drought stress is the most commonly used method in investigating drought stress responses. However, such studies

have limited relevance on the development of drought-resistant crops (Blum, 2014). Therefore, a chronic drought assay was implemented in this study. A time-course comparison of suberin production was performed in WT under normal water levels, drought stress, and re-watering after drought stress. After 2, 3 and 4 weeks of drought stress, leaf biomass was lower compared to plants at the same age under control conditions ($p<0.05$ by student t-test; Figure 2-2a). Total suberin content in plants subjected to 2 or 3 weeks of drought stress was 41% and 22% higher compared to the same aged plants under control conditions, respectively (Figure 2-2b). During the time course of 4-7 weeks, plants under drought stress reached the highest suberin content after 3 weeks of drought (Figure 2-2b), while plants at control conditions reached the highest suberin content at 6 weeks (representing '4 weeks after drought' in Figure 2-2b). These results indicate an induction or an acceleration of suberin production by drought stress. However, total suberin content at full maturity (6 weeks age) was similar in both control and drought-stressed plants. Re-watered plants re-gained biomass to the same amount as the control plants after two weeks of re-watering (Figure 2-2a). There was no net gain in total suberin content during re-watering, indicating reduced suberin production upon cessation of the water deficit (Figure 2-2b). These results provide evidence for the controlled regulation of suberin biosynthesis under different water levels.

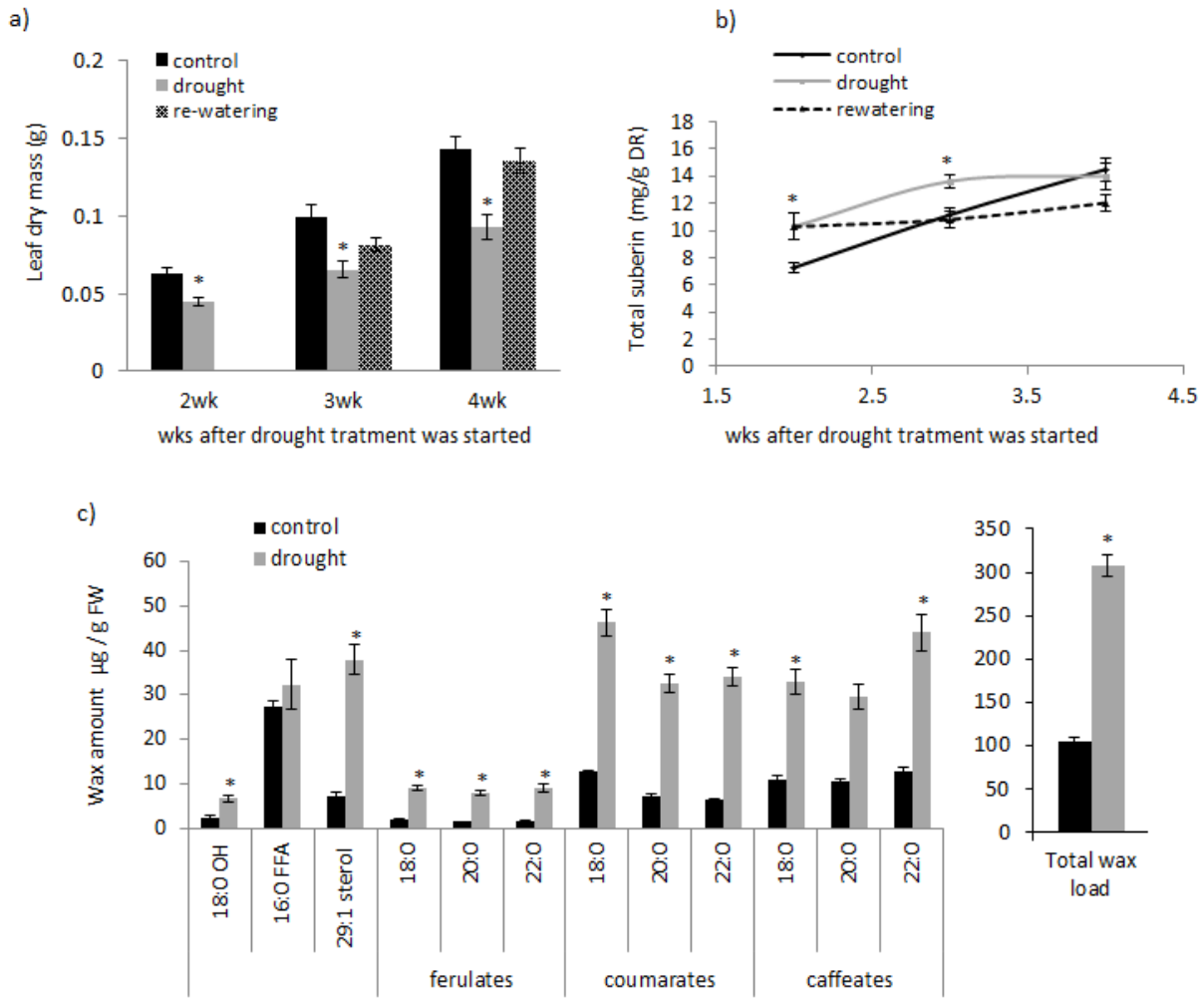

Figure 2-2. Comparison of leaf dry biomass, root suberin content and root wax amount in wild-type (Col-0) plants. a) Leaf biomass, b) total root suberin content at different time points under control, drought and re-watering condition and c) chloroform extractable surface wax amount from 3 weeks stressed, 5-week old tap root surfaces. The drought treatment was at 5% (v/v) water level). In a) and b), plants were subjected to re-watering (20% water level) after two weeks of drought treatment (e.g. 3 weeks = 2 weeks drought + 1 week re-watering and 4 weeks = 2 weeks drought + 2 weeks re-watering). Data points shown are mean values in grams for leaf dry mass from 10 replicate plants, milligrams of total suberin per gram of delipidated dry residue

from five replicate samples (a replicate consisted of a pool of 4 plants), micrograms of total wax amount per gram of fresh weight from 4-5 replicate samples (a replicate consisted of 10 tap roots) ± SE. Asterisks indicate $p<0.05$ by student's t-test comparing the values of the control and treatment. FFA= Free fatty acid.

I also analyzed induction of solvent-extractable surface waxes in 5-week-old WT taproots after 3 weeks of drought stress. Compared to the control plants, drought increased the total surface wax load by a factor of three, indicating induction of surface waxes by drought stress (Figure 2-2c). All AHCs increased about proportionally and also the 29:1 sterol.

2.4.2 *Cyp86a1-1 cyp86b1-1* and *myb92-1 myb93-1* mutants have reduced total suberin content, but only *cyp86a1-1 cyp86b1-1* has altered lamellae structure

Although *MYB92* and *MYB93* were identified previously as lateral root regulators (Gibbs *et al*., 2014), the root suberin composition was not analysed. Detailed suberin composition analysis was carried out in the *cyp86a1-1 cyp86b1-1* and *myb92-1 myb93-1* double mutants. Compared to wild-type, *cyp86a1-1 cyp86b1-1* had a 60% reduction in total suberin content (Figure 2-3). The decrease was associated with significant reductions in ferulate, 22:0 FA, and all chain lengths of DCAs and OH-FAs. Compared to wild-type, the *myb92-1 myb93-1* had a 33% reduction in total suberin content. In *myb92-1 myb93-1*, the monomers with significant reductions were 20:0 and 22:0 FAs, 16:0, 18:1, 18:0 and 24:0 DCAs, and 16:0, 18:2, 18:1, 18:0 and 20:0 OH-FAs (Figure 2-3).

I then compared the suberin composition in WT, *cyp86a1-1 cyp86b1-1* and *myb92-1 myb93-1* with their root periderm suberin lamellae ultrastructure under control conditions using

transmission electron microscopy (TEM). In contrast to the suberin lamellae of WT root periderm, *cyp86a1-1 cyp86b1-1* did not contain the light and dark banding pattern (Figure 2-5d). However, the lamellae structure in *myb92-1 myb93-1* was not different than that of WT (Figure 2-5f), despite the 33% reduction in total suberin content. *Myb92-1 myb93-1* had more DCA and omega-hydroxy FA content than that of *cyp86a1-1 cyp86b1-1* (Figure 2-3). Therefore, the results suggest that the DCA and omega-hydroxy FA composition play an important role in the formation of suberin ultra-structure.

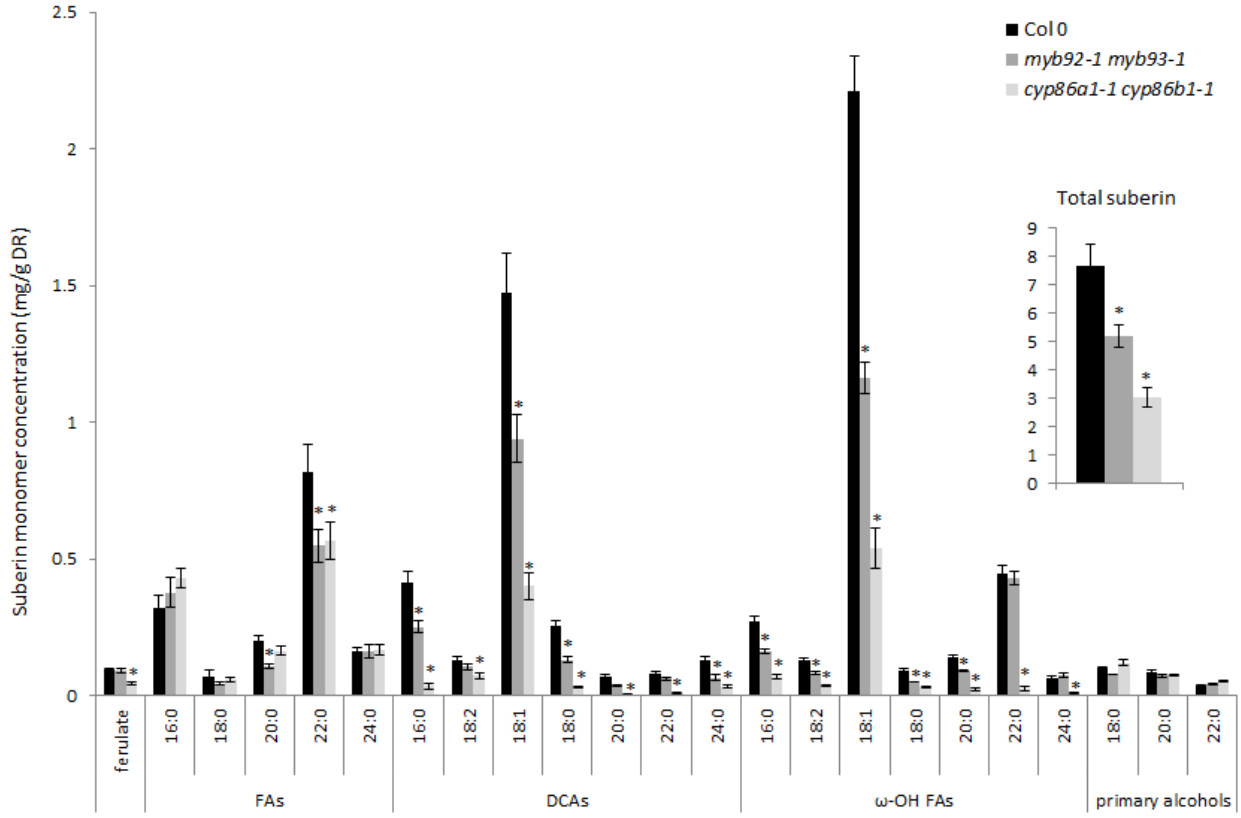

Figure 2-3. Comparison of root suberin monomer composition between wild-type (Col-0) and mutants *myb92-1 myb93-1* and *cyp86a1-1 cyp86b1-1*. Mean values are shown in milligrams of suberin per gram of delipidated dry residue (DR) from 3-4 replicate samples ± SE. A replicate consisted of a pool of 4 plants. Inset represents the total suberin content for the three genotypes.

Asterisks indicate significant differences compared to WT by Student's t-test at $p<0.05$. FA: Fatty acids; DCA: Dicarboxylic acids; ω-OH: Omega hydroxy fatty acids.

2.4.3 Drought stress did not affect the mutants more than wild-type

To test whether the mutants are more susceptible to drought stress than wild-type, I investigated biomass of plant tissues and biomass allocation patterns in roots and shoots and relative water content in leaves. The chronic drought stress imposed here had a negative effect on growth of all genotypes, including wild-type (Table 2-1 and Figure 2-4). Drought reduced the total biomass in all genotypes (Figure 2-4a). Based on the ANOVA tests, this effect varied among the genotypes (Table 2-1). Wilting symptoms were not displayed in any of the mutants, suggesting that none of the mutants were affected by the drought stress more than wild-type. *Abcg2-1 abcg6-1 abcg20-1* had the lowest total biomass under control conditions, but recorded only a very small percent reduction in total biomass by drought stress (Figure 2-4a). Under drought stress, total biomass in *abcg2-1 abcg6-1 abcg20-1* was not different to WT (Figure 2-4a). The drought effect on root dry mass varied among genotypes (Table 2-1 and Figure 2-4b). Relative to control, drought treatment did not reduce root dry mass in *cyp86a1-1 cyp86b1-1* (Figure 2-4b). Despite the altered root suberin composition in *cyp86a1-1 cyp86b1-1* and *abcg2-1 abcg6-1 abcg20-1* (Figure 2-3, Yadav *et al.,* 2014), mutant roots were able to acclimatize to the drought stress. Even though the drought stress imposed here did not affect these mutants more so than WT, I investigated if there was nonetheless a relationship between drought tolerance and suberin depending on alterations in monomer composition and lamellae structure, as there seemed to be variation among genotypes. The relative water content (RWC) is a measure of the water content in leaves relative to its saturated state. Compared to control condition, drought

significantly reduced RWC in all genotypes except for *cyp86a1-1 cyp86b1-1* (Figure 2-4c). Under control conditions, *cyp86a1-1 cyp86b1-1* had the lowest average RWC, indicating that *cyp86a1-1 cyp86b1-1* was the most stressed genotype in terms of water content in leaves, even under control condition. Also, RWC in *cyp86a1-1 cyp86b1-1* did not respond to further limitations in water availability (Figure 2-4c). Root mass ratio (RMR) represents the ratio between root dry mass and total dry mass. All genotypes increased the biomass allocation to roots in response to drought (Figure 2-4d). However, the drought effect on the RMR was not variable among genotypes (Table 2-1). With the strong response in biomass allocation to roots, *cyp86a1-1 cyp86b1-1* was still able to acclimatize to drought stress.

Table 2-1. ANOVA test results of the drought stress experiment.

The measured and calculated traits, total dry mass (TDM), root dry mass (RDM), root mass ratio (RMR), relative water content (RWC) and suberin content (S) were considered as the dependent variables, and genotypes (WT and mutants) and the two levels of water treatment (control and drought stress) as independent variables. ***$p < 0.001$; **$p < 0.01$; *$p < 0.05$.

Trait	R^2	*n*	F-ratio		
			Genotype	Water Treatment	Genotype X Treatment
TDM	0.81	97	41.1^{***}	202.8^{***}	4.3^{**}
RDM	0.66	97	31.3^{***}	25.9^{***}	5.4^{***}
RMR	0.40	97	3.3^{*}	41.4^{***}	0.9
Leaf RWC	0.39	93	1.9	36.1^{***}	2.7^{*}
Root S	0.92	45	61.8^{***}	86.2^{***}	3.9^{**}

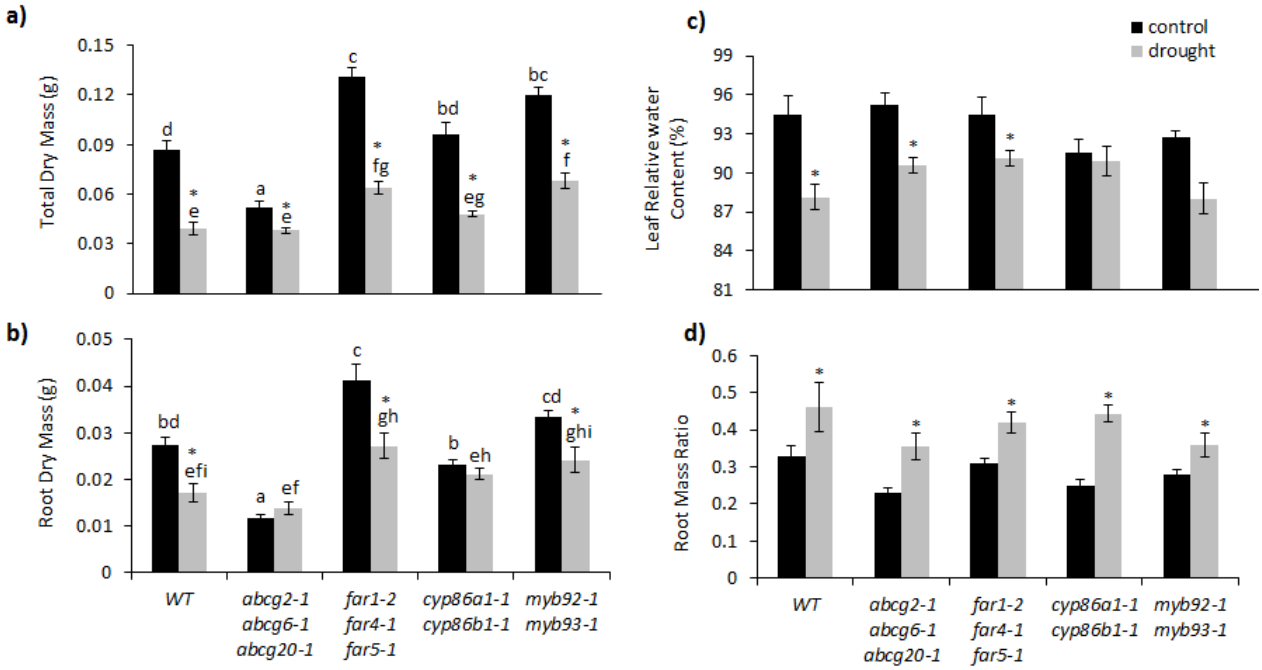

Figure 2-4. Comparison of drought stress responses between wild-type and mutants. a) Total biomass (above ground plant parts and roots); b) Root dry mass; c) Leaf relative water content of a representative leaf of an individual plant; d) Root mass ratio (ratio between root dry mass and total dry mass). Mean values are from ten replicate samples ± SE. Each replicate represents tissues from a single plant. Post-hoc Turkey test was carried out when ANOVA results indicated a significant difference in genotype and treatment interaction. Significant differences are indicated in letters by Tukey test at $p<0.05$ comparing genotypes at control (a,b,c,d) and drought stress (e,f,g,h,i) conditions. Comparisons in a) and b) were done separately for control and drought treatments; in b) asterisks indicate significant differences by student's t-test at $p<0.05$ comparing control and treatment. RWC data revealed that, relative to WT, mutants were not different when Tukey test was performed separately under control and drought condition. Hence, only the results from student's t-test are included for RWC.

2.4.4 Drought increases suberin in wild-type and the suberin mutants tested, but does not alter the lamellae structure

I next examined whether there were changes in suberin structure under control and drought stress conditions. Drought increased total root suberin content in all genotypes (Table 2-1 and Figure 2-5a). Despite the variability in abundance of different monomer groups, the effect of drought stress in each monomer group in all genotypes was shown to be similar except for some low abundance monomers (Figure 2-6). Compared to the control condition, there was a 89% increase in total suberin content in WT by drought stress (Figure 2-5a) with increases in all monomer groups (Figure 2-6). Drought doubled the amount of suberin in *myb92-1 myb93-1* (Figure 2-5a). The FAs, DCAs and OH-FAs in *myb92-1 myb93-1-1* were increased by drought (Figure 2-6d). Relative to control plants, *cyp86a1-1 cyp86b1-1* recorded a 42% increase in total suberin content despite no changes in OH-FAs. However, there were small increases in FAs and DCAs in *cyp86a1-1 cyp86b1-1* due to drought stress (Figure 2-6c). Under drought stress, lamellae structure was disrupted in *cyp86a1-1 cyp86b1-1,* but no different than that under control conditions (Figure 2-5e). Further, the lamellae structure in *myb92-1 myb93-1* drought condition was similar to the control condition (Figure 2-5g). Drought stress caused an increase in total suberin content in *abcg2-1 abcg6-1 abcg20-1* and *far1-2 far4-1 far5-1* (Figure 2-5a). My results demonstrate that even though drought increased the total suberin content in both *cyp86a1-1 cyp86b1-1* and *myb92-1 myb93-1*, there were no changes in the lamellae structure. Transmission electron microscopic studies on *abcg2-1 abcg6-1 abcg20-1* and *far1-2 far4-1 far5-1* previously showed that there is no alteration in the lamellae structure of *far1-2 far4-1 far5-1* (Delude *et al.*,2016), but lamallae is disrupted in *abcg2-1 abcg6-1 abcg20-1* (Yadev *et al.,* 2014).

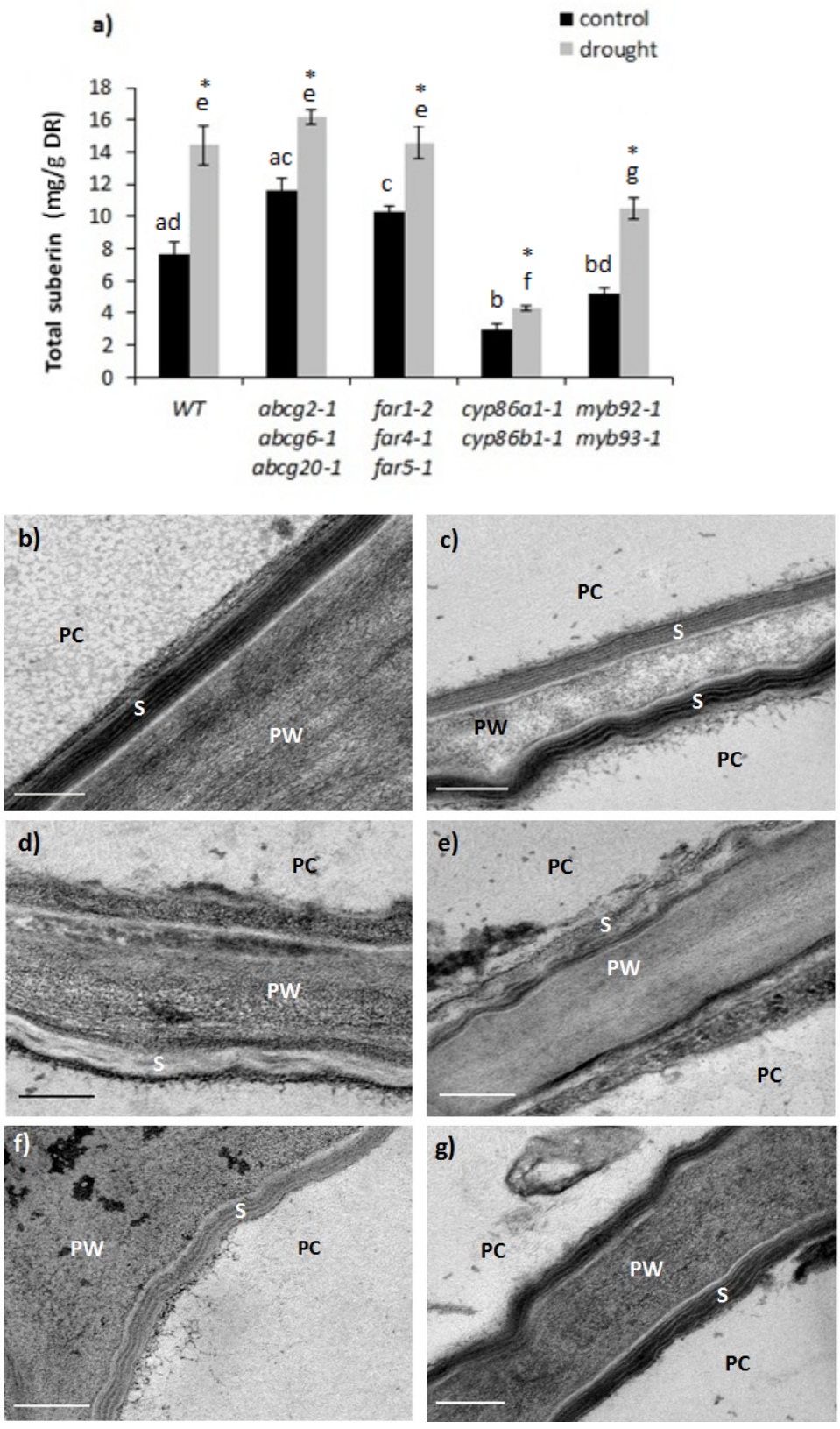
a)
control
drought
Total suberin (mg/g DR)
0
2
4
6
8
10
12
14
16
18
ad
ac
c
b
bd
e
f
g
WT
abcg2-1
abcg6-1
abcg20-1
far1-2
far4-1
far5-1
cyp86a1-1
cyp86b1-1
myb92-1
myb93-1
b)
c)
d)
e)
f)
g)
PC
S
PW

Figure 2-5. Total suberin content and TEM images of *A. thaliana* root sections of wild-type and mutants showing suberin lamellae in the periderm under control and drought stress. a) Total suberin content. Mean values of suberin conents are given in milligrams of suberin per gram of delipidated dry residue (DR) from 3-4 replicate samples ± SE. Each replicate consisted of four roots at 4 weeks old. Comparisons in a) were done separately for control and drought treatments. Significant differences among genotypes are indicated in letters by Tukey test at $p<0.05$ comparing genotypes at control (a,b,c,d) and drought stress (e,f,g) conditions. Asterisks indicate significant differences by student's t-test at $p<0.05$ comparing control and treatment. b) wild-type, control; c) wild-type, drought; d) *cyp86a1-1 cyp86b1-1,* control; e) *cyp86a1-1 cyp86b1-1*, drought; f) *myb92-1 myb93-1*, control; g) *myb92-1 myb93-1,* drought. Sections were taken from tap root periderm tissue of 4week-old wild-type, *cyp86a1-1 cyp86b1-1* and *myb92-1 myb93-1* plants grown under control and drought stress conditions. Suberin lamellae (S), primary cell wall (PW), periderm cell (PC). Scale bar = 200 nm.

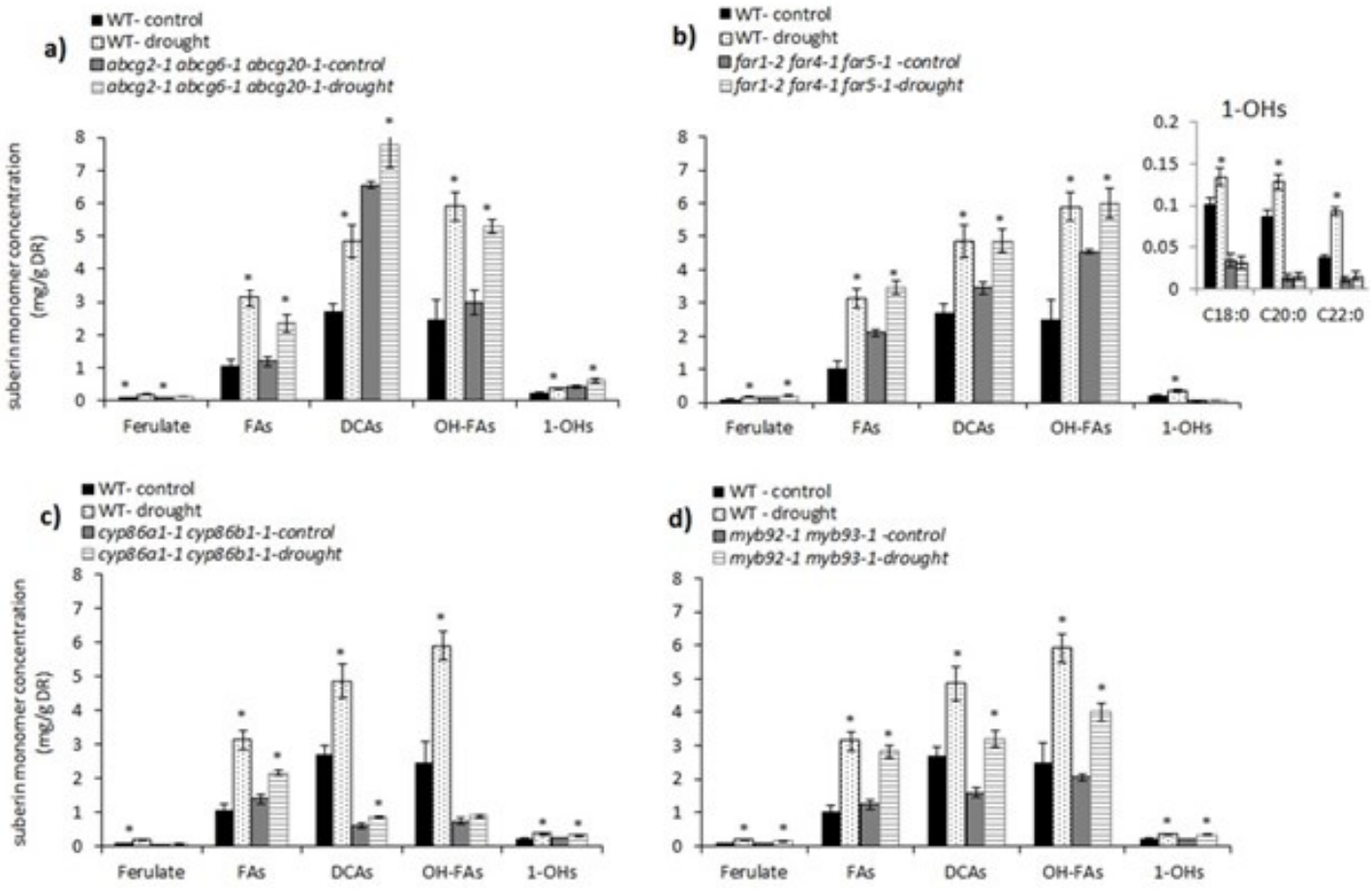

Figure 2-6. Suberin monomer composition under control and drought stress in wild-type and suberin mutants. a) *abcg2-1 abcg6-1 abcg20-1*, b) far1-2 far4-1 far5-1 (inset shows changes in fatty alcohol composition), c) *cyp86a1-1 cyp86b1-1,* and d) *myb92-1 myb93-1.* Mean values are shown in milligrams of suberin monomers per gram of delipidated dry residue (DR) from 3-4 replicate samples ± SE. Each replicate represents four intact roots at 4 weeks old. FAs: fatty acids, DCAs: dicarboxylic acids; OH-FA: hydroxy fatty acids; 1-OH: primary alcohols. Asterisk indicates $p<0.05$ by student's t-test comparing control and drought stressed plants.

2.4.5 Suberin deficiency and deformed ultra-structure increased water loss in root periderm

The mutant c*yp86a1-1 cyp86b1-1* recorded the lowest RWC, indicating it was the most stressed mutant of all the genotypes tested here. This prompted me to examine whether it experienced a more severe stress than other genotypes, as it had reduced suberin content and altered monomer composition as well as deformed lamellae structure. Therefore, I analysed the the amount of water loss in mature root periderm segments of c*yp86a1-1 cyp86b1-1* and compared them with WT. At 45 min, drought-stressed periderm segments of WT and *cyp86a1-1 cyp86b1-1* had lost a higher amount of water than their corresponding control plants (Figure 2-7). Relative to drought-stressed WT roots, drought-stressed c*yp86a1-1 cyp86b1-1* roots recorded an increased amount of water loss at 45 min and 75 min ($p<0.01$ by student's t-test). To confirm the relationship between suberin and water loss in roots, I analysed the amount of water loss in periderm segments of two additional mutants, *gpat5-1* and *esb1-2,* which have lower and higher amounts of suberin than WT, respectively (Beisson *et al.,* 2007; Baxter *et al.,* 2009). Water loss through the *esb1-2* root periderm was less than that of wild-type (Figure 2-8a) at 75 min. The RWC in *esb1-2* was greater than WT, which was not changed by the drought stress (Figure 2-8b). In a preliminary investigation involving a comparison of suberin content in WT, *gpat5-1* and *esb1-2* under control conditions, it was found that e*sb1-2* had 30% more suberin than WT (Figure 2-8c). When analysed for the amount of water loss under control conditions, *gpat5-1* was similar to c*yp86a1-1 cyp86b1-1* after 40 min. (Figure 2-8a).

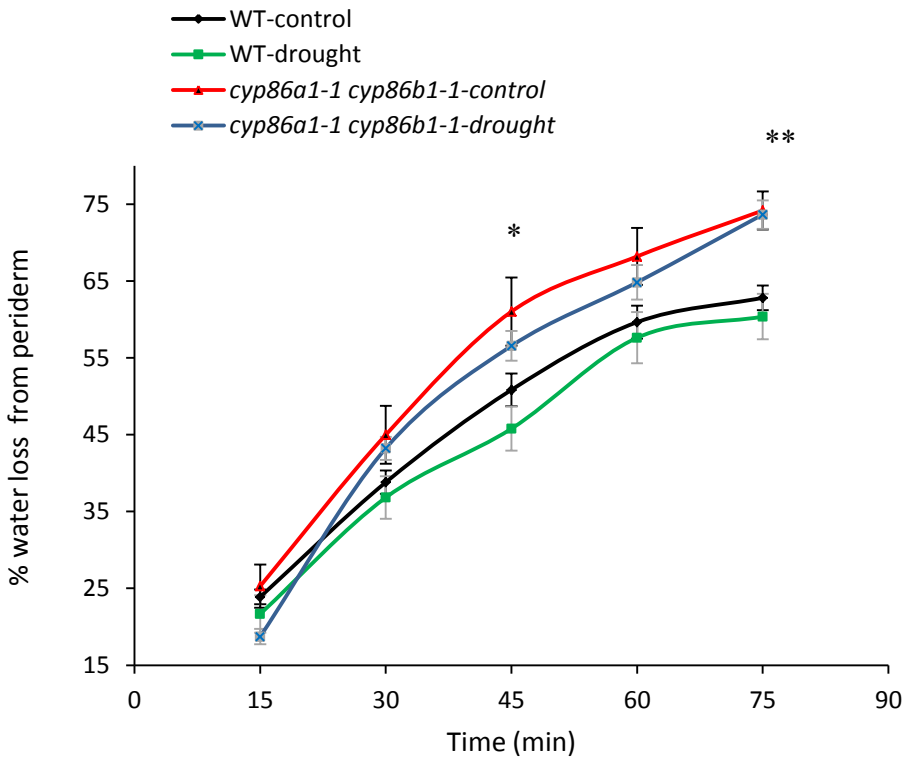

Figure 2-7. Comparison of amount of water loss in wild-type and *cyp86a1-1 cyp86b1-1* root periderm segments. From each genotype, weights were taken from a pool of three periderm segments with the same developmental stage at 15 min time intervals and the percent of water loss relative to the initial weight was recorded. Values are mean ± SD of five replicate samples. Significant differences between wild-type-drought and *cyp86a1-1 cyp86b1-1*-drought conditions are shown by asterisks (* $p<0.05$ and ** $p<0.01$ calculated by student's t test).

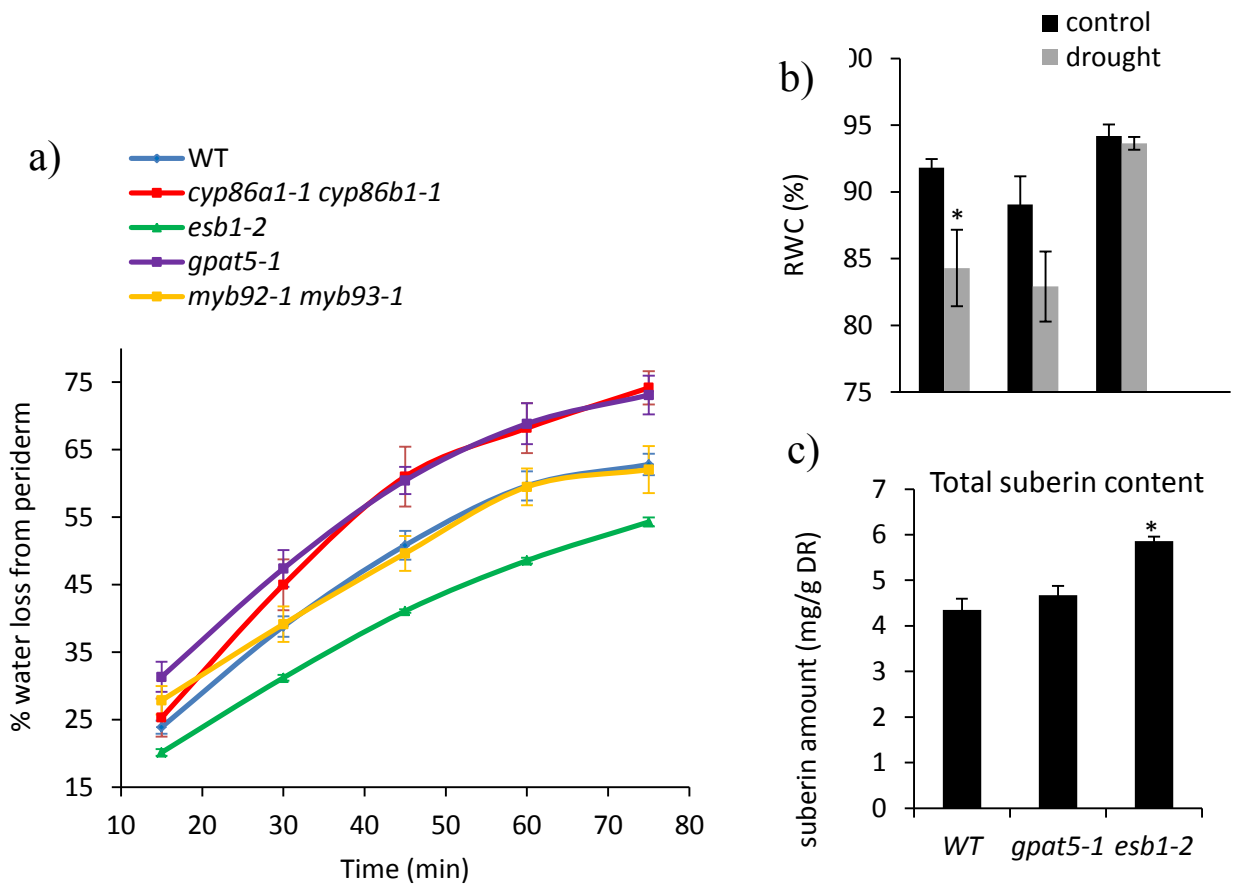

Figure 2-8. Comparison of the amount of water loss, leaf relative water content (RWC) and total suberin content in wild-type and mutants. a) Amount of water loss in WT, *cyp86a1-1 cyp86b1-1, esb1-2*, *gpat5-1* and *myb92-1 myb93-1* root periderm segments (n=5, with each replicate representing 3 periderm segments from different plants. b) Relative water content (RWC) in WT, *gpat5-1* and *esb1-2* under control and drought stress (n=10, with each replicate representing one leaf of an individual plant. Asterisk indicates the significance at $p<0.05$ in the difference in mean by student's t-test comparing control and drought stressed plants. c) Total root suberin content in WT, *gpat5-1* and *esb1-2* under control conditions (n=4-5, with each replicate representing 4 intact roots at 4 weeks of age. Asterisk indicates the significance at $p<0.05$ in the difference in mean by student's t-test comparing the WT plants. Values represent mean ± SD.

Investigation of the TEM images revealed the light and dark banding pattern of the suberin lamellae in *gpat5-1* was discontinuous under both control and drought stress (Figure 2-9). Consistently, mutants with lower suberin content and/or distorted ultra-structure had a higher amount of water loss in root periderm.

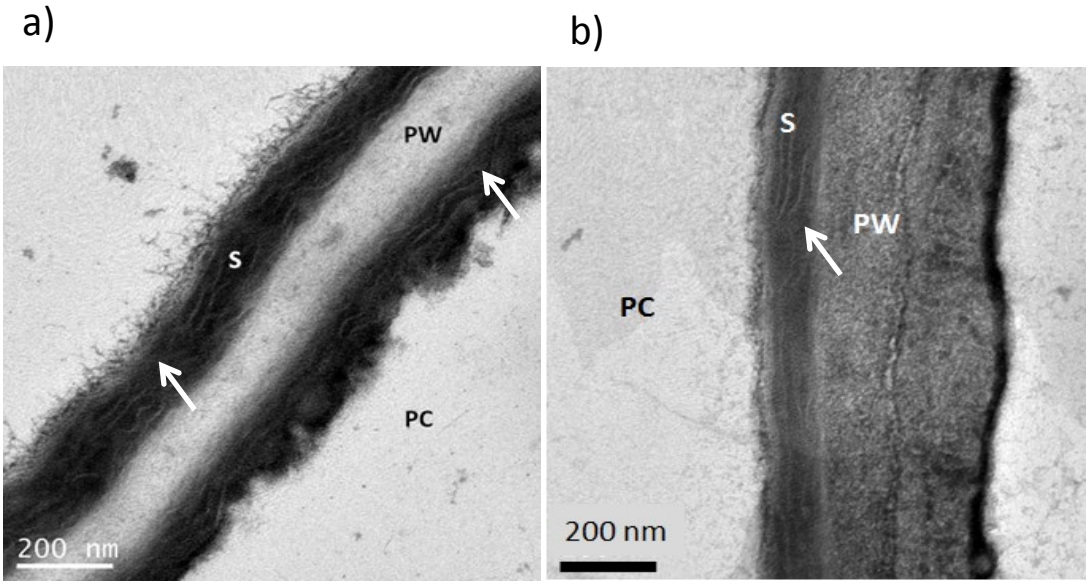

Figure 2-9. TEM images of *gpat5-1* root periderm sections under control and drought conditions. Sections of 4 week old *gpat5-1* plants grown under control (a) and drought stress (b) condition. White arrows indicate discontinuous suberin lamellae. Suberin lamellae (S), primary cell wall (PW), periderm cell (PC).

2.4.6 *Abcg2-1 abcg6-1 abcg20-1* mutant was very sensitive to NaCl treatment

To investigate salt stress responses, I exposed WT and suberin mutants to salt stress conditions (100 mM NaCl). All genotypes had significantly reduced biomass under the high salt conditions, indicating the plants were experiencing severe stress (Figure 2-10). At 100 mM NaCl, there was a very high rate of mortality in the *abcg2-1 abcg6-1 abcg20-1* plants. Therefore, due to lack of plant material, data on *abcg2-1 abcg6-1 abcg20-1* mutant was not included for the 100 mM NaCl treatment. When *abcg2-1 abcg6-1 abcg20-1* plants were instead exposed to 50 mM NaCl, there was a steep reduction in plant growth (Figure 2-10). *Abcg2-1 abcg6-1 abcg20-1* had a lower total biomass than wild-type plants even under control conditions (Figure 2-11a). In all other genotypes, total biomass at control or 100 mM NaCl conditions were not different than each other (Figure 2-11a; Table2-2).

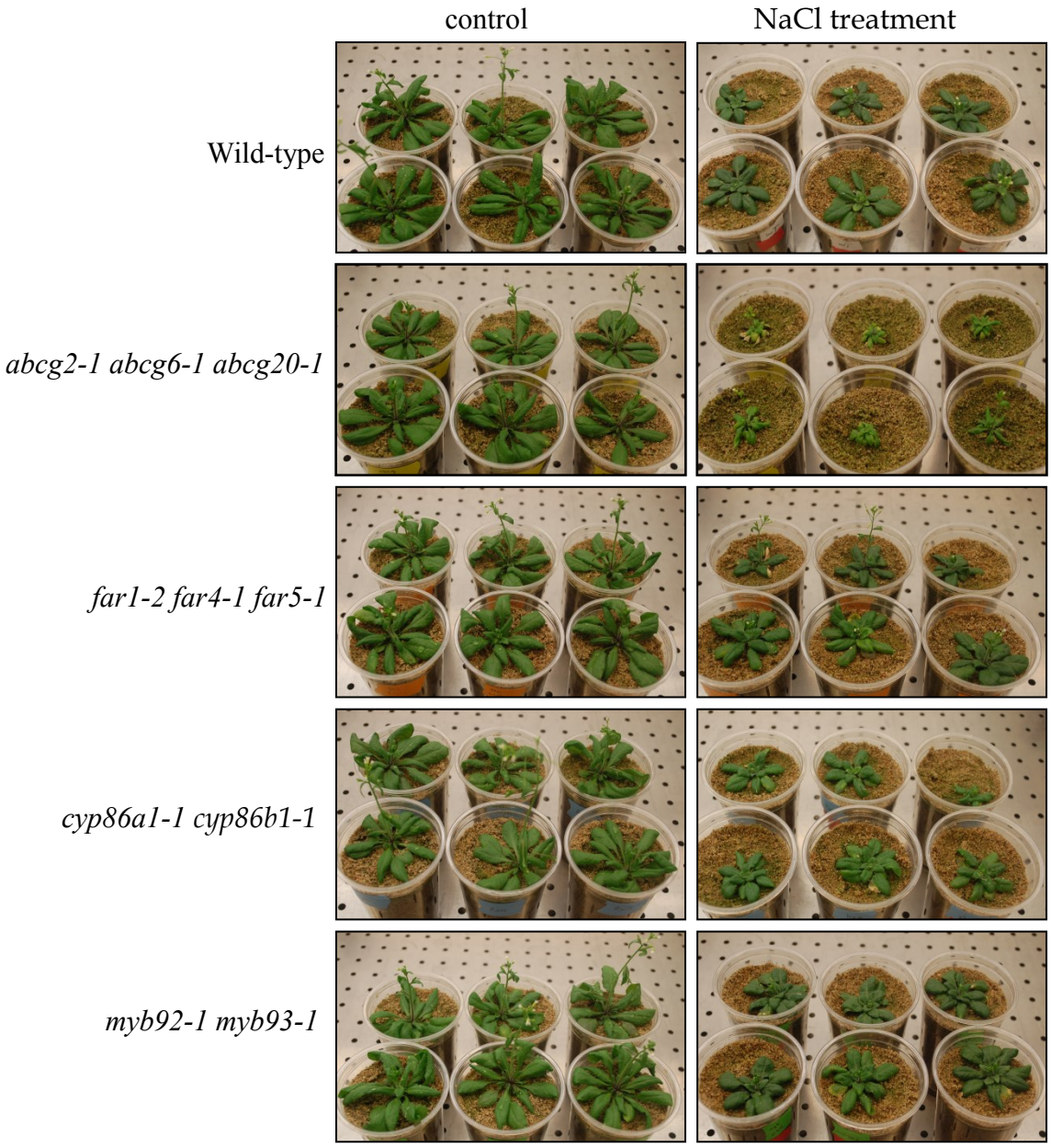

Figure 2-10. Comparison of genotypes grown at control (0 mM NaCl) and 2 weeks 100mM NaCl treatment. WT, *far1-2 far4-1 far5-1, cyp86a1-1 cyp86b1-1* and *myb92-1 myb93-1* plants were maintained at 100 mM NaCl and *abcg2-1 abcg6-1 abcg20-1* at 50 mM NaCl. Reduced plant size in *abcg2-1 abcg6-1 abcg20-1* indicates the sensitivity to NaCl at 50 mM NaCl.

2.4.7 Salt stress induced suberin biosynthesis in wild-type, but not in the suberin mutants

The effect of NaCl treatment on total suberin production varied among genotypes (Table 2-2). Relative to control plants, wild-type plants had a 22% increase in suberin content by 100 mM NaCl treatment (Figure 2-11b). The increase was associated with increases in DCAs and OH-FAs, while FAs were reduced by NaCl treatment in WT (Figure 2-12). Relative to the control condition, *far1-2 far4-1 far5-1* did not have a significant difference in total suberin content by NaCl treatment (Figure 2-11b). However, in the *far1-2 far4-1 far5-1* mutant, DCAs and OH-FAs were increased and FAs were decreased by NaCl treatment (Figure 2-12b). On the other hand, relative to control plants, *cyp86a1-1 cyp86b1-1* and *myb92-1 myb93-1* had 41% and 21% decreases in total suberin content after NaCl treatment (Figure 2-11b). It should be noted, however, that *cyp86a1-1 cyp86b1-1* had the lowest and *myb92-1 myb93-1* the second lowest amount of suberin content at control conditions. Further, there was no increase in any of the monomer groups in *cyp86a1-1 cyp86b1-1* and *myb92-1 myb93-1* by the 100 mM NaCl treatment (Figure 2-12c and d). In fact, the NaCl treatment in *cyp86a1-1 cyp86b1-1* caused reductions in the most abundant monomer groups (FAs, DCAs and OH-FAs) (Figure 2-12c). FA content in *myb92-1 myb93-1* displayed a 50% reduction by 100 mM NaCl treatment (Figure 2-12d). Primary alcohols were not affected by NaCl treatment in any of the genotypes (Figure 2-12).

Table 2-2. Results of the salt stress experiment.

ANOVAs of total dry mass (TDM), root suberin content, leaf Na and K content, and K/Na ratio as the dependent variables, and genotypes (WT and mutants) and the two levels of salt treatment (control and 100mM NaCl) as independent variables. Data for *abcg2-1 abcg6-1 abcg20-1* are not included in statistical analysis. ***p < 0.001; **p < 0.01; *p < 0.05

Trait	R^2	*n*	F-ratio		
			Genotype	100 mM NaCl treatment	Genotype X Treatment
TDM	0.61	79	2.7^{*}	101.4^{***}	0.7
Root suberin	0.91	36	86.9^{***}	0.2	5.3^{**}
Leaf Na	0.90	40	8.2^{***}	261.3^{***}	2.6^{*}
Leaf K	0.75	40	16.8^{***}	36.9^{***}	4.1^{**}
K/Na ratio	0.93	40	11.9^{***}	443.3^{***}	0.2

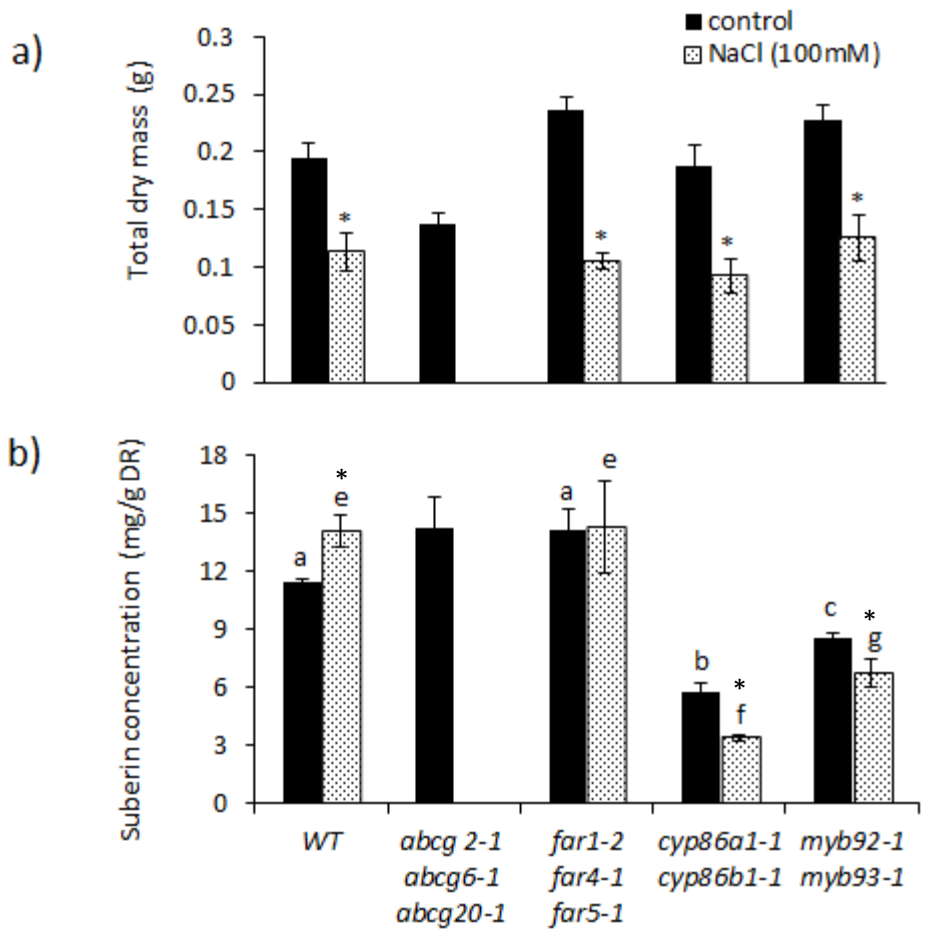

Figure 2-11. Comparison of total dry mass and total suberin content in WT and mutants under control and 100 mM NaCl treatment. a) Total dry mass; b) Total suberin content. *Abcg2-1 abcg6-1 abcg20- 1* NaCl treatment data are not included in the figure due to hypersensitivity to 100 mM NaCl. *Abcg2-1 abcg6-1 abcg20- 1* mutant was also excluded from the statistical analysis. Mean values in dry mass are given in grams from ten replicate samples ± SE. Each replicate consisted of one individual plant. Mean values of suberin contents are given in milligrams of suberin per gram of delipidated dry residue (DR) from 3-4 replicate samples ± SE. Each replicate consisted of 4-5 intact roots from separate plants. In a), asterisks indicate significant differences by student's t-test at $p<0.05$ comparing control and treatment . In b),

different letters at control (a,b,c) and NaCl treatment (e,f,g) indicate statistically significant differences between means by two-way analysis of variance (ANOVA) with Tukey separation of means ($P<0.05$). Comparisons among genotypes were done for control and NaCl treatments seperately.

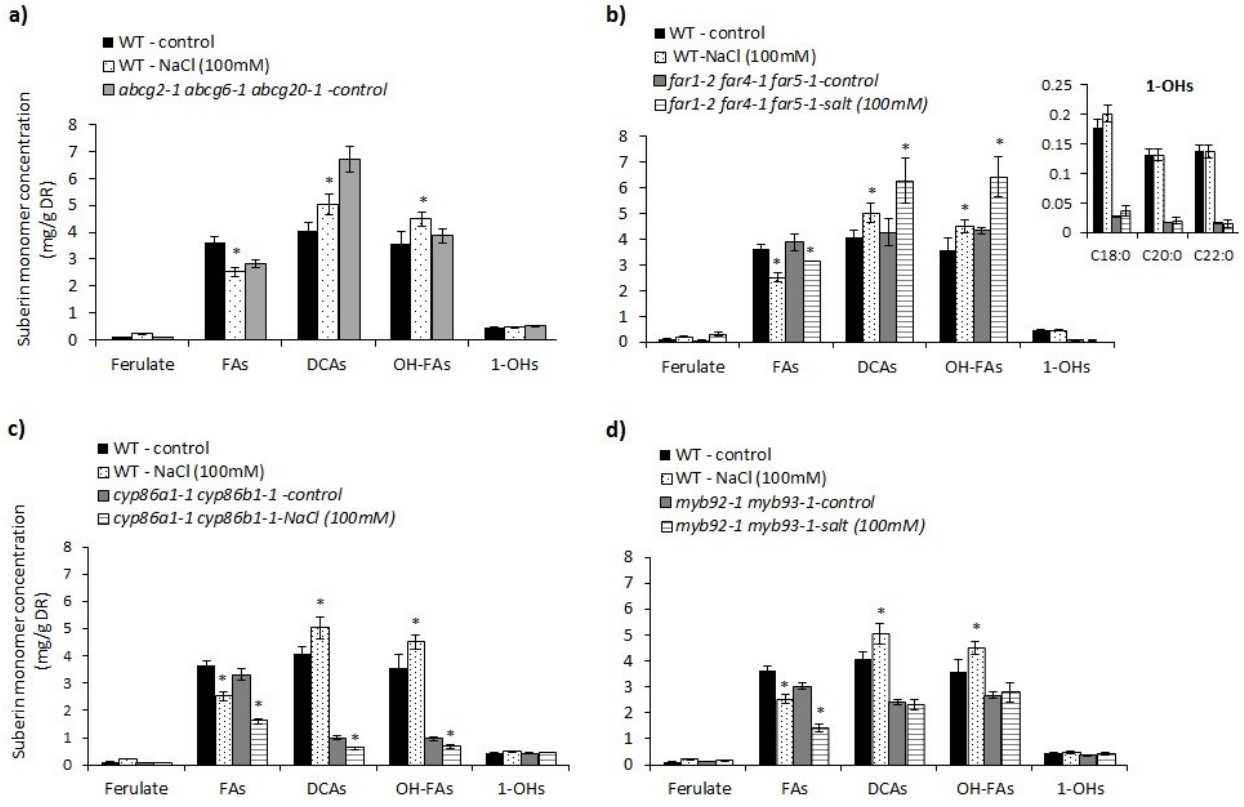

Figure 2-12. Comparison of root suberin monomer composition in mutants and WT under control and NaCl treatment. a) *abcg2-1 abcg6-1 abcg20-1,* b) *far1-2 far4-1 far5-1* (inset showing changes in fatty alcohol composition), c) *cyp86a1-1 cyp86b1-1* and d) *myb92-1 myb93-1*. *Abcg2-1 abcg6-1 abcg20-1* data for 100 mM NaCl treatment are not included as they incurred a high rate of mortality. Mean values are shown in milligrams of suberin monomer per gram of delipidated dry mass from 3-4 replicate samples ± SE. Each replicate represented 4-5 intact roots of separate plants at 4 weeks old. FAs: fatty acids; DCAs: dicarboxylic acids; OH-FAs: omega

hydroxy fatty acids; 1-OH: primary alcohols. Asterisk indicates $p<0.05$ by student's t-test comparing control and drought stressed plants.

The salt stress responses in suberin associated waxes were also investigated in WT plants. There was no significant increase in total wax content by 100 mM NaCl treatment. Significant increases were only observed in 18:0 ferulate and 20:0 and 22:0 coumarates (Figure 2-13). However, induction of root waxes by NaCl was previously reported by Kosma *et al.* (2015). Despite the higher variation in the sample error bars, most of the waxes had an increasing trend in their amount after introducing the drought stress.

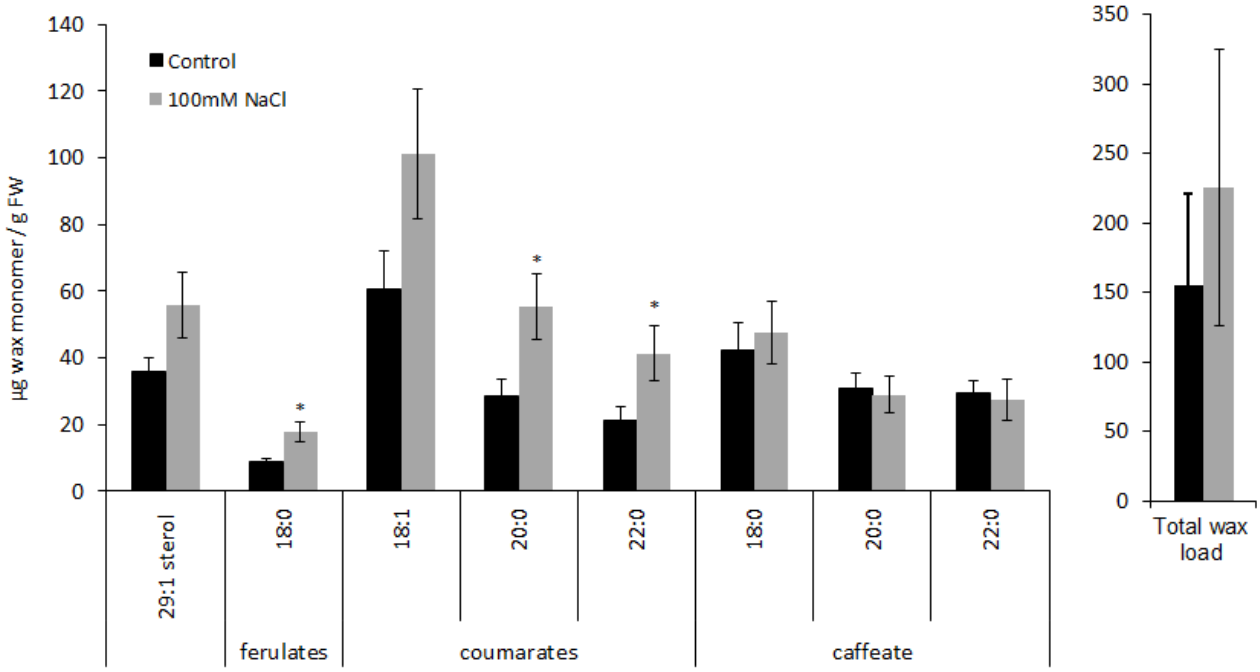

Figure 2-13. Comparison of root-associated wax composition in wild-type plants under control conditions and after 3 weeks 100 mM NaCl treatment. Mean values are shown in micrograms suberin monomer per gram of fresh weight from 3-4 replicate samples ± SE.Each replicate

represented 10 periderm root segments of separate plants. Asterisks indicate $p<0.005$ by student's t-test comparing the values of the control plants.

2.4.8 NaCl treatment caused ion imbalances (K/Na) in mutants with altered suberin composition and lamellae structure

To test whether altered suberin content and/or deformation in suberin lamallae structure changes the amount of solute transported into the shoot, I measured the elemental composition of leaf material from WT and mutants grown under control and 100 mM NaCl treatment. Principal component analysis (PCA) of elemental composition of each genotype indicated separation of *abcg2-1 abcg6-1 abcg20-1* plants from all other genotypes under the control condition (Figure 2-14). Separation implies that *abcg2-1 abcg6-1 abcg20-1* behaves differently than the other genotypes in terms of solute transport to shoot.

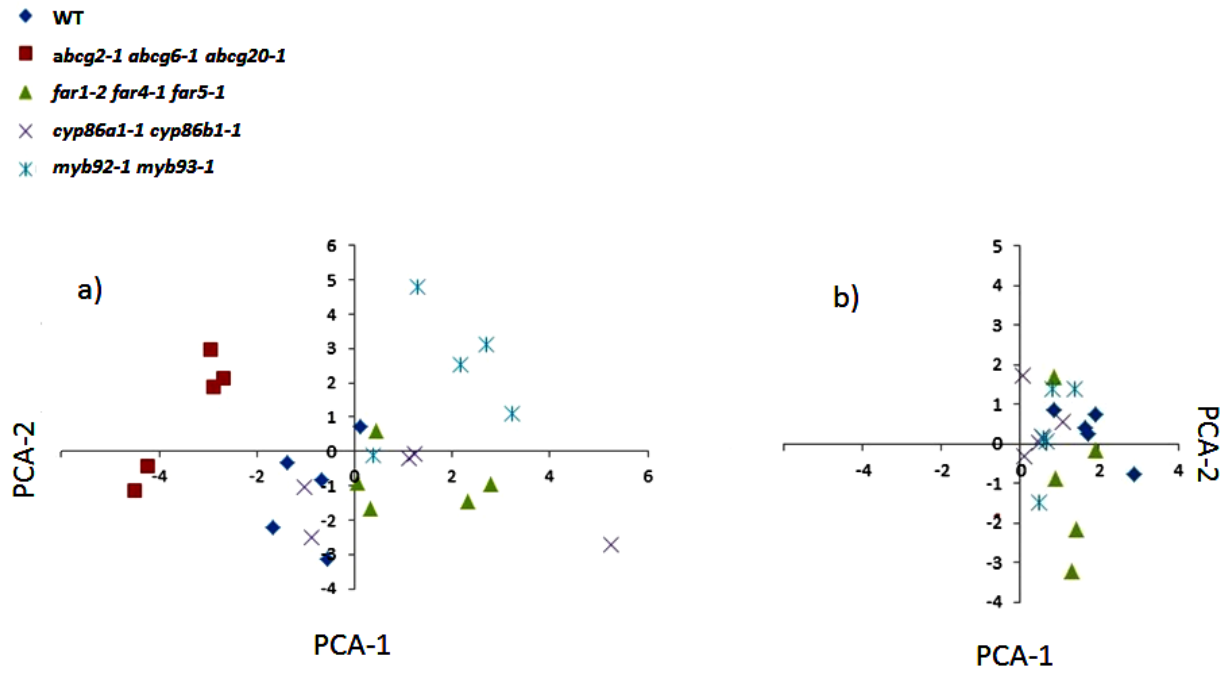

Figure 2-14. Segregation of leaf ionomic phenotypes in wild-type and mutants. a) Plants under control condition, b) Plants after 100 mM NaCl treatment. Data represents a) 30 % variance in x-axis (PCA1) and 21% variance in y-axis (PCA2); in b), 43% variance in x-axis (PCA1) and 14 % variance in y-axis (PCA2). There is a separation of data in *abcg2-1 abcg6-1 abcg20-1* from other genotypes in control plants.

Further, at 0 mM NaCl condition, *abcg2-1 abcg6-1 abcg20-1* had higher shoot Na concentration and lower shoot K concentration (and thus lower K/Na ratio) than any other genotype (Table 2-3 and Figure 2-15a, b and c). This suggests that *abcg2-1 abcg6-1 abcg20-1* is highly vulnerable to ion imbalance even under control condition. In fact, *abcg2-1 abcg6-1 abcg20-1,* which did not survive 100 mM NaCl salt conditions, had a Na content under control conditions closer to the amount found in WT and *far1-2 far4-1 far5-1* plants treated with 100 mM NaCl (Figure 2-15a and Table 2-3).

The effect of NaCl treatment on leaf Na content varied among genotypes (Table 2-2, Figure 2-1a). Ionomic analysis of leaf tissues sampled from both *cyp86a1-1 cyp86b1-1* and *myb92-1 myb93-1* showed a 20 fold increase in average leaf Na content while WT and *far1-2 far4-1 far5-1* displayed a 10 fold increase (Table 2-3).

Table 2-3**.** Analysis of elements in leaf tissues. *Abcg2-1 abcg6-1 abcg20-1* data are not included under NaCl treatment due to hypersensitivity at 100 mM NaCl. For each element, data is derived from 4-5 plants, concentrations given in parts per million (ppm) ± SE under non-stressed (control) and 100 mM NaCl treatment. Data in bold represents the significant differences compared to the control plants of the same genotype ($p<0.05$ by student's t-test). Asterisks indicate the differences relative to wild-type control plants at $P<0.05$ by student's t-test.

	Wild-type (Col-0)		*abcg2-1 abcg6-1 abcg20-1*	*far1-2 far4-1 far5-1*		*cyp86a1-1 cyp86b1-1*		*myb92-1 myb93-1*	
	Control	NaCl	Control	Control	NaCl	Control	NaCl	Control	NaCl
Na	2383.15±421.3	**24319.16±6646.9**	13626.72±2909.3	2208.46±723.1	**24240.87±7979.2**	3351.56±560.6	***64392.33±25442.0**	1834.52±288.7	**39941.14±25507.2**
K	34334.085±1908.6	**26253.93±3935.0**	13423.18±1892.6	27132.87±3592.4	**23250.75±3462.4**	26565.26±4095.1	***14219.72±3953.1**	22492.32±2777.2	19991.80±3616.2
Mg	1471±158.0	2412±263.6	1859±186.4	1397±218.7	26439±273.8	1420±86.8	2110±226.7	1248±207.3	2567±241.9
Ca	19166±716.8	19331±1202	**21200±956**	16587±688	**21061±1462**	16930±1802	**20648±697**	*13477±751	**20122±36**
Cd	0.08±0.0	**0.45±0.0**	0.05±0.0	0.07±.0.00	**0.47±0.0**	0.06±0.0	**0.56±0.0**	0.05±0.0	**0.37±0.0**
Mo	2.51±0.3	**1.52±0.1**	2.44±0.2	2.73±0.4	1.92±0.4	2.21±0.3	1.75±0.1	2.20±0.2	1.67±0.7
Zn	25.8±0.6	**41.6±2.3**	28.8±2.1	23.9±0.7	39.6±3.3	24.0±0.4	**35.2±0.7**	*20.3±1.2	**36.3±2.1**
Si	91.8±7.8	**65.2±9.1**	111.8±15.2	130.3±27.8	108.8±15.2	79.3±5.6	76.8±10.9	61.6±16.4	47.2±3.3
B	44.2±2.5	47.5±2.9	57.7±13.9	*29.8±1.1	**25.9±1.4**	*28.5±2.3	**19.2±0.2**	*27.7±0.4	26.8±2.4
Li	0.17±0.0	**0.04±0.0**	0.08±0.0	*0.50±0.1	**0.04±0.0**	0.42±0.2	0.15±0.0	0.26±0.1	**0.08±0.28**
Al	153.94±30.5	**53.50±13.7**	*52.74±8.3	*507.69±165.4	**40.16±8.5**	*410.07±120.7	**108.61±20.9**	*269.25±84.8	76.0±7.9
Cr	1.48±0.3	1.10±0.1	1.15±0.1	1.11±0.0	1.21±0.1	1.38±0.1	1.31±0.1	1.08±-.1	1.14±0.4
Mn	175.95±11.6	**118.13±10.7**	146.84±6.1	145.27±10.2	**116.90±10.6**	186.92±21.4	**124.43±10.6**	123.49±7.8	**97.96±2.3**
Fe	422.50±98.6	**207.39±40.3**	*230.31±14.8	*792.85±165.6	**183.81±12.6**	*1017.88±480.9	317.09±72.8	*689.12±197.9	242.87±12.2
Co	1.13±0.04	1.56±0.3	0.98±0.1	1.30±0.05	1.24±0.1	1.28±0.1	0.88±0.1	1.03±0.1	1.19±0.5
Ni	0.88±0.12	0.88±0.13	0.78±0.04	0.75±0.04	0.84±0.1	1.11±0.1	0.88±0.1	0.86±0.1	0.91±0.4
Cu	8.73±0.2	8.24±0.16	9.70±0.7	8.23±0.3	8.85±0.3	8.36±0.3	8.39±0.5	6.54±0.5	**7.61±0.8**
As	0.07±0.01	0.06±0.0	0.05±0.0	0.06±0.0	0.06±0.0	0.07±0.0	0.07±0.0	0.04±0.0	0.06±0.1
Se	0.27±0.0	0.09±0.0	0.21±0.1	0.13±0.1	0.17±0.0	0.26±0.1	0.08±0.0	0.11±0.0	0.11±0.0

Cyp86a1-1 cyp86b1-1 had the highest average Na content at control condition and NaCl treatment (Figure 2-15a), suggesting that altered composition and ultra-structure in *cyp86a1-1 cyp86b1-1* impaired the barrier function for the transport of Na into the shoot. The effect of NaCl treatment on K content varied among genotypes (Table 2-2). WT had the highest K content under both control and salt stress condition (Figure 2-15c). *Cyp86a1-1 cyp86b1-1* and *myb92-1 myb93-1* recorded lower values than WT and *far1-2 far4-1 far5-1* under both conditions (Figure 2-15c). *Abcg2-1 abcg6-1 abcg20-1,* even at control conditions, had a lower value for K than the values measured in the other genotypes under NaCl treatment (Figure 2-15c). The ratio between K and Na was analysed to investigate the salt tolerance in mutants. *Cyp86a1-1 cyp86b1-1* and *myb92-1 myb93-1* showed a stronger response in the K/Na ratio to NaCl treatment than WT or *far1-2 far4-1 far5-1* (Figure 2-15b). *Cyp86a1-1 cyp86b1-1* had the lowest value for K/Na ratio, indicating that it was more severely affected by NaCl treatment than the other mutants. The observed imbalance in Na and K contents indicates that *abcg2-1 abcg6-1 abcg20-1*, *cyp86a1-1 cyp86b1-1*, and *myb92-1 myb93-1* were more susceptible to NaCl treatment than wild-type. The ionomic analysis of micro elements revealed no clear relationship between suberin composition and elemental composition. However, there were differences in B, Si, Mn and Cu contents among genotypes ($p<0.5$ by Kruskal- wallis test for the genotypic effect). Also, Li, Al, Mn, Fe, Zn, Se, Mo, Cd, Ca and Mg contents in genotypes were altered by NaCl treatment ($P<0.5$ by Kruskal- wallis test for the treatment effect).

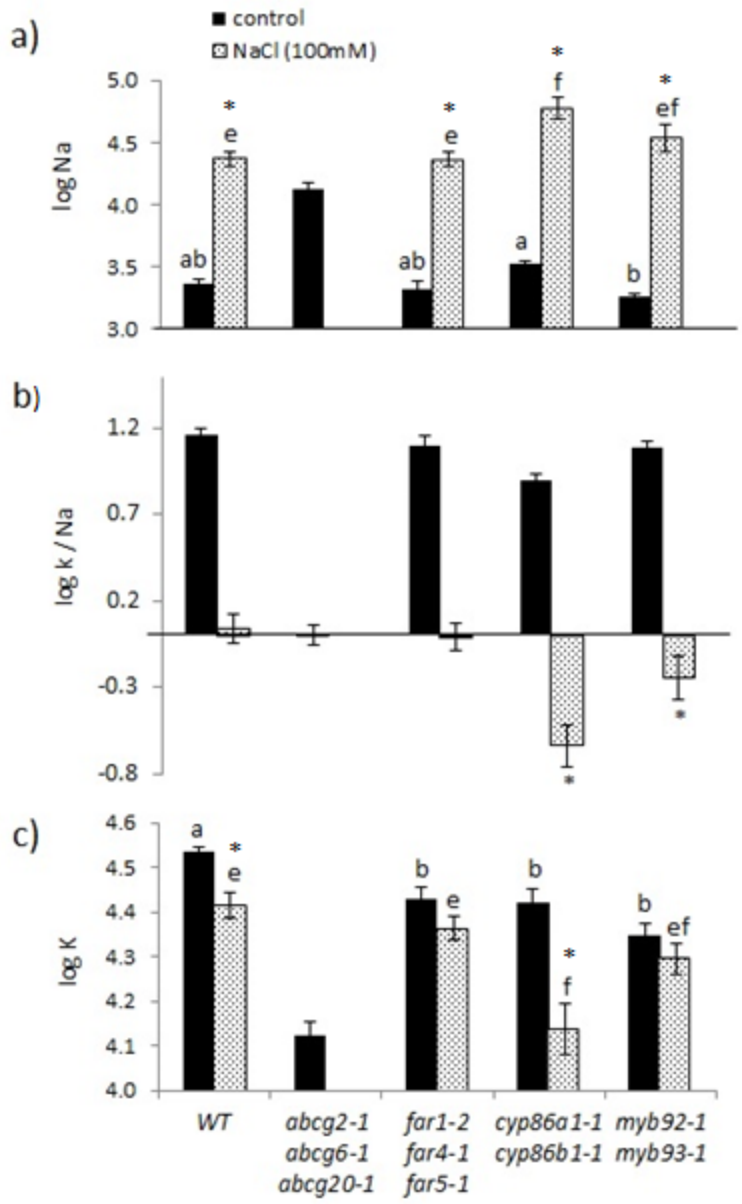

Figure 2-15. Comparison of Na, K/Na and K in leaves of wild-type and mutants under control and NaCl treatment. Log transformed data from Table 2-3 were plotted against each genotype. a) log Na ; b) log K/Na; c) log K. *Abcg2-1 abcg6-1 abcg20-1* NaCl treatment data are not included in the figures and statistical analysis due to hypersensitivity to 100 mM NaCl. *Abcg2-1 abcg6-1 abcg20- 1* mutant was also excluded from the statistical analysis. Mean values are from 4-5 replicate samples ± SE. Each replicate represented leaves from an individual plant. Different

letters at control (a,b) and NaCl treatment (e,f) indicate statistically significant differences between means by two-way analysis of variance (ANOVA) with Tukey separation of means ($P<0.05$). Comparisons were done separately for control and NaCl treatment. Asterisks indicate the differences at $p<0.05$ by student's t-test comparing the control and treatment in a) and c), and NaCl treated wildtype and mutant plants in c).

2.5 Discussion

In this study, I identified how suberin production varied under different water and salt levels. Both total suberin composition and lamellae structure are important for the barrier function against water loss through root periderm, which is important to maintain the water balance. Altered salt stress responses in mutants proved that suberin composition and lamellae structure are also important to maintain ion balance.

Studies investigating suberin induction under stress conditions over a time-course are rare (Pereira, 2016). The data presented in this study showed that during root development, suberin monomers increase with plant age and reach a steady state at maturity (Figure 2-1). The increased suberin production may have been associated with initiation of secondary growth in roots, which was previously reported to take place around 3 weeks of age in Arabidopsis (Dolan *et al*., 1993). A similar pattern of suberin production was also observed in wild-type Arabidopis plants grown in tissue culture conditions (Delude *et al*., 2016). I found here that plants under drought stress reached its highest suberin production before the plants under non-stress conditions. Analysis of the amount of water loss in roots revealed that suberin is important in preventing roots from drying out. Drought treatment caused increases in suberin production and this was correlated with reduced water loss in roots. As speculated by Hose *et al.* (2001), perhaps

the acceleration of suberin synthesis benefited plant endurance to drought stress. The observed increase in suberin-associated waxes implies further reinforcement of suberin barrier function against drought stress. Drought tolerance can also be improved by deposition of suberin associated waxes in root periderm, which reduces the risk of cavitation in xylem conduits (Soliday *et al*., 1979; Lens *et al.,* 2013). The drought stress and cessation of drought (re-watering) directly influenced suberin production (Figure 2-2a and b). Barberon *et al*., (2016) provided evidence for plasticity in endodermal suberization in response to a range of nutrient availabilities in Arabidopsis. Suberization was delayed in young Arabidopsis seedlings under Fe, Mn and Zn deficient conditions, and it was enhanced under K and S deficient conditions. They also found that suberin development is induced by the stress hormone abscisic acid (ABA). Drought stress leads to induction of ABA (Schroeder, *et al*. 2001). Additionally, Barberon *et al*., (2016) observed a decrease in suberin accumulation in response to ethylene. Therefore, it is possible that re-watering caused ABA levels to diminish and/or ethylene levels to increase, with concomitant cessation of suberin biosynthesis.

Although the suberin mutants tested here were not more susceptible to drought stress than wild-type, the responses to drought were different among genotypes. *Cyp86a1-1 cyp86b1-1,* which was deficient in suberin content and had deformed lamellae structure, was able to acclimatize to the chronic drought stress. *Cyp86a1-1 cyp86b1-1* was able to maintain RWC and root dry mass to the same level as control condition after the drought stress. Due to an increased in the amount of water loss in mature roots, it is possible that the *cyp86a1-1 cyp86b1-1* mutant may have experienced a more severe drought stress than the other genotypes and then had a stronger response to the drought stress. Further, the correlation between low root suberin in

cyp86a1-1 cyp86b1-1 and increased rate of water loss implies that suberin plays a role in preventing uncontrolled water loss in roots.

A lower rate of water loss is key to maintain plant water balance suitable for metabolic processes and to improve water use efficiency (WUE) under drought stress (Li *et al.,* 2017). An increased amount of suberin deposition was reported in *esb1-2,* which was associated with higher WUE (Baxter *et al*., 2009; Hosmani *et al.,* 2013). *Esb1-2* has an increase in all aliphatic suberin monomer components in roots compared to wild-type (Baxter *et al*., 2009). Analysis of water evaporation rate in *esb1-2* mutant further comfirmed the relationship between increased suberin and reduced water loss in mature roots that could have resulted in the improved WUE reported by Baxter *et al.,* (2009).

The amount of water loss in root periderm of *gpat5-1* was similar to *cyp86a1-1 cyp86b1-1*. *Gpat5-1* has 50% less aliphatic suberin than wild-type in young roots (Beisson *et al.,* 2007) and has a discontinuous suberin lamellae structure (Figure 2-8 and 2-9). These results provide evidence that distorted lamellae results in higher amount of water loss in roots. However, in contrast to *cyp86a1-1 cyp86b1-1*, decreased root suberin content in *myb92-1 myb93-1* was not associated with deformed lamellae structure. Detailed analysis of monomer composition indicated that *myb92-1 myb93-1* had a lower amount of DCA monomers, relative toWT, rather than ω-OH FAs. Specifically C16, C18:1, C18:0, and C24 DCA monomers were reduced. Despite these defects, *myb92-1 myb93-1* had intact suberin lamellae structure. On the other hand, compared to WT and *myb92-1 myb93-1*, *cyp86a1-1 cyp86b1-1* had less DCAs as well as ω-OH FAs of all chain lengths: C16, C18:2, C18:1, C18, C20, C22 and C24. The suberin lamellae structure in *cyp86a1-1 cyp86b1-1* was deformed. Based on the results of the above two mutants, it is challenging to infer which specific type(s) of monomers are important for the ultra-structure

arrangement seen by electron microscopy. Perhaps the compositional differences and total amount of monomers or a combination of several factors distrupted the lamellae in *cyp86a1-1 cyp86b1-1*. However, the results did indicate that the native ultra-structure of suberin is functionally critical in reducing backward water flow under drought stress. *Abcg2-1 abcg6-1 abcg20-1* is different, which has more suberin content than WT but fails to form the lamellae (Yadav *et al.,* 2014). The drought stress responses observed in *far1-2 far2-1 far5-1* were similar to WT, which indicates that primary alcohols in suberin do not play a major role in drought tolerance. Despite the large reduction in primary alcohols, neither the total suberin content nor suberin lamellae was altered in *far1-2 far4-1 far5-1* (Delude *et al.,* 2016).

The presence of salt in the medium affected growth in the *abcg2-1 abcg6-1 abcg20-1* mutant. The reduced survival rate observed at 100 mM NaCl in *abcg2-1 abcg6-1 abcg20-1* was the first evidence indicating the increased toxic effect of salinity. A key issue for salt tolerance is the ability of a plant to reduce Na transport to shoot, while maintaining K content unaffected (Negrao *et al.,* 2017). *Abcg2-1 abcg6-1 abcg20-1* recorded a very high Na content and a very low K content even under control conditions. Therefore, salinity could have generated a major disruption of ion balance in this mutant. Compared to other genotypes grown at 100 mM NaCl, reduced biomass in *abcg2-1 abcg6-1 abcg20-1* at 50 mM NaCl treatment provides evidence for hypersensitivity due to deformed lamellae structure (Figure 2-10). Additionally, *abcg2-1 abcg6-1 abcg20-1* has defects in lateral root formation that could have reduced water uptake, thereby affecting WUE (Yadav *et al.,* 2014).

Exposing plants to 100 mM NaCl resulted in increased deposition of suberin in wild-type. The increased root suberin in WT under salt stress may have diminished Na transport into the shoot. Krishnamurthy *et al.* (2011) also detected a similar relationship among rice cultivars that

varied in tolerance to salinity. The salt tolerant cultivar Pokkali has more suberin in its roots than the salt sensitive cultivar IR20. Exposure of both cultivars to 100 mM NaCl resulted in deposition of additional suberin, which reduced accumulation of Na in the shoot and improved survival of plants when subjected to 200 mM NaCl (Krishnamurthy *et al.,* 2011). Relative to WT and *far1-2 far4-1 far5-1,* the increased Na accumulation in shoots of *cyp86a1-1 cyp86b1-1* and *myb92-1 myb93-1* after NaCl treatment suggests that root suberin amount plays an important role in limiting Na translocation into the shoot. However, NaCl treatment failed to increase the overall amount of suberin associated waxes in WT plants (Figure 2-13). Detailed analysis of suberin monomer composition in WT revealed drought stress increased all suberin monomerss, while NaCl increased only DCAs and OH-FAs. Production of FAs in all the mutants was also affected by NaCl treatment and not by drought stress. Therefore, even though the drought stress increased total suberin content in all the genotypes, 100 mM NaCl increased the total suberin content only in WT. Altogether, these results indicate that suberin biosynthesis in mutants was suppressed by NaCl treatment, perhaps due to the ion imbalance caused by increased uptake of Na. The data presented in this study also showed that the increase in Na was related to a decrease in K, as high Na is know to cause increases in K efflux (James *et al.,* 2011). A plant's ability to maintain high K/Na ratio, either by retention of K or by preventing Na from accumulating in leaves, was a key feature for salt tolerance in barley (Chen *et al.,* 2007). Increased susceptibility to salt treatment displayed by two mutants, *abcg2-1 abcg6-1 abcg20-1* and *cyp86a1-1 cyp86b1-1,* implies that suberin content, composition and lamellae structure are important factors in reducing uncontrolled Na transport into the shoot, which improves tolerance to salinity. As reported by Doblas *et al.,* (2017), the variability in accumulation of micro-elements observed in

this study perhaps could have been due to the selective barrier function of suberin for different minerals.

Beased on these results, several comparisons can be made between the phenotypic responses of Arabidopsis under drought or salt stress conditions. Salt stress increased suberin production only in wild-type, whereas drought stress increased suberin in both wild-type and suberin mutants. Further, the amount that was increased by salt stress was much smaller than the drought stress. Mutants with altered suberin monomer composition and distorted suberin lamellae structure were not more susceptible to drought stress than wild-type probably because they could acclimatize the drought stress conditions tested here. However, in the suberin mutants, acclimatization responses were not evident under salt stress. Altogether, these observations imply that perturbation of suberin chemical composition and structure disturbs whole plant physiology more so when subjected to salt stress than drought stress.

In summary, the results presented here indicate that suberin synthesis shows plasticity at different water levels and prevents root dehydration under drought stress. This is important to maintain water balance in plants. Increased suberin specifically in root periderm may therefore present opportunities for developing enhancing drought resistance in crops. I also provide evidence that suberin composition and structure plays an important role in limiting uncontrolled transport of Na under high salinity conditions. Altogether, the results of this study indicates that the regulated deposition of suberin in specific tissues provides protection against different stresses. These findings may contribute to future research targeting enhanced stress resistance in crops.

Chapter 3: Seed coat suberin forms an effective barrier against chromium (Cr^{3+}) during early seed germination in *Arabidopsis thaliana*

3.1 Abstract

The seed coat contains various lipid-based (suberin and cutin), carbohydrate-based (mucilage) and phenolic-based (proanthocyanidin) polymers that are thought to influence seed coat permeability to various solutes. I investigated here the role of these polymers in preventing chromium (Cr^{3+}) penetration of the seed coat prior to seed germination in the model plant *Arabidopsis thaliana*. Wild-type (WT) and mutants impaired in one or more of the seed coat polymers were exposed to different Cr^{3+} concentrations (0, 50, 100, 200, 400 and 800 mg/L) during seed stratification and early imbibition. Mutants with major reductions in suberin lipid polyester amount in the seed coat were highly sensitive to Cr^{3+} relative to wild-type in terms of seed germination. At the highest level of Cr^{3+} (800 mg/L), mutants deficient in suberin also had significantly reduced embryo viability, indicating that chromium was more easily passing through the seed coat and damaging the embryo directly. This was correlated with increased permeability of the seed coats to tetrazolium salts. A mutant with reduced cutin lipid polyester, which is deposited in a different layer of the seed coat, was not affected by high concentrations of Cr^{3+}, similar to wild-type. Some mucilage-altered mutants had slightly increased sensitivities to Cr^{3+} in terms of seed germination rates, but not at the level of sensitivities observed with suberin-deficient mutants. Although many proanthocyanidin mutants displayed reduced seed germination in the presence of Cr^{3+}, their embryo viability was only slightly reduced at high Cr^{3+} concentrations. I speculate that seed coat imposed dormancy was increased in proanthocyanidin mutants, and the embryo damage by penetration of Cr^{3+} through the seed coat was not increased

similar to the seeds reduced in seed coat suberin. Altogether, these findings provide evidence for the effective barrier function of seed coat suberin on the imposition of impermeability to Cr^{3+}. Additionally, the results highlight the risks associated with Cr^{3+} toxicity on the persistence of seeds that have relatively low seed coat suberin in soils contaminated with high levels of chromium.

3.2 Introduction

Industrialization has led to the incorporation of pollutants into natural resources such as soil, water and air. Increased amounts of heavy metals in soil is one of the main environmental issues impacting plants and humans (Rodriguez *et al*., 2015). During storage in the soil, seeds are often subjected to various hazardous conditions, which could affect the persistence of viable seeds in soil. In recent years, chromium mining for industrial purposes has drawn considerable attention due to the risks associated with chromium toxicity on seed germination and overall plant health (Rodríguez *et al.,* 2015; Lukina *et al.,* 2016; Lopez-Luna *et al.,* 2009; Shanker *et al.,* 2005). The mechanisms underlying the seed persistence in soil have been addressed mostly with respect to chemical defense. This study focused on the protection provided by the seed coat that envelops the embryo against chromium toxicity during storage in soil and early seed germination. I hypothesised that the ability of a seed to germinate in contaminated soil is expected to depend on the constituents of seed coat.

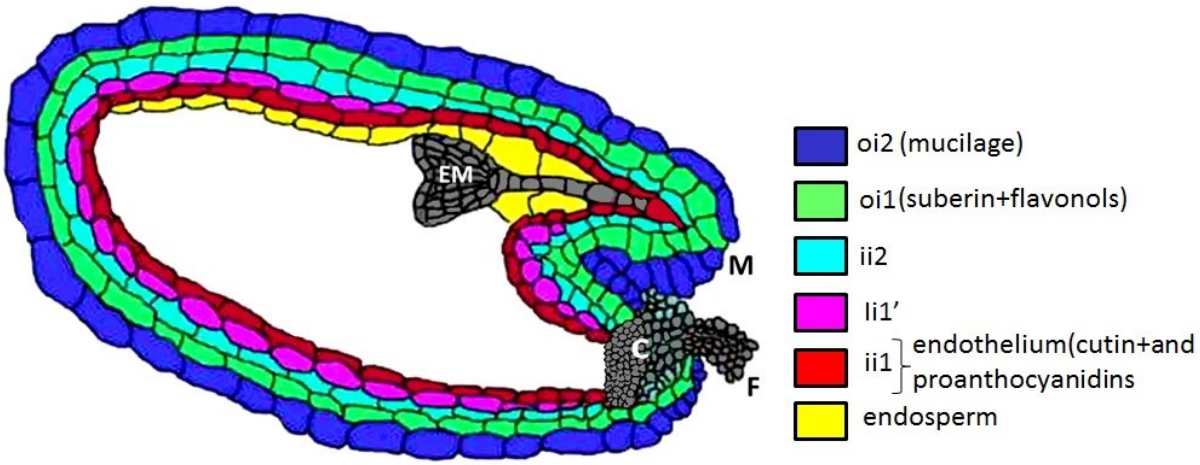

Figure 3-1. Illustration of *A. thaliana* seed anatomy at the heart stage of embryogenesis. A longitudinal section modified from (Debeaujon *et al.*, 2003). oi, outer integument; ii, inner integument; C, chalaza; M, micropyle; EM, embryo; F, funiculus.

The seed coat develops from the ovule integuments after fertilization. Providing a physical barrier around the embryo is one of the important roles played by the seed coat. The barrier properties vary depending on the composition and structure of the seed coat (Vishwanath *et al.,* 2013; Molina *et al.,* 2008; Mendu *et al.,* 2011). Seed coat differentiation has been well studied in the model plant, *Arabidopsis thaliana* L. (Beekman *et al.*, 2000; Haughn and Chaudhury, 2005). During development, the Arabidopsis seed coat is composed of two integuments; the inner (ii) and outer (oi) integuments, each consisting of two cell layers (Figure 3-1). An additional layer that reaches about two-thirds the distance from the chalaza towards the micropyle develops from the inner integument (ii1′) (Schneitz, 1995). At maturity, the Arabidopsis seed coat (testa) consists of dead cells corresponding to the five cell layers that originate from ovule integuments. Except for the outer most cell layer, other cell layers are

largely collapsed and crushed together and contain brown pigments (Haughn and Chaudhury, 2005).

Arabidopsis seed coat integuments deposit different polymers that may influence permeability to various solutes, including environmental toxins. The outermost layer of the integument (epidermal cells) of the Arabidopsis seed coat synthesizes and secretes large quantities of the polysaccharide mucilage (Figure 3-1) (Haughn and Western, 2012). The mucilage is separated into non-adherent and adherent layers. The pectin rhamnogalacturonan I (RG I) is the main constituent of both mucilage layers (Western 2012; Western *et al.,* 2000). The non-adherent layer represents 65% of total mucilage and is easily detached from the seed. The adherent layer forms the remaining mucilage and is difficult to remove from the seed. In parallel to mucilage production, the cytoplasm forms a volcano shaped column in the center of the cell that plays a role in the attachment of mucilage on the seed (Western *et al.,* 2000). The adherent layer is associated with ray-like structures that radiate outwards from these columns (Sullivan *et al.,* 2011).

Suberin and cutin are two distinct lipid-based polyesters deposited in the seed coat (Molina *et al.,* 2008). Suberin is a polyaromatic and polyaliphatic heteropolymer located in the outer integument 1 (oi1) layer of the Arabidopsis seed coat (Figure 3-1) (Molina *et al.,* 2008). The aliphatic portion of suberin is thought to impose the barrier function against water and solute permeability (Franke and Schreiber, 2007). Aliphatic suberin consists of long-chain (C16 and C18) and very-long-chain (≥C20) aliphatics, such as α,ω-dicarboxylic acids, ω-hydroxy fatty acids, unsubstituted fatty acids, and primary fatty alcohols, as well as esterified ferulate and glycerol (Graca, 2015; Schreiber *et al.,* 1999; Vishwanath *et al.,* 2015). It often forms a lamellae structure when deposited in the cell wall (Graça and Santos, 2007). Cutin is a fatty acid- and

glycerol-based polyester mainly composed of inter-esterified hydroxy and epoxy-hydroxy fatty acids with chain lengths of 16 and 18 carbons (Nawrath, 2002). Cutin is located in the inner cell layer of the inner integument (ii1 or endothelium; Figure 3-1) (Molina *et al.,* 2008). During late maturation of seeds, suberin is also deposited in the chalazal region of the seed (Molina *et al.,* 2009; Beisson *et al.,* 2007). Seed flavonoids are also deposited in the seed coat. Three major flavonoids present in Arabidopsis are proanthocyanidins (PAs), or condensed tannins, which turn a brown colour after oxidation, flavonol glycosides (yellow), and anthocyanins (red to purple) (Poucel *et al.,* 2005). Similar to the synthesis of phenolics found in suberin and suberin-associated waxes, the precursors of flavonoids, including proanthocyanidins, are derived from products of phenylpropanoid pathway. PAs are polymers made up of flavan-3-ol subunits such as catechin and epicatechin (Poucel *et al.,* 2005). These flavonoids accumulate in vacuoles of the seed coat endothelium (Figure 3-1) and are known to play protective roles in plant-environment interactions (Debeaujon *et al.,* 2003). Seed coat suberin and flavonoids in *A. thaliana* contribute to seed coat-imposed dormancy by providing a barrier to water and oxygen (Fedi *et al.,* 2017; North *et al.,* 2010). Flavonoids are also thought to play a role in controlling germination though dormancy imposition (Debeaujon *et al.,* 2000).

The seed germination process in Arabidopsis starts with early imbibition phase followed by a plateau phase of water uptake in which metabolism is reactivated in embryo tissues and ends with protrusion of the radicle through the micropyle (Weitbrecht *et al.,* 2011). Upon first contact with water, Arabidopsis seeds extrude mucilage. Mucilage helps to maintain seed hydration and promotes seed germination especially in dry environments (Western *et al*., 2000). Seeds of many plant species, including Arabidopsis, exhibit primary dormancy after release from the mother plant. Primary dormancy is an intact, viable state of a seed that blocks germination

even under favorable germination conditions (Bewley, 1997; Chahtane *et al.,* 2017). When seeds are unable to germinate because of the constraints in the seed coat, it is called seed coat imposed primary dormancy (Debeaujon *et al.,* 2000). After release from primary dormancy, the non-dormant seeds can become dormant again if the external environmental conditions become unfavorable for germination. This is known as secondary dormancy (Chahtane *et al.,* 2017; Momoh *et al.,* 2002).

Arabidopsis mutants affected in one of the seed coat polymers without causing changes in seed viability are important tools in investigating the protective functions of the seed coat. The protective roles of these polymers against adverse environmental conditions, such as heavy metal toxicity have not been fully explored. A large number of *A. thaliana* mutants have been identified that are impaired in one or more of the seed coat polymers described above (Vishwanath *et al.,* 2013; Molina *et al.,* 2008; Beisson *et al*. 2007; Xiao *et al*.,2004; Western *et al.*, 2001; Debeaujon *et al.,* 2000). By taking advantage of these mutants, my aim was to determine which of the seed coat polymers are important for protecting the embryo against chromium toxicity prior to seed germination. Viability of seeds exposed to contamination was tested by employing seed germination assays. I found that amongst the different polymers deposited in Arabidopsis seed coat, suberin is the key polymer that forms a physical barrier against Cr^{3+} penetration.

3.3 Materials and Methods

3.3.1 Plant materials and seed amplification

A. thaliana ecotypes Columbia (Col)-0 and Landsberg *erecta* (L*er)* were used in this study. Mutants defective in mucilage (*mum2-1, mum4-1, men4-1* and *mum4-1 men4-1*) are as

described in Western *et al.* (2001). The T-DNA insertion lines of other mutants were obtained from the Arabidopsis Biological Resource Centre (ABRC), Ohio State University (Appendix IV). Seeds were stratified at 4°C for 3 days and sown on a 1:1:1 mixture of Promix PGX soil-less medium (Premier Horticulture), vermiculite, and perlite and grown in an environmental chamber at 21°C to 22°C, 40% to 60% humidity, and a 16 hr / 8 hr light/dark cycle. All seeds were amplified in identical environmental conditions and harvested on the same day. Homozygous T-DNA insertion lines altered in suberin or cutin were confirmed by PCR genotyping using primers given in Appendix II. Homozygous mutant lines altered in mucilage or flavonoids were confirmed by phenotypic characterization using the ruthenium red and vanillin assays, respectively. Suberin and cutin mutants were confirmed phenotypically by chemical analysis of seed coat polyesters. Seeds harvested from dry siliques were stored at room temperature in paper bags for two weeks, cleaned, and stored in micro-centrifuge tubes prior to the start of germination assay.

3.3.2 Preparation of chromium (Cr^{3+}) solutions and germination assay

Chromium chloride hexahydrate (Catalog number: 27096; CAS: 10060-12-5; Sigma-Aldrich Canada Co, Oakville, Ontario) was used as a source of Cr^{3+} due to its high solubility in cold water and >98% purity. Following a previous toxicological study (Lukina *et al.,* 2016), doses were selected to reflect ecologically relevant levels of Cr^{3+} in pristine soils (i.e. 0, 50, and 100 mg kg^{-1}), as well as those levels found in soils near contaminated sites relevant to any mining area (i.e. 200, 400, and 800 mg kg^{-1}). Each dose was prepared separately by weighing the appropriate amounts of $CrCl_3 \bullet 6H_2O$ and mixing it with 50 ml of deionized water. Once thoroughly mixed, one ml of each dose (in triplicate) was transferred into a microcentrifuge tube

already containing *A. thaliana* seeds (at least 25 seeds) and stored in the dark at 4°C for 3 days. On the 4th day, the tubes with seeds were transferred to a controlled growth chamber at 21°C, 40% to 60% humidity, and a 16 hr / 8 hr light/dark cycle to expose seeds to early imbibition before seeds start to crack open. To avoid embryos directly coming into contact with the chromium solution, seeds were imbibed for only 16-18 hr after stratification. The Cr^{3+} solution was then discarded and seeds were rinsed with deionized water three times. Seeds were sown on wet filter paper (Fisherbrand qualitative –P5; cat. No. 09-801C) in 6 cm plastic petri dishes. Seed germination was monitored for 2 weeks. Deionized water was added to the filter paper when necessary to avoid dryness of seeds. Seeds were scored as germinated when the two cotyledons were visible. Cumulative germination percentage (%) was recorded every second day over 15 days by taking images of the petri plate using a stereomicroscope (SteREO Discovery V20 microscope, Carl Zeiss Microscopy). Imaging software used was Zen 2012 (Blue Edition), Carl Zeiss Microscopy. When seeds of plants with two mutant alleles of the same gene displayed a similar germination response and permeability properties, the data of only one allele was included in the main results.

3.3.3 Seed coat polyester analysis

Both suberin and cutin polyesters were analyzed together as these compounds are very difficult to separate from each other because of their chemical similarities (Molina *et al.,* 2008). Seed lipid polyester (suberin/cutin) analysis was performed with some modifications to Molina *et al.,* (2006). Approximately 100 mg of dry seeds for each replicate were ground in liquid nitrogen using a mortar and pestle, immersed in hot isopropanol, and then the mixture was transferred to solvent-rinsed glass GC tubes and heated for 15 min at 85^{o}C. After cooling, tissues

were finely ground with a polytron and incubated with isopropanol at room temperature for 24 hrs. Soluble lipids were removed from the crushed seeds using successive solvent extractions with chloroform: methanol (2:1, v/v) and chloroform: methanol (1:2, v/v) at room temperature for 24 hours each on a tube rotator (Boekel Scientific) set at 60 rpm. The residue was air dried in a fume hood for 2-3 days. The residue was then extracted successively with 100% methanol (30 min), sterile water (30 min), 2 M NaCl (1 hr), sterile water (30 min), and 100% methanol (30 min), 1:2 (v/v) chloroform: methanol (overnight), and 2:1 (v/v) chloroform: methanol (overnight). Samples were dried in a fume hood at room temperature for 2-3 days and then in a desiccator for another 5 days before being used for lipid polyester analysis. Seed coat lipid polyester analysis was carried out using base-catalyzed transmethylation followed by acetyl derivatization. The solvent-extracted dried residues were weighed, and 10 to 30 mg of each sample was depolymerized by transmethylation at 60°C for 3 h with periodic vortexing in 0.9 ml of methanol, 0.0225 ml of methyl acetate and 0.375 ml of sodium methoxide. Twenty micrograms each of methyl heptadecanoate (17:0 FAME) and pentadecanolactone (OPL) were used as internal standards. After cooling, the reaction mixtures were acidified with glacial acetic acid to adjust pH to 4–5. To recover the fatty acid methyl esters (FAMEs), 2 ml of saline solution (0.5 M NaCl) was added and FAMEs were extracted with dichloromethane (2.5 ml) followed by centrifugation at 800g for 5 min at room temperature to promote phase separation. The organic phase was transferred to a fresh glass tube and washed three times with dilute saline solution (0.5 M NaCl) and dried over anhydrous Na_2SO_4. The solvent was evaporated to dryness under N_2. The samples were heated at 60°C for 1 hr with 100 µl each of acetic anhydride and pyridine. Acetylated samples were evaporated to dryness under N_2 (without heating) and dissolved in 100 µl hexane for analysis by gas chromatography.

3.3.4 Gas chromatography

Quantification of suberin and cutin monomers was done with a Varian-3900 Gas Chromatograph equipped with a flame ionization detector (GC-FID) and a HP-5MS capillary column (30 m length, 0.25 mm inner diameter, 0.25 μm film thickness). One μL aliquot of the sample was injected in splitless mode, and high-purity helium was used as the carrier gas at a flow rate of 1.5 ml min^{-1}. The temperature of the injector was held at 250°C and the column oven temperature was ramped from 140°C to 310°C at 3°C min^{-1}, and then held for an additional 10 min at 310°C. The flame ionization detector (FID) was held at 350°C and high purity helium was used as the carrier gas at a flow rate of 1.5 ml per min. For peak identification, representative samples were analyzed on a gas chromatograph (Thermo Scientific, TRACE 1300) coupled to a mass spectrometer (GC-MS; Thermo Scientific ISQ LT Single Quadrupole) on a TG-5MS column (30 m length, 0.25 mm inner diameter, 0.25 μm film thickness), following the program detailed in Molina *et al*. (2006).

3.3.5 Seed coat permeability assay

The tetrazolium assay was performed as described by Vishwanath *et al.* (2014). Dried seeds (50 mg) for each genotype were placed in a 1.5 ml microcentrifuge tube. Each sample was assayed in triplicate. A milliliter of aqueous solution of tetrazolium red (2,3,5-triphenyltetrazolium chloride, Sigma-Aldrich), 1% (w/v), was added to each tube containing seeds. These tubes were placed in a microfuge tube rack covered with aluminium foil and seeds incubated in an air incubator at 30°C for 24 h. A negative control was performed using water instead of tetrazolium salt. After incubation, seeds were observed for changes in seed colour and seeds imaged using a stereomicroscope (SteREO Discovery V20 microscope, Carl Zeiss

Microscopy) with Zen 2012 (Blue Edition) imaging software, Carl Zeiss Microscopy. For the extraction of formazans, tube contents (seeds and the 1% tetrazolium red solution) were transferred into a mortar using a one ml pipette. Then, tetrazolium red solution was removed from the mortar using a glass pasteur pipette. Seeds were washed with distilled water twice using a pasteur pipette and 1 ml of 95% ethanol added to the seeds in the mortar. Seeds were finely ground using a pestle and the whole ground seed material in ethanol solution transferred to a fresh microfuge tube using a pasteur pipette and the final volume adjusted to 1.5 ml with 95% ethanol. The tubes were immediately centrifuged at 15,000 rpm for 3 min. Supernatant was collected into a spectrophotometer cuvette and the absorbance of the formazan extracts measured at 485nm using a spectrophotometer. As the blank, 95% ethanol solution was used.

3.3.6 Analyses of seed coat mucilage by ruthenium red

Seeds were characterized for the presence of mucilage by the ruthenium red staining assay as described in McFarlane *et al.* (2014). Twenty seeds were placed in a cleaned microcentrifuge tube. After adding 800 µl of an aqueous solution of 0.01% ruthenium red to each tube, seeds were incubated by shaking at 400 rpm for 1 h at room temperature. The ruthenium red solution was removed and replaced with distilled water. Seeds were mounted on a slide in water and observed using a stereomicroscope (SteREO Discovery V20 microscope, Carl Zeiss Microscopy) with Zen 2012 (Blue Edition) imaging software, Carl Zeiss Microscopy.

3.3.7 Analysis of seed coat proanthocyanidins by vanillin

The presence of proanthocyanidins in Arabodopsis seed coat was observed by the vanillin stain as described in Xuan *et al.* (2014). Phenotypes of the mutants were confirmed by

comparing the seed coat color with wild-type. The vanillin reagent (1% w/v) was freshly prepared by mixing with 6 M HCl. Ten dry seeds were placed in a microcentrifuge tube incubated in 800 µl of vanillin reagent at room temperature for 1 h. After incubation, a few seeds were placed on a slide mounted with vanillin reagent and covered with a cover slip. Stained seed coats were observed using a stereomicroscope (SteREO Discovery V20 microscope, Carl Zeiss Microscopy) with Zen 2012 (Blue Edition) imaging software, Carl Zeiss Microscopy.

3.3.8 Seed viability test by tetrazolium salt

All respiring tissues including seed embryos are capable of converting the colourless compound tetrazolium salt (TZ) (2,3,5 triphenyl tetrazolium chloride) to a red coloured, water-insoluble formazan by hydrogen transfer reaction catalysed by cellular dehydrogenases (Verma and Majee, 2013). This concept was used in testing seed viability. TZ enters both living and dead embryos, but only living cells can catalyse the formation of formazan which is non-diffusible and stains the viable seeds red, whereas the absence of respiration prevents formazan production making the dead seeds remain unstained.

After seeds were incubated in 800 mg/L of Cr^{3+} solution, they were rinsed with distilled water for three times. Then, seeds were scarified in 1 ml of scarification solution for 15 min. Scarification solution was made by mixing 20 ml commercial bleach and 100 µl Triton X-100 in 100 ml autoclaved water. To prepare 1% tetrazolium solution, 1 g of 2,3,5 triphenyl tetrazolium chloride was added to an amber coloured bottle and topped with 100 ml of autoclaved distilled water and mixed thouroughly.

Clearing agent (lactophenol solution) was prepared fresh by mixing lactic acid: phenol: glycerine: water in a ratio of 1:1:2:1. Then 800 µl of tetrazolium solution was added to the microcentrifuge tubes and incubated at 30°C for 24 h in the dark. After staining, seeds were washed 2-3 times with distilled water and observed using a stereomicroscope (SteREO Discovery V20 microscope, Carl Zeiss Microscopy) with Zen 2012 (Blue Edition) imaging software, Carl Zeiss Microscopy.

3.3.9 Statistical analysis

Statistical analyses were performed using SYSTAT 13 (Systat Software Inc., Chicago, IL, USA). Two-way ANOVA was not performed as normality was not met in all three mutant categories. Therefore, to evaluate the effect of chromium on seed germination, one-way ANOVA tests were performed separately for each genotype. Prior to analyses, log or second or third power transformation of data was done, if necessary, to obtain a normal distribution. Kruskal-Wallis test was conducted when assumptions of normality were not met.

3.4 Results

Chromium is a relatively abundant and naturally existing element usually found in trivalent (Cr^{3+}) or hexavalent (Cr^{6+}) forms. Chromium toxicity results in growth inhibition in plants. It interferes with several metabolic processes causing toxicity to plants and is manifested in part by reduced seed germination (Hayat *et al.,* 2012). The trivalent form (Cr^{3+}) was used in this study since it is the most abundant form found in chromite mineral (Zayed and Terry, 2003). The Cr^{3+} concentrations used here are similar to the levels found by natural chromite deposits,

such as those in the Ring of Fire region of Northern Ontario (Lukina *et al.,* 2016), as well as contaminated sites.

3.4.1 Mutants used in this study and characterization of their seed coat phenotypes

I used Arabidopsis mutants with alterations in various aspects of mucilage, suberin, cutin, or proanthocyanidin deposition in seed coats to test the relative contributions of each polymer in preventing chromium from reducing seed germination. *Mum4-1, men4-1* and *mum4-1 men4-1* are reduced in mucilage rhamnose content by 10%, 35% and 40%, respectively (Arsovski *et al.,* 2009). *MUM4* codes for RHAMNOSE BIOSYNTHESIS 2, which is involved in the production of rhamnogalacturonan-I (RGI) that makes up pectin in mucilage. *MUCILAGE ENHANCERS (MEN)* are additional genes acting on mucilage synthesis. *Men4* was identified by screening for enhanced mucilage phenotypes in the *mum4* mutant background (Arsovski *et al.,* 2009) Mutants with impaired cellulose synthesis affecting mucilage in the adherent layer (i.e. *cesa5-2*, *cesa9-1, and cesa2-1 cesa5-1 cesa9-1*) (Sullivan *et al.,* 2011; Mendu *et al.,* 2011), mutants with modified mucilage attachment (i.e. *sos5-2, fei2-1,* and *cobl2-1*) (Harpaz-Saad *et al.,* 2011; Ben-Tov *et al.,* 2015), and mutants with defects in mucilage release (i.e. *mum2-1*) (Dean *et al.,* 2007) were also tested. Previous studies found that ruthenium red-stained adherent mucilage from *cesa5-1* more closely resembled that of the *mum3-1* mutant. Therefore, *mum3-1* is an allele of the *CESA5 (CELLULOSE SYNTHASE 5)* gene *(*Sullivan *et al.,* 2011). However, the ruthenium red phenotype that I observed for the *mum3-1* mutant was not comparable to what was previously reported by Sullivan *et al*. (2011). Therefore, for assays reported in this thesis, I used the *cesa5-2* single mutant that has a similar phenotype to that of *cesa5-1* seeds (Sullivan *et al.,* 2011). *CESA2* and *CESA9* serve in radial wall reinforcement, as does *CESA5*, but *CESA5* also functions in

mucilage biosynthesis (Mendu *et al.,* 2011). Mutations in any one of these three genes resulted in lower cellulose content, a loss of cell shape uniformity, and reduced radial wall integrity (Mendu *et al*.,2011). To test the cumulative functional defects of radial wall reinforcement and mucilage biosynthesis, the triple *cesa2-1 cesa5-1 cesa9-1* was used (Mendu *et al.,* 2011).

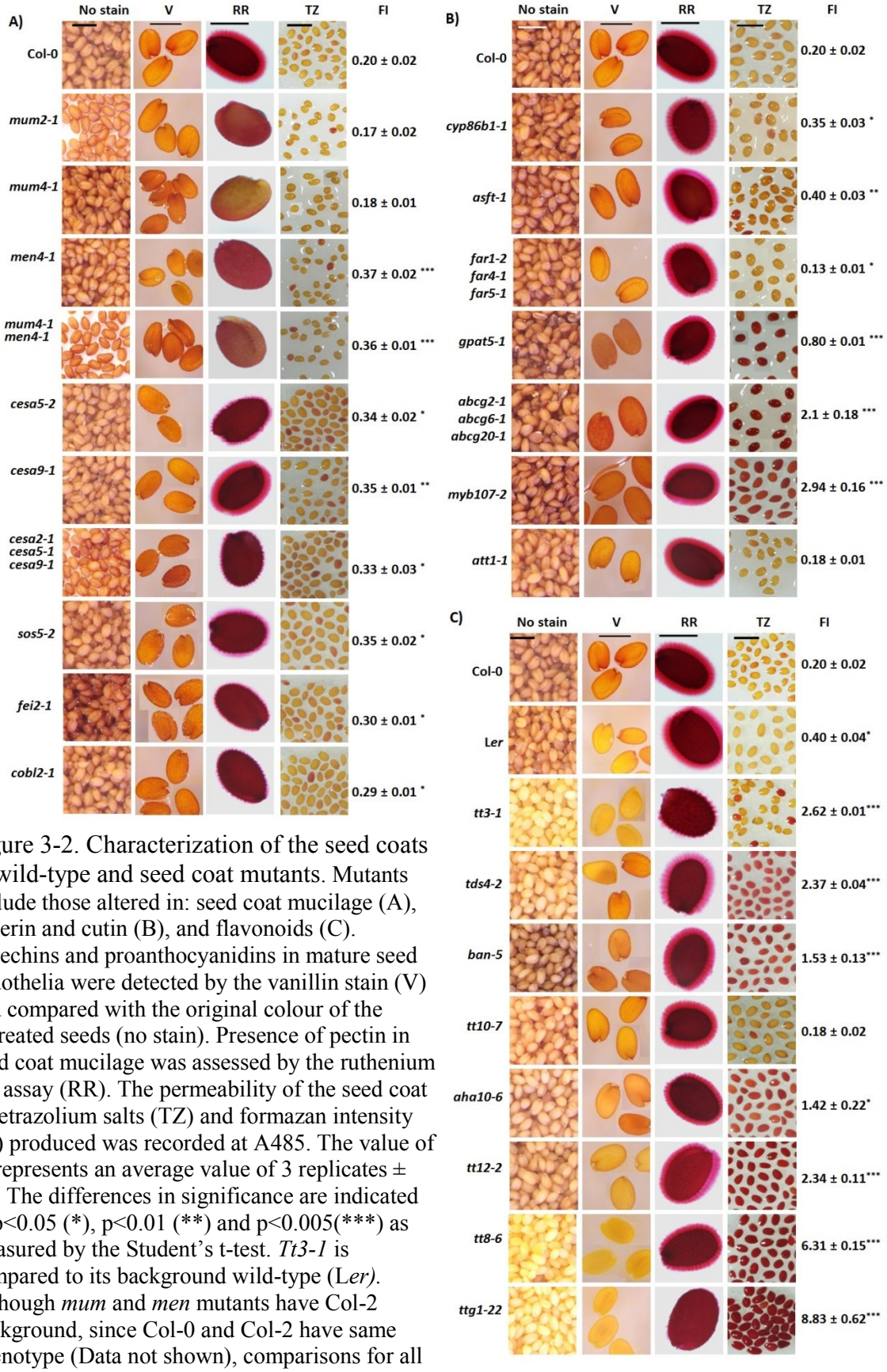

Figure 3-2. Characterization of the seed coats in wild-type and seed coat mutants. Mutants include those altered in: seed coat mucilage (A), suberin and cutin (B), and flavonoids (C). Catechins and proanthocyanidins in mature seed endothelia were detected by the vanillin stain (V) and compared with the original colour of the untreated seeds (no stain). Presence of pectin in seed coat mucilage was assessed by the ruthenium red assay (RR). The permeability of the seed coat to tetrazolium salts (TZ) and formazan intensity (FI) produced was recorded at A485. The value of FI represents an average value of 3 replicates ± SE. The differences in significance are indicated in $p<0.05$ (*), $p<0.01$ (**) and $p<0.005$(***) as measured by the Student's t-test. *Tt3-1* is compared to its background wild-type (L*er).* Although *mum* and *men* mutants have Col-2 background, since Col-0 and Col-2 have same phenotype (Data not shown), comparisons for all other mutants were done with the Col-0. Scale bars: 1 mm for seeds without stain and TZ and 0.05 mm for V and RR.

Characterization of seed coat proanthocyanidins, mucilage and permeability to tetrazolium salt are presented in columns 'V' (vanillin stain), 'RR' (ruthenium red) and 'TZ' (tetrazolium red), respectively, of Figure 3- 2. Seed pigmentation without staining (Figure 3-2, column: 'No stain') varied from brown in the wild-type to very pale yellow (*tt3-1, tt8-6* and *ttg1-22*), to in between very pale yellow and brown (*tds4-2, tt10-7, aha10-6, tt12-2*), to dark brown (*ban-5*). The wild-type L*er* ecotype had reduced levels of mucilage compared to Col-0, as reported previously (Passardi *et al.,* 2007). Further, these results confirmed earlier observations of flavonoid altered mutants (Appelhagen *et al.,* 2014). At least some mucilage release upon imbibition was observed in all genotypes except for the *mum* and *men* mutants, and *ttg1-22.* Compared to WT, intermediate amounts of mucilage were observed in the *cesa* mutants, *sos5-2*, *fei2-1, cob12-1* and *tt3*-1. These phenotypes are in agreement with previous reports (Arsovki *et al.,* 2009; Harpaz-Saad *et al.*, 2011; Mendu *et al.,* 2011).

The tetrazolium penetration assay is commonly used for testing seed coat permeability. Colourless tetrazolium salts turn into red-colored formazan by active dehydrogenases (NADH-dependent reductases) in the embryo of seeds after penetrating the cells of the seed coat (Vishwanath *et al.,* 2014). The investigation of seed coat permeability by the tetrazolium assay revealed that mutants altered in mucilage composition did not have different permeability than WT (Figure 3-2A, columns TZ and FI). Seed coats of the suberin-altered mutants *gpat5-1*, *abcg2-1 abcg6-1 abcg20-1*, and *myb107-2* had higher permeabilities to tetrazolium salts than WT (Figure 3-2B, columns TZ and FI). The mutant *att1-1,* which is altered in seed coat cutin, was not more permeable to tetrazolium salt than WT. Except for *tt10-7*, all the proanthocyanidin mutants had increased level of permeabilities to tetrazolium salt compared to WT. The *tt8-6* and

ttg1-22 mutants had the highest level of tetrazolium salt uptake (Figure 3- 2C, columns TZ and FI).

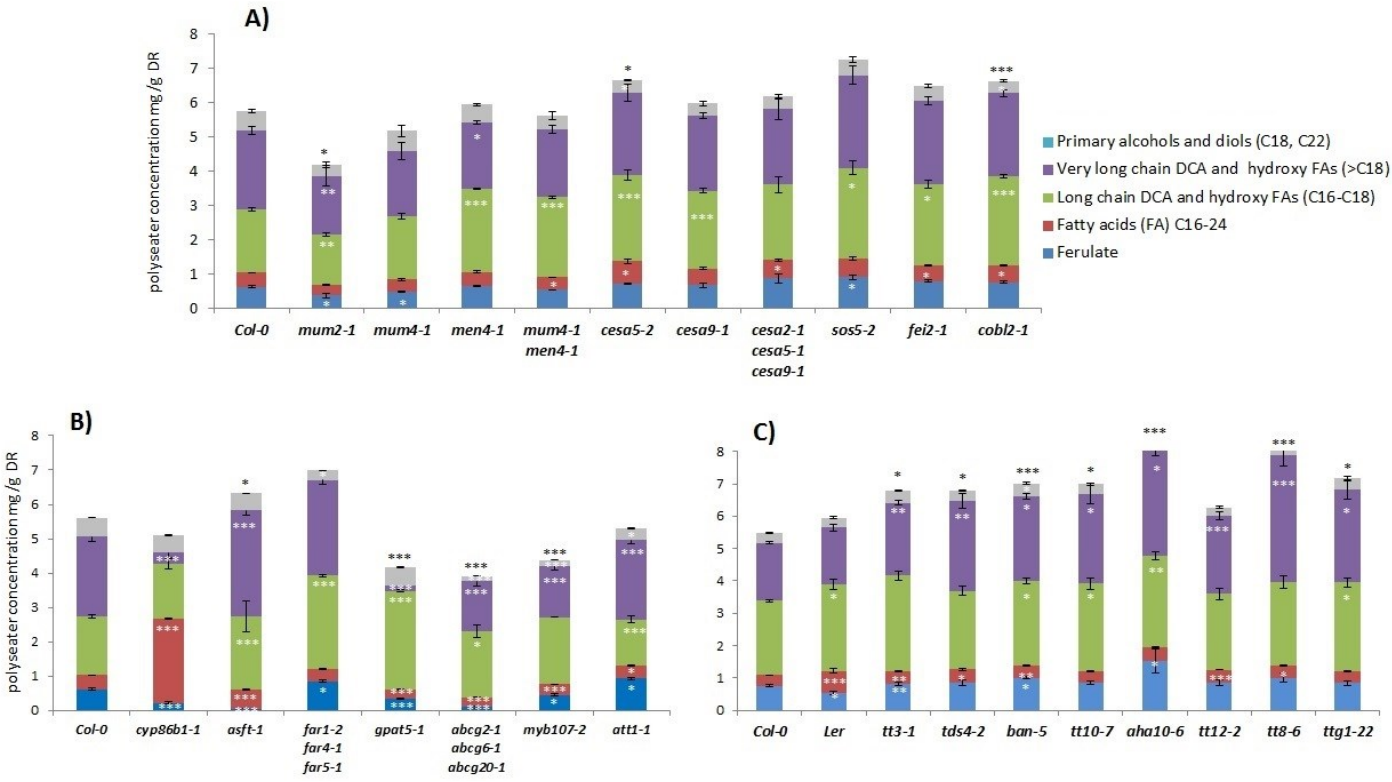

Figure 3-3. Seed coat polyester composition in wild-type and mutants. Mutants primarily altered in seed coat mucilage (A), suberin or cutin (B), or flavonoids (C) were analysed after depolymerisation of solvent-extracted seed residues by base-catalyzed transmethylation and quantified using a GC-FID. Since 20:0 primary alcohol co-elutes with 18:2 DCA, the amount for 20:0 primary alcohol is included with 18:2 DCA. Mean values are shown in milligrams per gram of delipidated dry residue (DR) from 3-4 replicate samples ± SE. Each replicate represented a pool of seeds from 3 individual plants. Compared to wild-type, significance differences in different monomer groups are indicated in white asterisks and for total amount in black asterisks at $p<0.05$ (*), $p<0.01$ (**), and $p<0.005$(***) by Student's t-test. *Tt3-1* is compared to its background wild-type (L*er)*, whereas all other mutants are compared with Col-0. DCA= Dicarboxylic acids, FAs=Fatty acids.

Table 3-1. Monomer composition of seed coat polyesters in wild-type (Col-0) and mucilage mutants. Data represent monomer amounts from depolymerization of solvent-extracted seed residues by base-catalyzed transmethylation and quantified using a GC-FID. Since 20:0 primary alcohol co-elutes with 18:2 DCA, the amount for 20:0 primary alcohol is included with 18:2 DCA. Mean values are shown in milligrams of polyester per gram of delipidated dry residue from 3-4 replicate samples ± standard error (SE). Each replicate represented a pool of seeds from 3 individual plants.

Polyester	Col-0	*mun2-1*	*mum4-1*	*men4-1*	*mum4-1 men4-1*	*cesa5-2*	*cesa9-1*	*cesa2-1 cesa5-1 cesa9-1*	*sos5-2*	*fei2-1*	*cobl2-1*
Hydroxy cinnamic acids											
Trans ferulate	0.616±0.03	0.358±0.06	0.464±0.01	0.647±0.02	0.533±0.00	0.696±0.02	0.656±0.06	0.856±0.13	0.696±0.02	0.777±0.03	0.741±0.04
Trans coumarate	0.061±0.00	0.045±0.00	0.047±0.00	0.054±0.00	0.063±0.00	0.083±0.01	0.073±0.01	0.125±0.03	0.083±0.01	0.094±0.01	0.101±0.00
Fatty acid methyl esters											
C16:0	0.141±0.01	0.110±0.00	0.116±0.00	0.138±0.00	0.137±0.01	0.356±0.08	0.216±0.05	0.272±0.04	0.356±0.08	0.173±0.01	0.201±0.02
C18:0	0.019±0.00	0.001±0.00	0.000±0.00	0.000±0.00	0.000±0.00	0.025±0.00	0.019±0.00	0.017±0.01	0.025±0.00	0.011±0.01	0.013±0.00
C20:0	0.041±0.00	0.030±0.00	0.036±0.00	0.041±0.00	0.040±0.00	0.050±0.00	0.046±0.00	0.038±0.01	0.050±0.00	0.048±0.00	0.048±0.00
C22:0	0.061±0.00	0.046±0.00	0.056±0.01	0.070±0.02	0.022±0.00	0.069±0.01	0.067±0.00	0.059±0.02	0.069±0.01	0.070±0.00	0.071±0.00
C24:0	0.144±0.00	0.115±0.01	0.155±0.02	0.150±0.00	0.154±0.01	0.165±0.01	0.147±0.01	0.145±0.03	0.165±0.01	0.167±0.01	0.155±0.01
Dicarboxylic acid methyl esters											
C16:0	0.120±0.00	0.099±0.02	0.131±0.00	0.199±0.00	0.191±0.00	0.212±0.03	0.163±0.01	0.136±0.05	0.212±0.03	0.161±0.01	0.188±0.01
C18:2	0.358±0.01	0.321±0.02	0.448±0.01	0.357±0.01	0.348±0.01	0.667±0.04	0.643±0.03	0.560±0.07	0.667±0.04	0.648±0.04	0.780±0.01
C18:1	0.260±0.02	0.221±0.03	0.311±0.01	0.510±0.01	0.498±0.02	0.291±0.02	0.250±0.01	0.225±0.03	0.291±0.02	0.250±0.01	0.300±0.01
C18:0	0.053±0.00	0.042±0.01	0.054±0.00	0.074±0.00	0.067±0.00	0.072±0.00	0.058±0.00	0.049±0.02	0.072±0.00	0.061±0.00	0.067±0.00
C20:0	0.033±0.01	0.017±0.00	0.022±0.00	0.033±0.00	0.028±0.00	0.029±0.00	0.023±0.00	0.020±0.01	0.029±0.00	0.023±0.00	0.027±0.00
C22:0	0.147±0.01	0.103±0.01	0.122±0.01	0.191±0.01	0.194±0.00	0.239±0.02	0.217±0.01	0.198±0.04	0.239±0.02	0.216±0.01	0.243±0.00
C24:0	0.882±0.06	0.727±0.13	0.744±0.11	0.539±0.01	0.593±0.04	0.949±0.12	0.819±0.04	0.837±0.16	0.949±0.12	0.932±0.04	0.915±0.05
ω-Hydroxy fatty acids											
C16:0	0.085 ± 0.00	0.091±0.06	0.079±0.00	0.127±0.00	0.113±0.00	0.112±0.01	0.092±0.00	0.077±0.03	0.112±0.01	0.097±0.00	0.109±0.01
10, 16-OH C16:0	0.039 ± 0.01	0.040±0.01	0.052±0.01	0.092±0.01	0.069±0.01	0.291±0.06	0.174±0.03	0.233±0.03	0.291±0.06	0.167±0.01	0.193±0.03
C18:2	0.133 ± 0.01	0.107±0.01	0.127±0.01	0.145±0.00	0.129±0.00	0.141±0.01	0.133±0.00	0.150±0.02	0.141±0.01	0.141±0.01	0.148±0.01
C18:1	0.197 ± 0.01	0.132±0.01	0.178±0.01	0.376±0.01	0.332±0.00	0.211±0.01	0.177±0.01	0.180±0.01	0.211±0.01	0.183±0.01	0.209±0.01
C18:0	0.014 ± 0.00	0.012±0.00	0.011±0.00	0.015±0.00	0.011±0.00	0.020±0.00	0.016±0.00	0.012±0.00	0.020±0.00	0.016±0.00	0.020±0.00
9,10.18-OH C18:1	0.584 ± 0.08	0.417±0.10	0.446±0.08	0.518±0.00	0.581±0.02	0.500±0.14	0.561±0.02	0.584±0.05	0.500±0.14	0.636±0.03	0.598±0.01
C20:0	0.029 ± 0.00	0.015±0.00	0.024±0.00	0.050±0.00	0.040±0.00	0.054±0.00	0.051±0.00	0.039±0.01	0.054±0.00	0.048±0.00	0.061±0.00
C22:0	0.264 ± 0.02	0.157±0.03	0.149±0.04	0.421±0.01	0.384±0.03	0.245±0.03	0.303±0.01	0.283±0.01	0.245±0.03	0.315±0.03	0.321±0.00
C24:0	0.959 ± 0.03	0.689±0.11	0.850±0.16	0.704±0.01	0.750±0.06	0.875±0.10	0.777±0.05	0.823±0.06	0.875±0.10	0.901±0.04	0.852±0.05
Alcohols and diols											
C18:0 (1-OH)	0.089 ± 0.01	0.055±0.02	0.059±0.00	0.158±0.00	0.138±0.01	0.027±0.01	0.041±0.03	0.077±0.03	0.027±0.01	0.075±0.03	0.029±0.01
C22:0 (1-OH)	0.259 ± 0.04	0.156±0.02	0.259±0.04	0.253±0.00	0.174±0.08	0.195±0.00	0.188±0.01	0.184±0.01	0.195±0.00	0.213±0.01	0.202±0.01
C22:0 (1,22-OH)	0.205 ± 0.01	0.116±0.04	0.265±0.14	0.121±0.03	0.066±0.05	0.139±0.01	0.116±0.03	0.119±0.02	0.139±0.01	0.133±0.03	0.126±0.02
Total	**5.791±0.13**	**4.222±0.48**	**5.206±0.39**	**5.983±0.1**	**5.653±0.28**	**6.710±0.22**	**6.027±0.1**	**6.297±0.33**	**7.317±0.24**	**6.557±0.28**	**6.720±0.08**

Lipid polyesters have been characterized previously in the mutants impaired in seed coat suberin and cutin, but the composition of seed coat lipid polyesters in mutants altered in mucilage or proanthocyanidins are not known. Except for *mum2-1*, *cesa5-2* and *cobl2-1*, the total amounts and monomer composition of seed coat lipid polyesters of the mucilage mutants were the same as WT (Figure 3-3A, Table 3-1). Compared to WT, *mum2-1* had reduced overall lipid polyester amount with significant reductions in long-chain and very-long-chain α,ω-dicarboxylic and ω-hydroxy fatty acids, as well as ferulic acid. Conversely, relative to WT, *cesa5-2* and *cobl2-1* had increased total seed polyester amounts with relative increases in fatty acids (C16-C24), long-chain α,ω-dicarboxylic and ω-hydroxy fatty acids, and primary fatty alcohols (Figure 3-3A). Compared to WT, the mutants *gpat5-1*, *abcg2-1 abcg6-1 abcg20-1* and *myb107-2* had decreased amounts of total seed coat polyester with reductions in almost all the monomer groups (Figure 3-3B). These results are consistent with previous observations (Beisson *et al.,* 2007; Yadav *et al.,* 2014; Gou *et al.,* 2017). As reported previously by Molina *et al.* (2009), the ferulate component of aliphatic suberin was absent in *asft-1* (Figure 3-3B). Relative to WT, the total seed coat polyester amount was not altered in *cyp86b1-1* and *far1-2 far4-1 far5-1.* In *cyp86b1-1,* relative to the monomer composition in WT, there was a significant reduction in very-long chain α,ω-dicarboxylic and ω-hydroxy fatty acids and ferulates, and an increase in fatty acids (Figure 3-3B). *Far1-2 far4-1 far5-1* showed major deduction in 18:0 and 22:0 fatty alcohols and 22:0 diol (Table 3-2). Since 20:0 alcohol co-eluted with 18:2 DCA in acetylated derivatives, 20:0 primary alcohol was not quatified separately in all mutants. Although *att1-1 and att1-2* showed slight changes in individual seed polyester amounts, the total polyester loads remained closer to WT (Table 3-2).

Table 3-2. Monomer composition of seed coat polyesters in wild-type (Col-0) and suberin- and cutin-altered mutants. Data represent monomer amounts from depolymerization of solvent-extracted seed residues by base-catalyzed transmethylation and quantified using a GC-FID. Since 20:0 primary alcohol co-elutes with 18:2 DCA, the amount for 20:0 is included with 18:2 DCA. Mean values are shown in mg of polyester per gram of delipidated dry residue from 3-4 replicate samples ± standard error (SE). Each replicate represented a pool of seeds from 3 individual plants.

Polyester	**Col-0**	***cyp86b1-1***	***cyp86b1-2***	***asft-1***	***asft-2***	***far1-2 far4-1 far5-1***	***gpat5-1***	***gpat5-2***	***abcg2-1 abcg6-1 abcg20-1***	***myb107-2***	***att1-1***	***att1-2***
Hydroxy cinnamic acids												
Trans ferulate	0.616 ± 0.03	0.212 ± 0.03	0.271 ± 0.02	0.021 ± 0.00	0.007 ± 0.00	0.841 ± 0.06	0.333 ± 0.02	0.396 ± 0.03	0.093 ± 0.00	0.446 ± 0.03	0.930 ± 0.07	1.033 ± 0.08
Trans coumarate	0.061 ± 0.00	0.031 ± 0.01	0.034 ± 0.00	0.004 ± 0.00	0.003 ± 0.00	0.076 ± 0.01	0.038 ± 0.00	0.042 ± 0.00	0.012 ± 0.01	0.027 ± 0.00	0.096 ± 0.00	0.112 ± 0.01
Fatty acid methyl esters												
C16:0	0.141 ± 0.01	0.141 ± 0.01	0.147 ± 0.00	0.139 ± 0.00	0.136 ± 0.00	0.124 ± 0.01	0.136 ± 0.00	0.160 ± 0.01	0.138 ± 0.01	0.096 ± 0.00	0.151 ± 0.01	0.123 ± 0.01
C18:0	0.019 ± 0.00	0.022 ± 0.00	0.019 ± 0.00	0.014 ± 0.00	0.017 ± 0.00	0.004 ± 0.00	0.015 ± 0.00	0.016 ± 0.00	0.021 ± 0.00	0.007 ± 0.00	0.016 ± 0.00	0.014 ± 0.00
C20:0	0.041 ± 0.00	0.056 ± 0.01	0.057 ± 0.00	0.054 ± 0.00	0.045 ± 0.00	0.033 ± 0.00	0.029 ± 0.00	0.031 ± 0.00	0.041 ± 0.00	0.037 ± 0.00	0.039 ± 0.00	0.041 ± 0.00
C22:0	0.061 ± 0.00	0.343 ± 0.02	0.386 ± 0.01	0.102 ± 0.00	0.099 ± 0.01	0.051 ± 0.00	0.037 ± 0.00	0.043 ± 0.00	0.043 ± 0.00	0.067 ± 0.01	0.047 ± 0.00	0.046 ± 0.00
C24:0	0.144 ± 0.00	1.902 ± 0.09	2.036 ± 0.06	0.267 ± 0.01	0.288 ± 0.03	0.149 ± 0.01	0.060 ± 0.00	0.062 ± 0.00	0.047 ± 0.00	0.098 ± 0.01	0.106 ± 0.00	0.093 ± 0.01
Dicarboxylic acid methyl esters												
C16:0	0.120 ± 0.00	0.102 ± 0.01	0.119 ± 0.00	0.256 ± 0.00	0.185 ± 0.01	0.127 ± 0.01	0.233 ± 0.01	0.277 ± 0.01	0.219 ± 0.00	0.058 ± 0.01	0.119 ± 0.01	0.132 ± 0.00
C18:2	0.358 ± 0.01	0.275 ± 0.04	0.340 ± 0.01	0.451 ± 0.01	0.490 ± 0.01	0.975 ± 0.04	0.331 ± 0.00	0.348 ± 0.01	0.399 ± 0.02	0.686 ± 0.04	0.109 ± 0.00	0.092 ± 0.01
C18:1	0.260 ± 0.02	0.213 ± 0.01	0.263 ± 0.00	0.349 ± 0.00	0.353 ± 0.01	0.326 ± 0.01	0.640 ± 0.02	0.689 ± 0.01	0.360 ± 0.02	0.222 ± 0.02	0.098 ± 0.00	0.107 ± 0.00
C18:0	0.053 ± 0.00	0.052 ± 0.00	0.060 ± 0.00	0.093 ± 0.00	0.062 ± 0.00	0.046 ± 0.00	0.048 ± 0.00	0.053 ± 0.00	0.193 ± 0.01	0.024 ± 0.00	0.042 ± 0.01	0.056 ± 0.01
C20:0	0.033 ± 0.01	0.015 ± 0.00	0.026 ± 0.01	0.043 ± 0.00	0.027 ± 0.00	0.033 ± 0.01	0.028 ± 0.00	0.029 ± 0.00	0.114 ± 0.00	0.018 ± 0.00	0.051 ± 0.00	0.056 ± 0.00
C22:0	0.147 ± 0.01	0.018 ± 0.00	0.028 ± 0.00	0.485 ± 0.00	0.333 ± 0.02	0.218 ± 0.02	0.018 ± 0.01	0.037 ± 0.01	0.386 ± 0.03	0.220 ± 0.00	0.160 ± 0.01	0.203 ± 0.01
C24:0	0.882 ± 0.06	0.100 ± 0.02	0.141 ± 0.00	1.791 ± 0.06	1.322 ± 0.14	1.220 ± 0.13	0.071 ± 0.03	0.099 ± 0.01	0.771 ± 0.05	0.513 ± 0.07	0.891 ± 0.05	0.932 ± 0.08
ω-Hydroxy fatty acids												
C16:0	0.085 ± 0.00	0.060 ± 0.00	0.072 ± 0.00	0.040 ± 0.00	0.029 ± 0.01	0.083 ± 0.01	0.210 ± 0.01	0.253 ± 0.01	0.059 ± 0.00	0.030 ± 0.00	0.106 ± 0.00	0.112 ± 0.00
10, 16-OH C16:0	0.039 ± 0.01	0.040 ± 0.01	0.068 ± 0.01	0.061 ± 0.01	0.059 ± 0.02	0.079 ± 0.02	0.054 ± 0.00	0.100 ± 0.02	0.020 ± 0.00	0.092 ± 0.02	0.109 ± 0.03	0.059 ± 0.02
C18:2	0.133 ± 0.01	0.146 ± 0.01	0.159 ± 0.00	0.128 ± 0.00	0.131 ± 0.01	0.326 ± 0.01	0.117 ± 0.00	0.125 ± 0.01	0.100 ± 0.01	0.134 ± 0.01	0.154 ± 0.01	0.170 ± 0.00
C18:1	0.197 ± 0.01	0.153 ± 0.01	0.192 ± 0.00	0.143 ± 0.00	0.117 ± 0.01	0.238 ± 0.01	0.667 ± 0.03	0.754 ± 0.01	0.119 ± 0.00	0.115 ± 0.01	0.202 ± 0.00	0.234 ± 0.01
C18:0	0.014 ± 0.00	0.026 ± 0.00	0.030 ± 0.00	0.010 ± 0.00	0.012 ± 0.00	0.008 ± 0.00	0.019 ± 0.00	0.025 ± 0.00	0.020 ± 0.00	0.007 ± 0.00	0.024 ± 0.00	0.031 ± 0.00
9,10.18-OH C18:1	0.584 ± 0.08	0.519 ± 0.09	0.661 ± 0.02	0.609 ± 0.03	0.742 ± 0.06	0.508 ± 0.16	0.522 ± 0.04	0.560 ± 0.06	0.436 ± 0.01	0.593 ± 0.02	0.390 ± 0.09	0.506 ± 0.02
C20:0	0.029 ± 0.00	0.037 ± 0.00	0.049 ± 0.01	0.030 ± 0.00	0.023 ± 0.00	0.035 ± 0.01	0.007 ± 0.00	0.007 ± 0.00	0.039 ± 0.00	0.039 ± 0.00	0.042 ± 0.00	0.052 ± 0.00
C22:0	0.264 ± 0.02	0.082 ± 0.01	0.092 ± 0.00	0.181 ± 0.02	0.096 ± 0.01	0.199 ± 0.06	0.000 ± 0.00	0.000 ± 0.00	0.047 ± 0.00	0.299 ± 0.00	0.220 ± 0.03	0.272 ± 0.01
C24:0	0.959 ± 0.03	0.077 ± 0.00	0.104 ± 0.00	0.552 ± 0.01	0.492 ± 0.06	1.077 ± 0.13	0.064 ± 0.00	0.071 ± 0.00	0.094 ± 0.00	0.403 ± 0.06	0.958 ± 0.05	0.875 ± 0.05
Alcohols and diols												
C18:0 (1-OH)	0.089 ± 0.01	0.122 ± 0.00	0.119 ± 0.01	0.094 ± 0.00	0.113 ± 0.01	0.021 ± 0.00	0.118 ± 0.00	0.123 ± 0.01	0.052 ± 0.00	0.025 ± 0.01	0.070 ± 0.00	0.089 ± 0.01
C22:0 (1-OH)	0.259 ± 0.04	0.378 ± 0.02	0.409 ± 0.01	0.204 ± 0.00	0.180 ± 0.01	0.149 ± 0.01	0.215 ± 0.00	0.224 ± 0.00	0.024 ± 0.00	0.083 ± 0.00	0.149 ± 0.01	0.140 ± 0.01
C22:0 (1,22-OH)	0.205 ± 0.01	0.007 ± 0.00	0.009 ± 0.00	0.206 ± 0.00	0.116 ± 0.02	0.115 ± 0.03	0.203 ± 0.01	0.211 ± 0.00	0.082 ± 0.00	0.071 ± 0.00	0.125 ± 0.03	0.142 ± 0.00
Total	**5.791±0.13**	**5.127±0.35**	**5.892±0.08**	**6.328±0.12**	**5.480±0.37**	**7.063±0.55**	**4.212±0.16**	**4.734±0.07**	**3.926±0.13**	**4.411±0.17**	**5.30±0.22**	**5.71±0.21**

In the proanthocyanidin mutant category, the total seed coat polyester amounts in nearly all mutants were moderately increased compared to WT, with the exception of *tt12-2* that had the same lipid polyester content as WT (Figure 3-3C, Table 3-3).

Table 3-3. Monomer composition of seed coat polyesters in wild-type (Col-0) and flavonoid altered mutants. Data represent monomer amounts from depolymerization of solvent-extracted seed residues by base-catalyzed transmethylation and quantified using a GC-FID. Since 20:0 primary alcohol co-elutes with 18:2 DCA, the amount for 20:0 is included with 18:2 DCA. Mean values are shown in milligrams of polyester per gram of delipidated dry residue from 3-4 replicate samples ± standard error (SE). Each replicate represented a pool of seeds from 3 individual plants.

	Col-0	***Ler***	***tt3-1***	***tds4-2***	***ban-5***	***tt10-7***	***aha10-6***	***tt12-2***	***tt8-6***	***ttg1-22***
Hydroxy cinnamic acids										
Trans ferulate	0.758±0.03	0.544±0.05	0.816±0.05	0.850±0.16	1.000±0.03	0.841±0.06	1.538±0.37	0.860±0.08	1.001±0.14	0.839±0.08
Trans coumarate	0.044±0.00	0.073±0.01	0.092±0.01	0.057±0.02	0.060±0.00	0.076±0.01	0.104±0.02	0.097±0.01	0.100±0.01	0.096±0.02
Fatty acid methyl esters										
C16:0	0.105±0.00	0.359±0.06	0.082±0.01	0.116±0.00	0.100±0.01	0.124±0.01	0.124±0.01	0.124±0.01	0.094±0.01	0.113±0.02
C18:0	0.013±0.00	0.038±0.00	0.012±0.00	0.014±0.00	0.015±0.00	0.004±0.00	0.003±0.00	0.007±0.00	0.005±0.00	0.006±0.00
C20:0	0.032±0.00	0.076±0.00	0.060±0.00	0.041±0.01	0.033±0.00	0.033±0.00	0.019±0.01	0.045±0.00	0.033±0.00	0.033±0.00
C22:0	0.045±0.00	0.075±0.01	0.067±0.00	0.059±0.00	0.066±0.00	0.051±0.00	0.060±0.01	0.068±0.00	0.055±0.00	0.050±0.00
C24:0	0.131±0.00	0.121±0.01	0.167±0.00	0.184±0.01	0.184±0.01	0.149±0.01	0.204±0.03	0.155±0.00	0.195±0.01	0.163±0.02
Dicarboxylic acid methyl esters										
C16:0	0.116±0.01	0.173±0.02	0.127±0.00	0.140±0.04	0.157±0.01	0.127±0.01	0.153±0.02	0.137±0.01	0.154±0.00	0.158±0.02
C18:2	0.723±0.02	0.912±0.06	1.265±0.04	0.732±0.04	0.832±0.08	0.975±0.04	0.799±0.09	0.744±0.02	0.698±0.00	0.647±0.04
C18:1	0.268±0.01	0.226±0.01	0.295±0.01	0.311±0.01	0.363±0.02	0.326±0.01	0.421±0.05	0.354±0.02	0.344±0.00	0.355±0.02
C18:0	0.044±0.00	0.066±0.01	0.045±0.00	0.053±0.01	0.052±0.00	0.046±0.00	0.039±0.01	0.044±0.00	0.054±0.00	0.054±0.01
C20:0	0.029±0.00	0.033±0.00	0.033±0.00	0.028±0.01	0.030±0.00	0.033±0.01	0.014±0.01	0.018±0.00	0.052±0.03	0.028±0.01
C22:0	0.165±0.01	0.234±0.01	0.243±0.01	0.249±0.01	0.284±0.01	0.218±0.02	0.324±0.04	0.239±0.01	0.318±0.03	0.287±0.04
C24:0	0.687±0.01	0.666±0.05	0.897±0.04	1.107±0.14	1.014±0.03	1.220±0.13	1.806±0.25	1.063±0.06	1.711±0.11	1.126±0.12
ω-Hydroxy fatty acids										
C16:0	0.080±0.01	0.089±0.01	0.085±0.00	0.090±0.01	0.108±0.01	0.083±0.01	0.107±0.01	0.089±0.01	0.102±0.00	0.094±0.01
10, 16-OH C16:0	0.053±0.00	0.402±0.11	0.068±0.01	0.094±0.01	0.076±0.01	0.079±0.02	0.139±0.03	0.085±0.01	0.088±0.02	0.140±0.05
C18:2	0.208±0.00	0.183±0.02	0.412±0.02	0.217±0.02	0.309±0.03	0.326±0.01	0.246±0.02	0.204±0.02	0.246±0.01	0.214±0.02
C18:1	0.196±0.01	0.145±0.01	0.187±0.01	0.220±0.01	0.273±0.01	0.238±0.01	0.318±0.02	0.249±0.02	0.255±0.01	0.261±0.02
C18:0	0.012±0.00	0.026±0.01	0.008±0.00	0.010±0.00	0.016±0.00	0.008±0.00	0.005±0.00	0.007±0.00	0.010±0.00	0.011±0.00
9,10.18-OH C18:1	0.606±0.02	0.462±0.01	0.467±0.09	0.564±0.09	0.413±0.11	0.508±0.16	0.590±0.11	0.431±0.13	0.636±0.19	0.811±0.06
C20:0	0.038±0.00	0.050±0.00	0.031±0.00	0.035±0.00	0.047±0.00	0.035±0.01	0.039±0.01	0.033±0.00	0.043±0.00	0.060±0.02
C22:0	0.194±0.01	0.287±0.02	0.233±0.03	0.250±0.03	0.275±0.05	0.199±0.06	0.271±0.04	0.182±0.04	0.415±0.11	0.250±0.02
C24:0	0.672±0.01	0.510±0.04	0.817±0.03	1.033±0.13	0.964±0.04	1.077±0.13	1.288±0.18	0.895±0.06	1.413±0.11	1.003±0.11
Alcohols and diols										
C18:0 (1-OH)	0.021±0.00	0.005±0.00	0.012±0.00	0.016±0.00	0.021±0.00	0.021±0.00	0.008±0.00	0.012±0.00	0.009±0.00	0.020±0.00
C22:0 (1-OH)	0.164±0.00	0.179±0.01	0.205±0.01	0.171±0.00	0.224±0.01	0.149±0.01	0.188±0.02	0.146±0.00	0.206±0.01	0.207±0.01
C22:0 (1,22-OH)	0.129±0.01	0.121±0.02	0.159±0.03	0.134±0.03	0.167±0.02	0.115±0.03	0.162±0.01	0.117±0.02	0.174±0.03	0.143±0.03
Total	**5.535±0.14**	**6.055±0.29**	**6.886±0.33**	**6.772±0.59**	**7.082±0.27**	**7.063±0.56**	**8.969±0.39**	**6.405±0.47**	**8.411±0.31**	**7.172±0.13**

3.4.2 Seed germination responses to chromium

3.4.2.1 Mucilage deficient mutants have moderately increased sensitivity to Cr^{3+}

To evaluate the effect of seed coat mucilage on Cr^{3+} sensitivity, I tested mutants with decreased overall amounts of mucilage biosynthesis (*mum4-1* > *men4* > *men4 mum4*). All *mum* and *men* mutants were in the Col-2 ecotype background. However, there was no difference in germination responses between Col-0 and Col-2 (data not shown). Hence, the comparisons were done with Col-0. Relative to *mum4, men4* has reduced mucilage content, while the double mutant *men4-1 mum4-1* has less mucilage than *mum4* or *men4* (Arsovski *et al.,* 2009). Unlike wild-type, seed germination of each mutant at 400 and 800 mg/L Cr^{3+} were significantly decreased relative to the control condition (0 mg/L Cr^{3+}) (Figure 3-4A), but the time course analysis indicated that there was no significant difference in germination between 400 and 800 mg/L (Figure 3-4A). The reduction in germination at day 15 increased as the amount of mucilage decreased in the three mutants (i.e. germination was 85% of control for *mum4-1, 80%* for *men4-1*, and 77% for *men4 mum4* ($p < 0.005$ by ANOVA) (Figure 3-4B). Compared to wild-type, tetrazolium salt uptake in *men4-1* and *mum4-1 men4-1* seeds were significantly increased, while *mum4-1* was not (Figure 3-2A, column TZ and FI). Some seeds in *mum* and *men* mutants displayed loss of viability when incubated in 800 mg/L Cr^{3+} (Figure 3-5). This indicates that some of the embryos in *mum* and *men* mutants were damaged by a high amount of Cr^{3+} passing through the seed coat. Similarly, germination at day 15 in *mum4-1* and *mum4-1 men4-1* mutants were significantly affected by Cr^{3+}. However, a proportion of the seeds was still viable after exposure to high Cr^{3+} concentrations. Therefore mutants reduced in RGI appear to be moderately affected by Cr^{3+}.

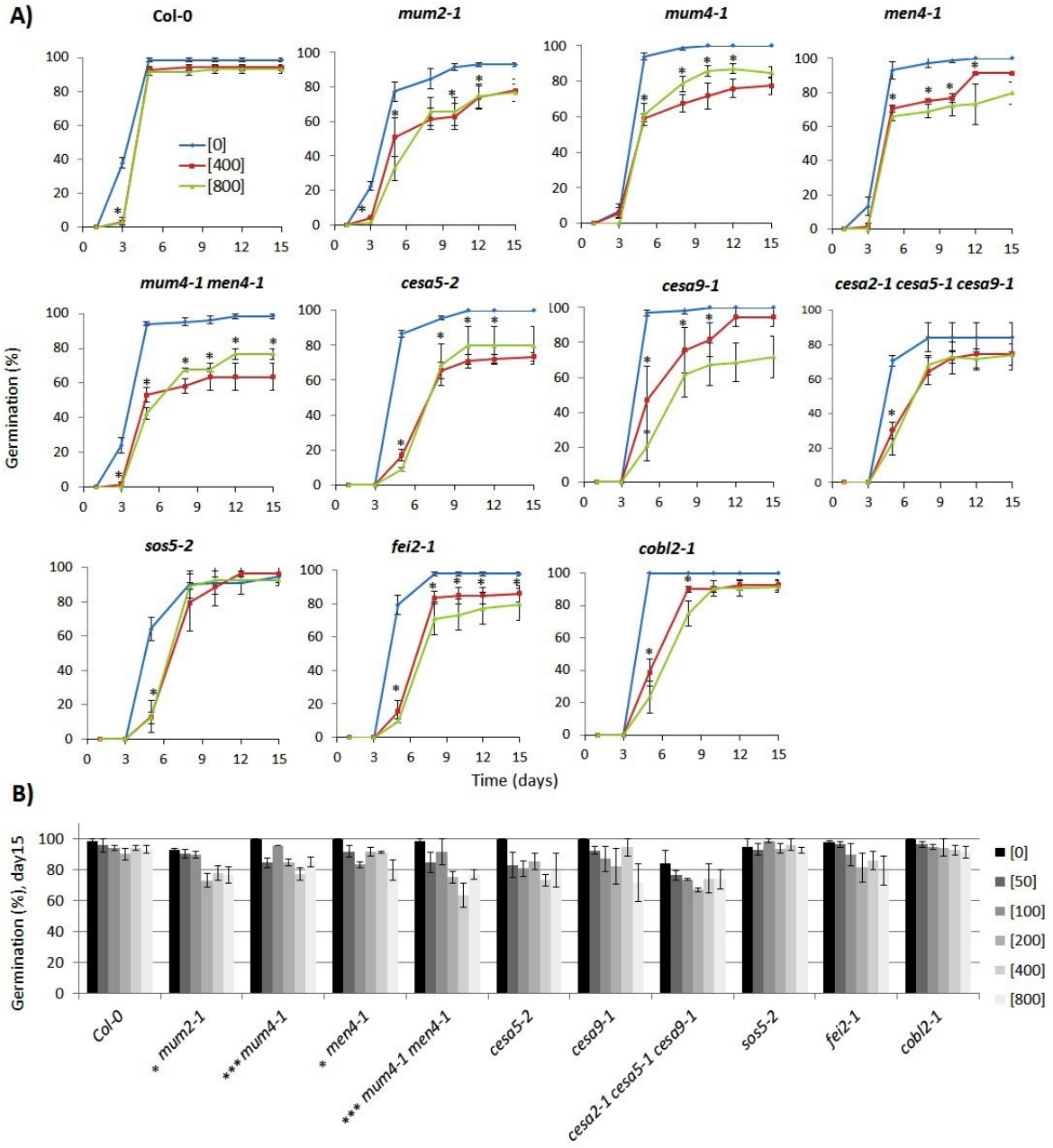

Figure 3-4. Comparison of germination responses to chromium treatment in wild-type (Col-0) and mutants altered in mucilage composition. A) Time course analysis of cumulative germination percentages (%) after incubation in 0, 400 and 800 mg/L Cr^{3+} concentrations; asterisks represent significant differences between [0] and [400] by student t-test at $P<0.05$. B)

Cumulative seed germination percentages on D15 after incubation in 0, 50, 100, 200, 400 and 800 mg/L Cr^{3+}. Values represent mean value ± standard error (SE), n=3, 25 seeds per replicate. One-way ANOVA was performed to test the chromium effect on individual genotypes (Table 3-4). The statistical significance at $p<0.05$ (*), $p<0.01$ (**) or $p<0.005$(***) are indicated in front of mutant.

The *MUM2* gene codes for a β-galactosidase enzyme, which is involved in mucilage modification following synthesis. The mutation causes defects in mucilage release but it contains the same level of mucilage as WT (Dean *et al.,* 2007). To learn if mucilage release affects seed germination, I used *mum2-1*. The dose effect of Cr^{3+} was significant in the ANOVA of *mum2-1*, which was associated with around 25% reduction in germination at each high 200, 400 and 800 mg/L Cr^{3+} concentration (Figure 3-4B) and reduction in seed viability at 800 mg/L Cr^{3+} relative to the control (Figure 3-5). However, it is not possible to conclude that reduced germination in *mum2-1* was related to the defects in mucilage release because *mum2-1* also has a reduced amount of seed polyester load (Figure 3-3A).

CESA2, CESA5 and *CESA9* are necessary for the stabilization of mucilage by production of rays of cellulose micro-fibrils that helps to keep the adherent-mucilage layer attached to the seed surface (Mendu *et al.,* 2011; Sullivan *et al*., 2011). They are also involved in secondary cell wall development (columella) (Francoz *et al.,* 2015; Harpaz- Saad *et al.,* 2011). To determine if the defects in mucilage attachment and alterations in columellate structure affect germination, I used *cesa5-2, cesa9-1* and *cesa2-1 cesa5-1 cesa9-1* mutants that are associated with alterations in seed columella and cellulose composition of the adherent mucilage layer (Sullivan *et al*., 2011; Ben-Tov *et al.,* 2015; Harpaz-Saad *et al.,* 2011). Further, in these mutants the mucilage is

not well attached to the seed (Mendu *et al.,* 2011). Disruption to *FEI2, SOS5* or *COBL2* genes also leads to reductions in the rays of mucilage cellulose of the adherent layer, which alters the structure of the mucilage. Therefore, defects similar to *cesa* mutants were reported in *sos5-2, fei2-1* and *cobl2-3* mutants (Harpaz-Saad *et al.,* 2011; Ben-Tov *et al.,* 2015). All the mutants that are defective in mucilage attachment did not show a difference in germination by Cr^{3+} treatment compared to WT control. When these seeds were incubated in 800 mg/L Cr^{3+}, viability was not affected (Figure 3-5A). Therefore, seed coat collumella does not appear to be important for the seed coat protective function against Cr^{3+}. Even though the overall mucilage amount was reduced in *fei2-1, sos5-2* and *cobl2-1*, relative to WT, the germination % on day15 was roughly equal and not affected by Cr^{3+} (Figure 3-4B), meaning the relative mucilage amount does not necessarily affect germination in the presence of Cr^{3+}. These results suggest that proper attachment of mucilage on the seed is not important for the protection against Cr^{3+}.

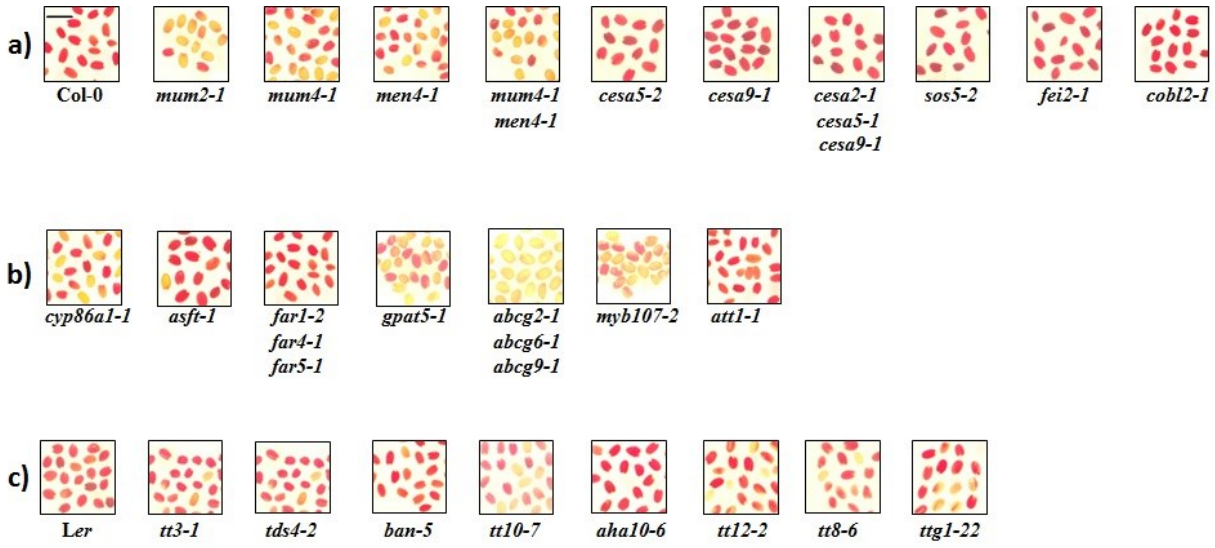

Figure 3-5. Results of the seed viability test. Seed viability was tested by incubating seeds in tetrazolium salts after exposure to 800 mg/L Cr^{3+}. Representative images of results for mucilage

related (a), suberin and cutin related (b), and proanthocyanidin related (c) mutants. Seeds in red indicate viable seeds and brown are dead seeds.

3.4.2.2 Suberin deficient mutants, but not a cutin deficient mutant, were severely affected by Cr^{3+} toxicity

Suberin and cutin are cell wall-associated lipid-based polymers that form important physical barriers and restrict the movement of water and solutes (Graça, 2015). In the suberin biosynthetic pathway, CYP86B1 is a cytochrome P450 enzyme that primarily hydroxylates very-long-chain fatty acids (mostly C22 and C24 chains) to yield ω-hydroxy fatty acids. In the *cyp86b1-1* loss-of-function mutant, C22- and C24 ω-hydroxy fatty acids and α,ω-dicarboxylic fatty acids are strongly reduced (Compagnon *et al.,* 2009; Molina *et al.,* 2009). ASFT is a feruloyl transferase and the mutant *asft-1* lacks ferulate in seed coat suberin and has slightly lower amounts of hydroxy-containing aliphatics (Molina *et al.,* 2009). The *FAR1*, *FAR4* and *FAR5* genes encode for alcohol-forming fatty acyl reductases that are specifically involved in the production of fatty alcohols found in suberin and its associated waxes (Domergue *et al.,* 2010; Vishwanath *et al.,* 2013). C22:0, C20:0 and C18:0 fatty alcohols are reduced in *far1 far4 far5* triple mutants (Vishwanath *et al*. 2013). *GPAT5* encodes for an acyl-CoA: glycerol-3-phosphate acyltransferase specifically involved in suberin biosynthesis (Beisson *et al.,* 2007). Very-long-chain α,ω-dicarboxylic fatty acids and ω-hydroxy fatty acids are reduced in the *gpat5-1* mutant (Figure 3-3B). Therefore, the above four mutants (*cyp86b1-1*, *asft-1*, *far1-2 far4-1 far5amiRNA,* and *gpat5-1*) were used to test if alterations in suberin seed coat composition increased the sensitivity to Cr^{3+} with regards to seed germination. MYB107 is a positive general regulator of gene expression for seed coat suberin synthesis (Gou *et al.,* 2017; Lashbrooke *et al.,* 2017). Loss-of-function mutations in *MYB107* therefore have lower seed coat suberin accumulation (all

monomers), altered suberin lamellar structure, and consequently have higher seed coat permeability and susceptibility to abiotic stresses (Gou *et al.,* 2017; Lashbrooke *et al.,* 2017). To form an effective suberin barrier in roots and seed coats, ABCG half-transporters (ABCG2, ABCG6, and ABCG20) are required in Arabidopsis. To investigate if global changes in suberin content or altered seed coat suberin lamellar structure is important for resisting chromium toxicity, the *myb107-2* and *abcg2-1 abcg6-1 abcg20-1* were used in this study. *ATT1* encodes CYP86A2, a cytochrome P450 monooxygenase catalyzing fatty acid oxidation in the cutin biosynthetic pathway (Xiao *et al.,* 2004). Loss-of-function *att1* mutations have about 70% reductions in each of 18:2 and 18:1 α,ω-dicarboxylic fatty acids in Arabidopsis seed coat (Molina *et al.,* 2008). To investigate if cutin in seed coat is important for protection against Cr^{3+}, the *att1-1* mutant was used.

Except for *cyp86b1-1* and *far1-2 far4-1 far5-1*, chromium treatment had a major effect on germination in all mutants altered in seed coat suberin levels relative to wild-type (Figure 3-6B). The time course analysis shows that seed germination in *gpat-5-1, abcg2-1 abcg6-1 abcg20-1* and *myb107-2* were severely affected at 400 mg/L Cr^{3+} and further reduced at 800 mg/L Cr^{3+} (Figure 3-5A). For all three mutants, germination on day15 was reduced with increasing concentrations of Cr^{3+} (Figure 3-6B). These mutants also displayed very high permeabilities to tetrazolium salt compared to WT (Figure 3-2B, column TZ and FI). When *abcg2-1 abcg6-1 abcg20-1* seeds were incubated with 800 mg/L Cr^{3+}, all the seeds lost their viability (Figure 3-5b). This indicates that the embryo tissues were totally damaged by chromium toxicity in this mutant. The compositional changes related to reduced ferulate in *asft-1* caused an intermediate effect on seed germination in the presence of higher Cr^{3+} concentrations. Seed germination or viability in the cutin-specific mutant *att1-1* was not affected by Cr^{3+}.

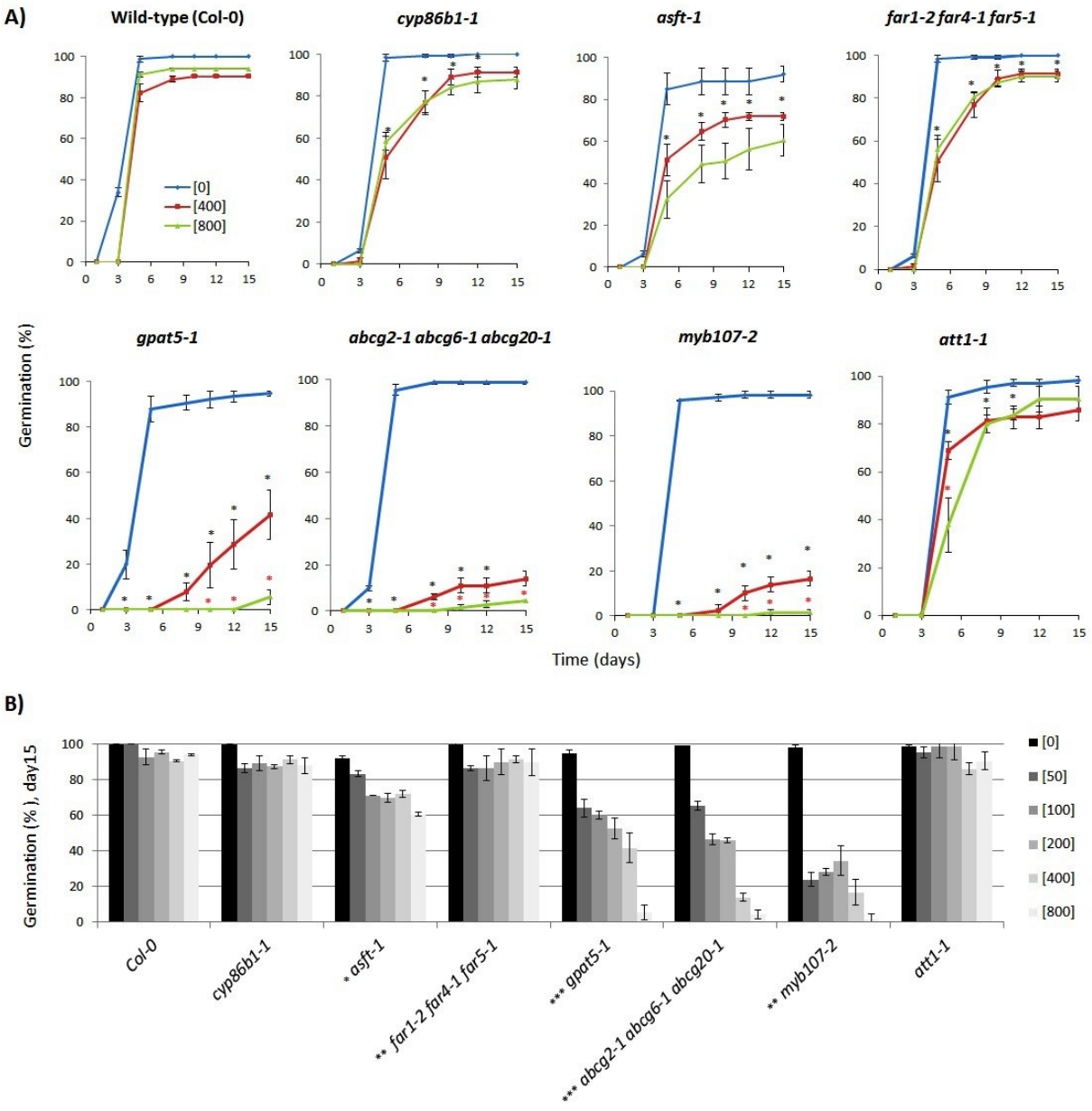

Figure 3-6. Comparison of germination responses to chromium treatment in wild-type (Col-0) and mutants altered in seed coat suberin or cutin composition. A) Time course analysis of cumulative germination percentages (%) after incubation in 0, 400 and 800 mg/L Cr^{3+} concentrations; asterisks represent significant differences between [0] and [400] mg/L Cr^{3+} in black and between [400] and [800] mg/L Cr^{3+} in red by student t-test at $P<0.05$.B). Cumulative seed germination percentages on day 15 (D15) after incubation in 0, 50, 100, 200, 400 and 800

mg/L Cr^{3+}. Values represent mean value ± standard error (SE), n=3, 25 seeds per replicate. One-way ANOVA was performed to test the chromium effect on individual genotypes (Table 3-S6). The significant differences at $p<0.05$ (*), $p<0.01$ (**) and $p<0.005$ (***) are indicated by asterisks in front of mutants.

3.4.2.3 Proanthocyanidin mutants were moderately affected by Cr^{3+} toxicity

Flavonoids are plant secondary metabolites whose biosynthetic pathway includes biosynthesis of monomeric anthocyanins and flavonols, and polymeric proanthocyanidins (PAs) (Abrahams *et al.,* 2003). The brown pigmentation in WT seeds are mainly due to PAs (also known as condensed tannins), which are the end products of the flavonoid biosynthetic pathway (Debeaujon *et al.,* 2000). The *TT3, TDS4* and *BAN* genes are involved in the PA biosynthetic pathway. *TT3* encodes dihydroflavonol 4-reductase (DFR), which represents a branch point in the flavonoid pathway, separating flavonol biosynthesis from anthocyanin- and PA-specific biosynthesis (Pourcel *et al.,* 2005). *TDS4* encodes for leucoanthocyanidin dioxygenase (LDOX) to produce anthocyanin precursors of PA. *Tds4* loss-of-function mutants have generally reduced PA levels (Abrahams *et al.,* 2003). LDOX precedes BANYULS (BAN) in the PA biosynthetic pathway and BAN is an anthocyanidin reductase (Pourcel *et al.,* 2005; Albert *et al.,* 1997). The *ban* loss-of-function mutant is characterized by its ability to produce enhanced amounts of anthocyanins at the expense of PA. The *ban* mutant displays dark brown pigmentation (Figure 3-2C, column under without stain). To determine whether alterations in PA or anthocyanin abundances affect seed germination in the presence of Cr^{3+}, I used the *tt3-1, tds4-2* and *ban-5* mutants. The *TTG1* and *TT8* genes encode regulatory factors for the expression of *BAN* (Baudry *et al.,* 2004). The loss-of-function *tt8-6* and *ttg1-22* mutants have pale yellow pigmentation in

their seed coats indicating that they have reduced PA content relative to WT (Figure 3-2C, columns No stain and V). The *ttg1-22* mutant was also affected in the columella structure that attached the mucilage to the seed and, therefore, very little mucilage was observed (Figure 3-2C, column RR). To test if these major alterations made the seeds more vulnerable to Cr^{3+} toxicity, I used the *tt8-6* and *ttg1-22* mutants. In the last step of PA biosynthesis, *TT10* is involved in the oxidation of PAs to brown colour pigments (Pourcel *et al.,* 2005). I therefore included *tt10-7* to determine if PA oxidation affects the imposition of impermeability to Cr^{3+}. The *TT12* gene is involved in the vacuolar accumulation of PA precursors and its mutation causes an absence of major flavonols and PAs in the seed (Marinova *et al.,* 2007). Autoinhibited H-ATPase isoform 10 (AHA10) is expressed in developing seeds and is involved in vacuole formation (Baxter *et al.,* 2005). A knock-out mutation of *AHA10* results in many small vacuoles, instead of a large central vacuole, and in light-coloured seeds presumably because PAs can no longer accumulate in the vacuole. A quantitative analysis of *aha10* mutants revealed a 100-fold reduction in PA (Baxter *et al.,* 2005). The effect of low / absent PA vacuolar accumulation on seed germination in the presence of Cr^{3+} was tested using *aha10-6* and *tt12-2* mutants.

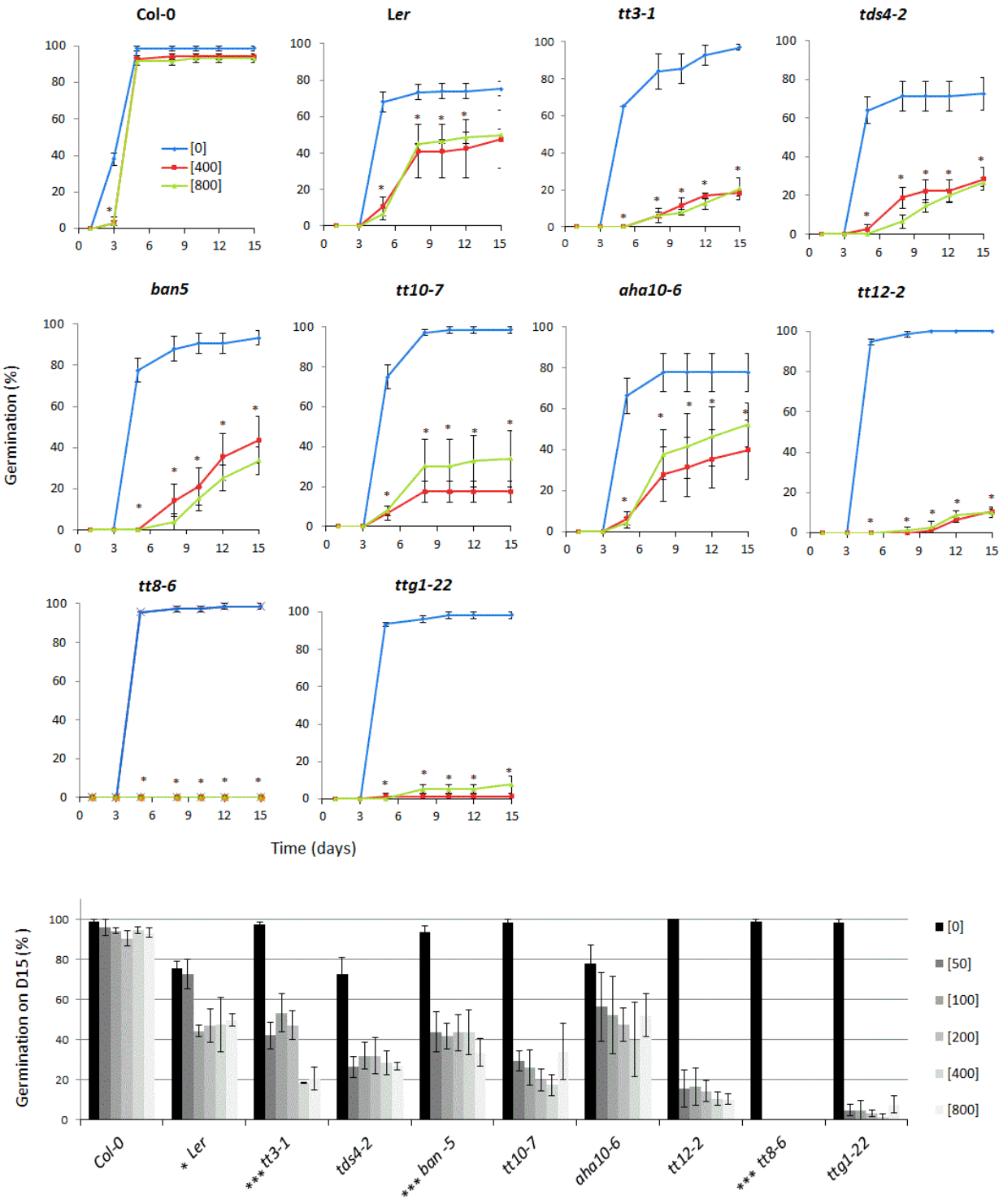

Figure 3-7. Comparison of germination responses to chromium treatment in wild-type (Col-0) and mutants altered in seed coat flavonoids. A) Time course analysis of cumulative germination

percentages (%) after incubation in 0, 400 and 800 mg/L Cr^{3+} concentrations; asterisks represent significant differences between [0], [400] or [800] mg/L Cr^{3+} by Student t-test at $p<0.05$. B). Cumulative seed germination percentages on day 15 (D15) after incubation in 0, 50, 100, 200, 400 and 800 mg/L Cr^{3+}. Values represent mean value ± standard error (SE), n=3, 25 seeds per replicate. One-way ANOVA was performed to test the chromium effect on individual genotypes (Table 3-S6). The significance at $p<0.05$ (*), $p<0.01$ (**) and $p<0.005$(***) is indicated by asterisks in front of mutant name.

For tests of germination in the presence of chromium, both Col-0 and L*er* ecotypes were tested here because one of the mutants (*tt3-1*) was in the L*er* background rather than the Col-0 background. The L*er* ecotype did not reach 100% germination even under control conditions (0 mg/L Cr^{3+}) by day 15. With the introduction of 50 mg/L Cr^{3}, *tds4-2, tt10-7, aha10-6, tt12-2* and *ttg1-22* mutants dropped their germination percentages. However, germination was not affected further by increasing Cr^{3+} concentrations (i.e. at 100, 200, 400 and 800 mg/L) indicating there was no dose effect by Cr^{3+} (Figure 3-7A and 7B). Statistical analysis by one-way ANOVA further confirms that the dose effect is not significant in these mutants (Table 3-4). Some mutants had massive reductions in germination (*tt8-6* and *ttg1-22*), while the others had germination reduced to around 20-50% at 800 mg/L Cr^{3+} after 15 days (Figure 3-7B). In the time course analysis, there was no difference in germination rates between 400 and 800 mg/L Cr^{3+} in all mutants (Figure 3-7A), which is different from what was observed in mutant seeds altered in suberin (*gpat-5-1, abcg2-1 abcg6-1 abcg20-1*, and *myb107-2*) (Figure 3-5A). In other words, the dose effect was significant in *gpat-5-1, abcg2-1 abcg6-1 abcg20-1*, and *myb107-2* . Even though statistical analysis indicated *tt3-1* and *ban-5* has a dose effect on germination, the average values

in germination at the highest Cr^{3+} level were higher than those recorded in suberin deficient mutants.

Table 3-4. Results of statistical analysis to test whether the germination percentages change with increasing chromium doses in individual genotypes. One-way ANOVA was performed for normally distributed data and non-parametric Kruskal-Wallis (KW) test when not normal. The significance at $p<0.05$ (*), $p<0.01$ (**) and $p<0.005$(***) is indicated by asterisks

Genotype	Type of analysis	P-value
Col-0	KW	0.168
mum2-1	KW	0.019*
mum4-1	ANOVA	0.000***
men4-1	ANOVA	0.017*
mum4-1 men4-1	ANOVA	0.001***
cesa5-2	ANOVA	0.166
cesa9-1	ANOVA	0.439
cesa2-1 cesa5-1 cesa9-1	ANOVA	0.542
sos5-2	KW	0.632
fei2-1	KW	0.227
cobl2-1	KW	0.277
cyp86b1	ANOVA	0.053
asft-1	ANOVA	0.020*
far1-2 far4-1 far5-1	ANOVA	0.009**
gpat5-1	ANOVA	0.009**
abcg2-1 abcg6-1 abcg20-1	ANOVA	0.000***
myb107-2	KW	0.015**
att1-1	KW	0.194
L*er*	ANOVA	0.301

tt3-1	ANOVA	0.038*
tds4-2	KW	0.000***
ban-5	ANOVA	0.003***
tt10-7	KW	0.132
aha10-6	ANOVA	0.590
tt12-2	KW	0.175
tt8-6	KW	0.005***
ttg1-22	KW	0.109

The results describe above prompted us to test the viability of seeds in samples incubated with 800 mg/L Cr^{3+} . During respiration, all tissues are capable of converting a colourless tetrazolium red (2,3,5 triphenyl tetrazolium chloride) stain to a red coloured water-insoluble formazan by hydrogen transfer reaction catalysed by the cellular dehydrogenases (Verma and Majee 2013). Due to the formation of formazan, the live tissues turn red in colour. This concept is used to confirm the viability of embryos. Embryo viability was tested after incubating seeds at 800 mg/L Cr^{3+} and by exposing the seeds to a tetrazolium red solution after stratification. The results from this assay revealed that most of the embryos in of *tt3-1* and *ban-5* were still viable, indicating that Cr^{3+} did not damage the embryos similar to suberin-deficient mutants (Figure 3-5c). Additionally, although *tt8-6* did not geminate at any of the Cr^{3+} levels investigated (Figure 3-7), most of the seed embryos remained viable (Figure 3-5c).

3.5 Discussion

The data presented here revealed that major decreases in Arabidopsis seed coat suberin (i.e. in mutants *gpat5-1*, *abcg 2-1 abcg 6-1 abcg 20-1* and *myb107-2*) impacts both seed germination and embryo viability in the presence of high Cr^{3+} concentrations. Reduced seed germination and embryo viability were correlated with increased permeability to tetrazolium salt in these mutants. Therefore, I conclude that seed coat suberin plays an important role on the imposition of impermeability to Cr^{3+}. Compared to WT, the more specific alterations in suberin monomer composition in the *cyp86b1-1*, *asft-1* and *far1-2 far4-1 far5-1* were not associated with major changes in seed germination or embryo viability, and therefore compositional perturbations in the suberin chemical make-up, even if affecting one type of constituent, does not necessarily lead to a defect in the suberin barrier properties, at least to this heavy metal. In addition to reduced total suberin content reported in *abcg 2-1 abcg 6-1 abcg 20-1* and *myb107-2*, defects in suberin lamellae structure were observed previously (Yadav *et al*., 2014; Gou *et al.,* 2017). However, the structure of the seed coat suberin lamellae in *gpat5-1* has not yet been analysed. Considering the major permeability defect and high Cr^{3+} sensitivity of the *gpat5-1* mutant, I would expect major deformations in the ultra-structure of suberin lamellae in seeds of *gpat5-1*. Germination responses of the mutants altered in flavonoid biosynthesis suggests that Cr^{3+} may alter seed dormancy and hence it is not reasonable to conclude whether PAs form an effective protective barrier against Cr^{3+} penetration. Most of the flavonoid (proanthocyanidin) mutants had higher amounts of viable seeds than dead seeds, even when incubated with 800 mg/L Cr^{3+} when germination was severely reduced (Figure 3-6B; Figure 3-5). In other words, seed germination was decreased but not embryo viability, unlike the most affected suberin mutants (*gpat-5-1, abcg2-1 abcg6-1 abcg20-1*, and *myb107-2*) (Figure 3-5B). Except for *tds4-2*,

all proanthocyanidin mutants reached the non-dormant state before germination and achieved complete germination (100%) under control condition (0 mg/L Cr^{3+}). However when incubated in 800 mg/L Cr^{3+}, even though they reduced their germination, most of the embryos remained viable. Additionally, the absence of germination observed in *tt8-6* was not associated with complete loss in seed viability when incubated in 800 mg/L Cr^{3+}. A possible reason for this observation could be that seeds reached a secondary dormancy state after the introduction of Cr^{3+}. Secondary dormancy is referred to a dormant state that is induced in non-dormant seeds by conditions unfavourable for germination (Bewley, 1997). In most of the proanthocyanidin mutants, there were no significant differences in percentage of germination between 50-100 mg/L, 100-200 mg/L, 200-400 mg/L, or 400-800 mg/L Cr^{3+}. This non- responsiveness in germination with increasing chromium concentration (i.e. 50 to 800 mg/L) observed in proanthocyanidin mutants further indicates that seeds may have reached the secondary dormancy state. The layer of endosperm located in-between the flavonoid-containing endothelium and the embryo is responsible for controlling seed dormancy by means of regulating two phytohormones, abscisic acid and gibberellic acid (Debeaujon *et al.,* 2007). In PA deficient mutants, Cr^{3+} may enter to the endosperm but not the embryo. The mechanism of Reactive Oxygen Species (ROS) distribution and sensing in seed embryos are involved in dormancy release (Rajjou *et al.*, 2012). The absence of favourable environmental conditions, such as presence of heavy matals in the environment, can induce secondary dormancy in imbibed seeds. Heavy-metals can alter the ROS distribution in seeds and subsequently impact dormancy release (Shahid *et al*., 2014). Therefore, Cr^{3+} may affect seed dormancy in PA mutants by penetrating through the PA defective endothelium without causing any damage to the embryo. On the other hand, Cr^{3+} can kill the suberin mutants as the the embryos are directly in contact with Cr^{3+}

through the chalazal region. A comprehensive study on gene activity during the development of Arabidopsis seeds showed that the endosperm in the chalazal region is functionally different to the endosperm in the peripheral region (Belmonte *et al.,* 2012). At seed maturity, suberin gene expression has been observed near the chalazal region (Molina *et al.,* 2008). Therefore, in suberin mutants, Cr^{3+} can directly kill the embryo. The results furrher support the idea that TZ penetration assay does not seem to reflect Cr^{3+} penetration. However, a small proportion of seeds in most of the proanthocyanidin mutants also showed seeds losing their viability in the presence of 800 mg/L Cr^{3+}. It is possible that in those seeds, some amount of Cr^{3+} could have damaged the embryos after penetrating through the defective proanthocyanidin layer before they reached the physiological dormancy state as speculated above (i.e. in this instance it should be secondary dormancy). However, it was obvious that seed viability in proanthocyanidin mutants was not completely lost in the presence of 800 mg/L Cr^{3+}. Therefore, if the seeds reached a secondary dormancy state, it is not possible to conclude that seed coat proanthocyanidins provide a physical protectitve function against Cr^{3+} toxicity.

To interpret the combined results from suberin deficient mutants and proanthocyanidin-altered mutants, it is important to reveal the route of Cr^{3+} entry to the embryo through different seed coat constituents. During seed development, the chalaza forms the connection between seed embryo and mother plant (Brown *et al*., 1999). At maturity, the chalazal/hilum region of the Arabidopsis seed gets sealed off with suberin (Beisson *et al.,* 2007). In suberin deficient loss-of-function *gpat5* mutants, tetrazolium salt penetration occurred first through the chalazal region (Beisson *et al.*, 2007). Therefore, in suberin deficient mutants, Cr^{3+} could have rapidly reached the embryo through the chalazal region. This speculation is further supported by the higher permeability to tetrazolium salt observed in all mutants defective in seed coat suberin (*gpat-5-1,*

abcg2-1 abcg6-1 abcg20-1, and *myb107-2*). However, seed polyester analysis of *tds4-2, ban-5, aha10-6 tt8-6* and *ttg1-22* had higher amounts of seed coat suberin, but yet showing higher permeabilities to tetrazolium salt than wild-type. It is then intriguing how tetrazolium salt or Cr^{3+} could have reached the embryo in proanthocyanidin-altered mutants, which have higher amounts of seed coat suberin. In addition to the chalazal area, suberin is detected in the inner layer of the outer integument (oi1) of the seed coat (Molina *et al.,* 2009). At maturity, Arabidopsis seed coat consists of dead cells corresponding to the five cell layers that originate from the ovule integuments (Beisson *et al.*, 2007). Although the epidermis (oi2) has the thick cell walls of the collumella and the mucilage secretory cells, during maturation, the layers below the epidermis collapse and get crushed together (Haughn and Chaudhury 2005). This process in proanthocyanidin mutants may leave gaps in-between the cells in suberin-containing integuments and cause Cr^{3+} to penetrate through the the non-chalazal region of the seed (i.e. proanthocyanidin-deficient endothelial layer). These observations suggest that suberin deficient mutants were more permeable to tetrazolium salt and Cr^{3+} at the chalazal region and proanthocyanidin mutants were more permeable at non-chalazal region. Therefore, I speculate that proanthocyanidins and suberin have different roles in imparting protection against Cr^{3+}. Perhaps, both suberin and proanthocyanidins are necessary for preventing the passage of molecules/ions through the seed coat, but in different locations. Thus, increasing one of the polymers may not compensate for the reduced amounts in the other. However, this model contradicts the previous observation of increased tetrazolium salt penetration through the non-chalazal region in the *fatb* mutant that has reduced seed coat polyesters (Molina *et al.,*2008). The *FATB* gene *(At1g08510)* encodes a plastid-localized acyl–acyl carrier protein (ACP) thioesterase with high activity towards palmitoyl–ACP (Salas and Ohlrogge, 2002). *FatB* mutant

seed polyesters has reductions (65–85%) in 16-hydroxy- and 10,16-dihydroxypalmitate and 1,16-hexadecane dioate. Further, similar to *gpat5-1*, *fatB* seeds had 45–65% reductions in the levels of straight-chain C20–24 suberin aliphatic components causing increased permeability to tetrazolium salt (Molina *et al.,* 2008). However, authors also express the view that due to some discrete differences in minor components of suberin aliphatic monomers and due to pleiotropic effects in *fatB,* changes in permeability may occur between *gpat5-1* and *fatB*.

The tetrazolium assay is commonly used to determine the permeability of the seed coat. Embryos turn red when formazans are produced by NADH-dependent reductases upon exposure to it non-colored tetrazolium salts (Berridge *et al.,* 1996). Although it was not tested with the studied mutants, it has been found that seed coat waxes do not contribute to seed coat impermeability to tetrazolium salts (Beisson *et al.,* 2007). The results of suberin deficient mutants show an negative relationship between seed coat suberin content and permeability to tetrazolium. That is, when mutants had major reductions in seed coat suberin content, they showed increased permeability to tetrazolium salt. This was confirmed by several studies previously (Beisson *et al.,* 2007; Yadav *et al.,* 2014; Gou *et al.,* 2017). However, results indicate that seed coat permeability to tetrazolim salts cannot always be used to monitor the permeability to Cr^{3+} unless the route of Cr^{3+} entry to the seed is known. Mutant *mum2-1* seeds did not have a significant increase in tetrazolium salt uptake (Figure 3-2A, column TZ and FI), despite having a reduced amount of seed coat suberin. Further, the flavonoid altered mutants *tds4-2, ban-5, aha10-6 tt8-6* and *ttg1-22* had higher amounts of seed coat suberin and their permeability to tetrazolium salt was greater than wild-type. Further, the results of proanthocyanidin mutants indicate that decreases in germination after exposure to Cr^{+3} was not always associated with increase in permeability to tetrazolium salt. Similarly, a previous study revealed that seed coat

permeability to water is best not measured by tetrazolium salts (Debeaujon *et al*., 2000). When non-dormant seeds did not stain red with tetrazolium salt, it was concluded that the tetrazolium assay is not appropriate to access water entry into the seed (Debeaujon *et al.,* 2000). Differences in the size of the TZ molecule and Cr^{3+} may be another reason for the contradictory results of the TZ penetration pattern in PA mutants and effects on embryo viability in the presence of Cr^{3+}. There are differences in thetwo methodologies assessing embryo viability versus seed coat permeability using tetrazolium salt. The seed coat is not intact when testing the embryo viability, whereas in the seed coat permeability it is intact. Also, when testing seed coat permeability, differences may occur in the intensities of formazan formed, depending on the route of TZ movement into the embryo in PA and suberin mutants.

The mutant *tt10-7* is not altered in PA or suberin amounts. Therefore, the results confirm that the permeability to tetrazolium salt in *tt10-7* was similar to wild-type and the oxidation of PA is not critical in changing the PA barrier property. The phenotypic deformations observed in *sos5-2, fei2-1* and *cobl2-1* mucilage mutants did not directly correlate with reduced seed germination. *Mum2-1* showed reduced germination and failed to release mucilage upon contact with water. *Mum2-1* had lower seed coat suberin content than wild-type. Therefore, it is likely that reduced suberin, but not the alteration in mucilage release, affected seed germination in *mum2-1*. Consequently, I cannot suggest that mucilage release directly affects germination in the presence of Cr^{3+}.

In summary, this study revealed that seed coat suberin protects the embryo against Cr^{3+} toxicity. Further, the results provide evidence of risks associated with the persistence of seeds with relatively low level of seed coat suberin in soils with high levels of chromium (Cr^{3+}), which may in turn affect species diversity. Further, this study provides insights into the implications of

heavy metal penetration through the seed coat of foods important for human consumption. During harvest and storage, seed contaminaton can occur due to inappropriate post harvest management. For example, rice being the first food given to babies has to be free from toxic materials. Seed coat or the pericarp in rice and the husk provide protection to the rice grain. Application of chemicals to eliminate pests in the field and storage is a general practice in the third word countries. Therefore, the protection of the food grain by the seed coat against toxic chemicals is important. However, if chromium is trapped in the seed coat, which is often consumed as a part of some food grains (e.g. pericarp in rice), there are health concerns for human consumption.

Chapter 4: Summary and Future Directions

Recent and rapid industrialization has led to many environmental issues, such as climate change and pollution of natural resources. Abiotic environmental factors such as drought and salinity are significant plant stressors that negatively impact plant development and productivity causing serious agricultural yield losses (Tester and Langridge, 2010; Agarwal *et al.,* 2013). Therefore, scientists are increasingly looking for solutions to improve world food security through classical and modern crop breeding techniques as well as improved agronomic practices. Genetic improvement of crops to better resist abiotic stresses requires detailed knowledge of the ways that plants naturally resist these stresses, such that they can be targeted.

Suberin is a hydrophobic hetero-polymer deposited in the cell walls of various internal and external tissues in plants. It plays multiple roles at plant-environment interfaces. One such function is forming a barrier for uncontrolled water and solute movement. However, there is a gap in our understanding of precisely how suberin protects plants from the variety of potential external stressors. The primary purpose of my thesis was to explore some of the specific roles of root suberin and seed coat suberin in the model plant *Arabidopsis thaliana* in relation to abiotic stress tolerance. All land plants deposit suberin in root endodermis and in periderm tissues. The primary root contains endodermis and the outer covering of the above-ground and below-ground tissues that undergo secondary development form a periderm. The second chapter of this thesis investigates the effects of drought and salinity stresses on suberin mutants, with the aim to understand the role of suberin and it associated waxes in drought and salinity stress tolerance mechanisms. In the future, this knowledge may guide crop improvement by genetic engineering.

Contamination of land or water by toxic materials is another major environmental issue.

Mining of chromium is concentrated in many parts of the world such as South Africa, several Asian countries, and potentially in Northern Ontario, Canada. High levels of chromium in soils can impact plant growth, including germination of seeds. Plants growing in such areas need a mechanism to cope with elevated levels of chromium in soil. The seed is an important organ of a plant as it carries the genetic make up of the plant to the next generation. The seed coat that covers the embryo is critical for its survival under unfavourable conditions. The seed coat is a complex organ that contains different polymeric substances such as mucilage, suberin, cutin, and proanthocyanidins. They are thought to act as barriers to different solutes. The third chapter of this thesis explored the roles of seed coat on seed germination under high chromium levels. By taking advantage of Arabidopsis mutants with alterations in different seed coat polymers, I investigated the functions of seed coat in relation to chromium stress tolerance.

4.1 Composition and ultra-structure of suberin play an important role in tolerance to drought and salinity in *Arabidopsis thaliana*

Apart from the constitutive deposition of suberin in root endodermis and periderm, environmental stresses also can induce suberin production in Arabidopsis roots (Barberon *et al*.,2016; Franke *et al*., 2012; Doblas *et al*., 2017). In the first part of Chapter 2, I analyzed the pattern of suberin accumulation over time in Arabidopsis WT (Col-0) after being exposed to different water stress conditions. The use of mutants defective in suberin composition is an important first step towards the understanding of the role of suberin in stress tolerance. The objective of the second part of the chapter was to identify the effects of salt on root suberin and again used suberin mutants to examine altered physiological responses.

4.1.1 Summary of findings

Suberin production increased with plant age and then reached a steady state at maturity with the transition from vegetative to reproductive stage. The analysis of suberin over a time-course revealed an acceleration of developmental suberin biosynthesis by drought stress. Additionally, there was a steep increase in the production of suberin-associated waxes by drought stress. The increase in suberin may be implicated in the early induction of root secondary growth to form a periderm-containing suberin-rich cork tissue, which may be a strategy to reduce root dessication. My results further revealed cessation of suberin production when the drought-stressed plants were re-watered. The responses demonstrated plasticity in suberin biosynthesis when plants are exposed to different water stress levels, similar to previously reported plasticity of suberin biosynthesis in response to different nutrient levels (Barberon *et al*., 2016).

The suberin mutants tested here were not more affected by chronic drought than wild-type. Relative to wild-type, wilting symptoms were not detected in any of the mutants with reduced suberin. However, drought stimulated the rate of suberin deposition in all genotypes. It is not clear which tissue (i.e. endodermis or periderm) increased suberin under drought stress. Even under control conditions, suberin-deficient mutants and those with deformed suberin lamellae lost water through the periderm faster than WT. Further, the increase in suberin caused by drought stress was related to slowing down of the amount of water loss though roots, indicating the importance of suberin in reducing water loss through roots. The differences in rate of water loss between control and drought stressed WT and *cyp86a1-1 cyp86b1-1* were less pronouncced than the difference between WT and *cyp86a1-1 cyp86b1-1* under control condition. This indicates that suberin deficiency had a greater influence on root water permeability than the

effect of drought stress (i.e., the genotypic effect is more important than treatment effect). In the investigation of drought tolerance, it is also important to consider the root system architecture, and in particular, where the suberized tissues are located for reducing water loss. The Arabidopsis mature root contains suberin primarily in the periderm. In contrast to the primary roots that deposit suberin in the endodermis, the periderm is located closer to the soil surface, where the effect of drought stress is more severe.

In order to minimize water loss and conserve water, protection by the suberized periderm is critical. On the other hand, in mature plants, young roots are normally located deeper in the soil where protection against dessication is not as critical as near the surface. When endodermal tissues are located in deeper soils, it provides an important function in controlling harmful solutes getting it to the root. Therefore, I speculate that suberin in endodermis and peridem impart independent and specific functions based on the location of suberized tissue in stress tolerance mechanism. Kreszies *et al.,* (2018) highlighted that water uptake relates to the deposition of suberized tissues in the endodermis by reducing the amount absorbed by roots. However, enhancing water uptake is also critical for drought tolerance which will not be enhanced by suberization in endodermis. Therefore, in contrast to the function of suberin in periderm, reduced suberin in endodermis may improve water uptake by underground soil profiles where water availability is higher than near the surface of a soil. This argument was supported by several previous studies. Hydraulic conductivity of the whole root system of an Arabidopsis c*yp86a1* suberin-deficient mutant was higher than in wild-type plants (Ranatunge and Schreiber, 2011). Perhaps reduced resistance at the endodermal barrier improves the uptake of water. However, the increase in suberin in *esb1* mutant failed to reduce root permeability below those of wild-type. It is possible that in *esb1,* the primary alteration in root permeability is due to

defective Casparian bands and the ectopic suberin deposition in cortex did not influence the radial movement of water in roots (Naseer *et al.,* 2012; Geldner**,** 2013; Andersen *et al.,* 2015). Therefore, the conventional assumption that the amount of root suberin negatively correlates with permeability has to be taken with caution (Kreszies *et al.,* 2018). Thus, suberization of the periderm may be more important for enhancing drought tolerance than endodermal suberization. Kreszies *et al.,* (2018) also emphasized that localization of suberin in different tissues has a more significant impact on suberin function. However, it is technically challenging to separate endodermis suberin from periderm suberin for chemical analyses in Arabidopsis because of the small size of roots and the amount of tissue needed for such analyses.

Kreszies *et al.,* (2018) also emphasized that monomer arrangements and its ultra-structure play an important role in proper functioning of the suberin polymer. Reduced levels of suberin and altered monomer composition in *cyp86a1-1 cyp86b1-1* caused deformation in lamellae structure. However reduced suberin in *myb92-1 myb93-1* did not result in a deformation of the suberin lamellae structure, suggesting that suberin composition, in particular C16-24 DCAs and OH-FAs, is vital in the formation of the lamellae structure observed by TEM. Even though *abcg2-1 abcg6-1 abcg20-1* had increased suberin amount than WT, this mutant has disrupted lamellae (Yadav *et al.,* 2014). The the location of suberin polymerization remains to be identified. However, it is likely that the polymerization step takes place on the cell wall similar to cutin biosynthesis (Yeats *et a*l., 2012) and *abcg2-1 abcg6-1 abcg20-1* is impaired in transport of monomers to the cell wall. TEM analysis of *cyp86a1-1 cyp86b1* and *gpat5-1* showed that reduced amounts of C16-24 DCAs and OH-FAs caused deformation in the suberin lamella, suggesting the importance of a balanced monomer composition in formation of the lamellae structure.

Unlike drought stress, some of suberin mutants tested here had increased sensitivity to NaCl. *Abcg2-1 abcg6-1 abcg20-1* did not survive the 100 mM NaCl treatment. Although all other mutants and wild-type survived under 100 mM NaCl, their total biomass was significantly reduced by NaCl treatment. However, *cyp86a1-1 cyp86b1-1* and *myb92-1 myb93-1* were affected by 100 mM NaCl more than wild-type and *far1-2 far4-1 far5-1*. *Cyp86a1-1 cyp86b1-1* and *myb92-1 myb93-1* leaf tissues had twice the amount of Na content than wild-type or *far1-2 far4-1 far5-1*. The increased leaf Na concentration was accompanied by a significant reduction in leaf K concentration, especially in *cyp86a1-1 cyp86b1-1* compared to WT. Decreased K concentration under salt stress in Arabidopsis has been reported to be mainly due to NaCl-stimulated K efflux in roots. Membrane depolarization due to Na entry leads to efflux of K, and additionally high NaCl concentration impairs the integrity of the plasma membrane, resulting in a release of cellular solutes including K (Nassery, 1979; Shabala *et al.*, 2006; Britto *et al.,* 2010). Therefore, mutants with either deformed suberin lamellae structure or reduced total suberin content showed reduced tolerance to salinity. None of the mutants increased suberin under NaCl treatment. Only the WT plants could increase suberin production, albeit marginally, under NaCl treatment. The inability to induce suberin in mutants indicates possible destruction to the metabolic activity related to suberin biosynthesis genes encoding enzymes or regulators controlling these enzymes due to the ion imbalance caused by NaCl treatment.

Overall, my investigation of drought and salinity stress responses provides knowledge on importance of chemical composition and structure for the barrier function against water loss and Na uptake in the tolerance mechanisms in Arabidopsis.

4.1.2 Future directions

Investigate the relationship between reduced root suberin and tolerance to drought and salinity

The mutants used in this study with reduced total suberin content were not affected by drought stress. Perhaps the magnitude of reduction in total suberin content in *cyp86a1-1 cyp86b1-1* and *myb92-1 myb93 -1* was not substantial enough to cause a significant effect on drought tolerance or the time period that plants were exposed to drought was not enough. Further, the decreases in K/Na ratio under salt stress conditions in *cyp86a1-1 cyp86b1-1* and *myb92-1 myb93 -1* was not reflected by changes in whole plant biomass.. A viable mutant with total suberin content reduced to the lowest possible amount might be susceptible to drought stress. Further, the increase in suberin production by drought stress displayed in the *myb92-1 myb93-1* double mutant indicates *MYB92* and *MYB93* genes mainly regulate developmental suberin biosynthesis and not stress induced suberin. A previous study reported that *MYB41* gene controls stress induced suberin in Arabidopsis roots (Kosma *et al.,* 2014). Also, a triple mutant loss-of-function *myb53 myb92 myb93* mutants have recently been developed (Rowland lab, unpublished) and displays ~70% reductions in suberin in young Arabidopsis roots. An investigation using a *myb41* loss-of-function mutant or a triple *myb53 myb92 myb93* mutant may provide evidence on the role of suberin in relation to drought tolerance.

Investigate the roles of suberin-associated waxes in drought and salinity tolerance

To date, no study has been reported on stress-induced suberin-associated waxes in Arabidopsis. The present work reported that relative to control condition, there was a three-fold increase in suberin-associated waxes in 5 weeks old Arabidopsis wild-type (Col-0) plants

exposed to 3 weeks of drought stress. Induction of suberin associated waxes could mean a physiologically important aspect in drought tolerance mechanism. Measurements on the sealing effect of root waxes at root-environment interphases to avoid formation of air cavities in xylem conduits (embolism) were not tested in the present study (Lens *et al.,* 2013). Such data may provide a link between suberin associated-waxes and drought tolerance. However, the present study investigated root tissues at 4 weeks of age and the *far1 far4 far5* and *abcg2 abcg6 abcg 20* mutants analyzed here have reduced levels of suberin-associated waxes relative to wild-type (Delude *et al.,* 2016; Yadav *et al*., 2014). However, suberin associated waxes are not eliminated in these mutants, nor were they examined in this mutants under stress conditions.

Do drought and salinity affect endodermal differentiation?

In the present study, induction of suberin was detected in wild-type by both drought and high salinity. However, it was not clear whether the increase in suberin was related to early induction of root secondary growth or acceleration of the endodermal differentiation process from stage I to stage II. This knowledge would help future researchers on crop improvement practices for drought and salinity tolerance.

Investigate the tissue specificity in suberin induction under drought and salinity stresses

My results indicated that root periderm suberin helps to reduce the amount of water loss through roots. However, increase in suberin in endodermis will likely reduce the amount of water that can uptaken by plants. Therefore, it is important to know about the tissue specifity of suberin induction to manipulate genes in development of stress resistant crops.

Investigate the transcription factors that regulate suberin synthesis under drought and salt stress

The results from the drought stress responses indicated a two-fold increase in suberin in *myb92-1 myb93-1* mutant. This observation suggests that there could be other MYB transcription factors that regulate suberin specifically under drought stress. Identification of transcription factors will further improve our strategies using genetic engineering for the development of stress tolerant crops.

4.2 Seed coat suberin forms an effective barrier against chromium in *Arabidopsis thaliana*

In recent years, soil contamination with chromium has become a threat to plant growth because of increasing chromium mining activities. Chromium is a non-essential and toxic element to plants. Mining-contaminated soil with high levels of chromium negatively impacts the growth and health of some plant species and subsequently affects other tropic levels in an ecosystem. Seed coat surrounds the embryo and protects it from environmental contaminations. During development, the seed coat undergoes cell differentiation and synthesis of polysaccharides, lipid polymers, and pigments. *Arabidopsis thaliana* seed coat cells accumulate several polymeric constituents, including pectin-rich mucilage, the lipid-polyesters cutin and suberin, and proanthocyanidins (oligomeric flavonoids). To test their barrier functions against Cr^{3+} penetration, mutants of Arabidopsis defective in these polymers were tested for changes seed germination and embryo viability, relative to wild-type, under a range of chromium Cr^{3+} concentrations.

4.2.1 Summary of findings

Mucilage-deficient mutants were moderately sensitive to Cr^{3+} toxicity. Therefore, the mucilage may contribute to the protection of seeds against chromium toxicity. Mutants affected in the attachment of mucilage on the seed were not affected in seed germination responses in the presence of chromium relative to wild-type. However, higher chromium levels did not reduce embryo viability when mucilage levels were reduced. Therefore, mucilage does not seem to form a major barrier againt Cr^{3+} penetration through the seed coat. Permeability in cutin-deficient seeds was the same as wild-type and seed germination rates were not reduced in the presence of chromium relative to wild-type. Conversely, I found strong evidence supporting the role of seed coat suberin in protecting the embryo against chromium toxicity. Mutants defective in seed coat suberin demonstrated an increased reduction in germination rate compared to wild-type in the presence of increasing chromium concentrations. Reduced embryo viability, in the presence of chromium, correlated with lower seed coat suberin levels, as well as with higher seed coat permeability to tetrazolium salt. Mutants altered in seed coat proanthocyanidins were also highly permeable to tetrazolium salt and showed reduced seed germination compared to wild-type in the presence of high chromium levels. However, this seemed to be an effect on seed dormancy rather than affecting chromium penetration to the embryo.

4.2.2 Future directions

Investigate the suberin lamellae structure in seed coat of gpat5-1

Previous studies provided evidence for deformed suberin lamellae structure in seeds of *abcg2-1 abcg6-1 abcg20-1* and *myb107-2* (Yadav *et al*., 2014; Gou *et al.,* 2017). The present study

revealed that *gpat5-1* also has major permeability defect and high Cr^{3+} sensitivity. However, the structure of the seed-coat suberin lamellae in *gpat5-1* has not yet been analysed. The knowledge about the ultra-structure in seed coat suberin in *gpat5-1* would further provide knowledge on the the importance of suberin lamellae for the barrier function.

Does suberin form a barrier to other heavy-metals?

It is known that suberin forms a barrier for selective uptake of solutes in Arabidopsis roots. Therefore as a follow up to the above research the same seed germination assay could be tested for several other toxic heavy metals such as Cu^{2+}, Pb^{2+} and Zn^{2+} using suberin deficient mutants. Recently, the use of chemical pesticides has been accelerated in the agriculture sector to increase crop yields. Common pesticides contain substantial concentrations of these metals (Gimeno-Garcia *et al.,* 1996). If the responses to Cu^{2+}, Pb^{2+} and Zn^{2+} metal toxicity are similar to chromium, I could generalize the functional role of seed-coat suberin barrier for protection against heavy metals. For further quantification of the movement of toxic metals through the seed coats in the different mutants, metal concentration in embryonic tissues should be analysed.

Investigate the effect of chromium (Cr^{3+}) on seed dormancy

The most common method of testing dormancy is by a germination assay. In this study, embryo viability was tested only in seeds incubated in 800 mg/L Cr^{3+} concentration. Some proanthocyanidin mutants had reduced seed germination at lower concentrations of Cr^{3+} (50 mg/L). Therefore, it is important to test the embryo viability after incubation in all Cr^{3+} concentrations and compare with the seed germination responses. Due to limitations in seed availability in this study, the viability test was carried out in only one sample. Better results could be obtained with multiple replicates thereby allowing to carry out statistical analysis to confirm the effect of chromium on seed dormancy.

References

Abrahams S, Lee E, Walker AR, Tanner GJ, Larkin PJ, Ashton, AR. 2003. The Arabidopsis *TDS4* gene encodes leucoanthocyanidin dioxygenase (LDOX) and is essential for proanthocyanidin synthesis and vacuole development. *The Plant Journal* **35,** 624-636.

Agrawal VP, Kolattukudy PE. 1978. Purification and characterization of a wound-induced omega-hydroxy fatty acid: NADP oxidoreductase from potato tuber disks (*Solanum tuberosum* L.). *Archives of Biochemistry and Biophysics* **191,** 452-465.

Albert S, Delseny M, Devic M. 1997. BANYULS, a novel negative regulator of flavonoid biosynthesis in the Arabidopsis seed coat. *The Plant Journal* **11,** 289-299.

Andersen TG, Barberon M, Geldner N. 2015. Suberization - the second life of an endodermal cell. *Current Opinion in Plant Biology* **28,** 9-15.

Andersen TG, Naseer S, Ursache R, Wybouw B, Smet W, De Rybel B, Vermeer JEM, Geldner N. 2018. Diffusible repression of cytokinin signalling produces endodermal symmetry and passage cells. *Nature* **555,** 529-533.

Appelhagen I, Thiedig K, Nordholt N, Schmidt N, Huep G, Sagasser M, Weisshaar B. 2014. Update on transparent testa mutants from *Arabidopsis thaliana*: Characterisation of new alleles from an isogenic collection. *Planta* **240,** 955-970.

Arsovski AA, Villota MM, Rowland O, Subramaniam R, Western TL. 2009. MUM ENHANCERS are important for seed coat mucilage production and mucilage secretory cell differentiation in *Arabidopsis thaliana*. *Journal of Experimental Botany* **60,** 2601-2612.

Armstrong J, Armstrong W. 2001. Rice and phragmites: effects of organic acids on growth, root permeability, and radial oxygen loss to the rhizosphere. *American Journal of Botany* **88,** 1359-1370.

Aroca R, Porcel R, Ruiz-Lozano J. 2012. Regulation of root water uptake under abiotic stress conditions. *Journal of Experimental Botany* **63**, 43–57.

Barberon M, Vermeer JE, De Bellis D, Wang P, Naseer S, Andersen TG, Humbel BM, Nawrath C, Takano J, Salt DE, Geldner N. 2016. Adaptation of root function by nutrient-induced plasticity of endodermal differentiation. *Cell* **164,** 447-459.

Barberon M. 2017. The endodermis as a checkpoint for nutrients. *New Phytologist* **213,** 1604-1610.

Baudry A, Heim MA, Dubreucq B, Caboche M, Weisshaar B, Lepiniec L. 2004. TT2, TT8, and TTG1 synergistically specify the expression of BANYULS and proanthocyanidin biosynthesis in *Arabidopsis thaliana*. *The Plant Journal* **39,** 366-380.

Baxter IR, Young JC, Armstrong G, Foster N, Bogenschutz N, Cordova T, Peer WA, Hazen SP, Murphy AS, Harper JF. 2005. A plasma membrane H-ATPase is required for the formation of proanthocyanidins in the seed coatendothelium of *Arabidopsis thaliana. Proceedings of National Academy of Sciences USA* **102,** 2649-2654.

Baxter I, Hosmani PS, Rus A. 2009. Root suberin forms an extracellular barrier that affects water relations and mineral nutrition in Arabidopsis. *PLoS Genetics* **5,** e1000492.

Beisson F, Li Y, Bonaventure G, Pollard M, Ohlrogge JB. 2007. The acyltransferase GPAT5 is required for the synthesis of suberin in seed coat and root of Arabidopsis. *The Plant Cell* **19,** 351-368.

Beisson F, Li-Beisson Y, Pollard M. 2012. Solving the puzzles of cutin and suberin polymer biosynthesis. *Current Opinion in Plant Biology* **15**, 329–337.

Bellows RS, Thomson AC, Helmstedt KJ, York RA, Potts MD. 2016. Damage and mortality patterns in young mixed conifer plantations following prescribed fires in the Sierra Nevada, California. *Forest Ecology and Management* **376,** 193-204.

Bernards MA, Lopez M L, Zajicek J, Lewis NG. 1995. Hydroxycinnamic acid-derived polymers constitute the polyaromatic domain of suberin. *Journal of Biological Chemistry* **270,** 7382–7386.

Bernards MA, Lewis NG. 1992. Alkyl ferulates in wound-healing potato-tubers. *Phytochemistry* **31,** 3409-3412.

Bernards M. 2002. Demystifying suberin. *Canadian Journal of Botany* **80,** 227-240.

Berridge MV, Tan A S, McCoy K D, Wang R. 1996. The biochemical and cellular basis of cell proliferation assays that use tetrazolium salts. *Biochemica* **4,** 15-19.

Beeckman T, De Rycke R, Viane R, Inze D. 2000. Histological study of seed coat development in *Arabidopsis thaliana*. *Journal of Plant Research* **113,** 139-148.

Ben-Tov D, Abraham Y, Stav S, Thompson K, Loraine A, Elbaum R, de Souza A, Pauly M, Kieber JJ, Harpaz-Saad S. 2015. COBRA-LIKE2, a member of the glycosylphosphatidylinositol-anchored COBRA-LIKE family, plays a role in cellulose deposition in Arabidopsis seed coat mucilage secretory cells. *Plant Physiology* **167,** 711–724.

Bewley JD. 1997. Seed germination and dormancy. *The Plant Cell* **9**, 1055-1066.

Blum A. 2014. Genomics for drought resistance- getting down to earth. *Functional Plant Biology*. **41,** 1191-1198.

Boesewinkel FD, Bouman F. 1995. Seed Development and Germination. In: Kigel J, Galili G. eds. *The Seed: Structure and Function.* New York: Marcel Dekker, Inc., 1-24.

Brown RC, Lemmon BE, Nguyen H, Olsen O. 1999. Development of endosperm in *Arabidopsis thaliana*. *Sexual Plant Reproduction* **12,** 32-42.

Bu Q, Lv T, Shen H, Luong P, Wang J, Wang Z, Huang Z, Xiao L, Engineer C, Kim TH, Schroeder JI, Huq E. 2014. Regulation of drought tolerance by the F-Box protein MAX2 in Arabidopsis. *Plant Physiology* **164,** 424-439.

Chahtane H, Kim W, Lopez-Molina L. 2017. Primary seed dormancy: a temporally multilayered riddle waiting to be unlocked. *Journal of Experimental Botany* **68,** 857-869.

Chen ZH, Zhou MX, Mendham N J, Newman IA, Zhang GP, Shabala S. (2007). Potassium and sodium relations in salinized barley tissues as a basis of differential salt tolerance. *Functional Plant Biology* **34,** 150–162.

Cominelli E, Conti L, Tonelli C, Galbiati M. 2013. Challenges and perspectives to improve crop drought and salinity tolerance. *New Biotechnology* **30,** 355-359.

Compagnon V, Diehl P, Benveniste I, Meyer D, Schaller H, Schreiber K, Franke R, Pinot F. 2009. CYP86B1 is required for very long chain ω-hydroxyacid and α,ω dicarboxylic acid synthesis in root and seed suberin polyester. *Plant Physiology* **150,** 1831-1843.

Cottle W, Kolattukudy PE. 1982. Abscisic acid stimulation of suberization: induction of enzymes and deposition of polymeric components and associated waxes in tissue cultures of potato tuber. *Plant Physiology* **70,** 775-780.

Dean BB, Kolattukudy PE. 1976. Synthesis of suberin during wound-healing in jade leaves, tomato fruit, and bean pods. *Plant Physiology* **58,** 411–416.

Dean GH, Zheng H, Tewari J, Huang J, Young DS, Hwang YT,Western, TL, Carpita, NC, McCann MC, Mansfield SD, Haughna GW. 2007. The Arabidopsis *MUM2* Gene Encodes a β-Galactosidase required for the production of seed coat mucilage with correct hydration properties. *The Plant Cell* **9,** 4007-4021.

Debeaujon I, Leon-Kloosterziel KM, Koornneef M. 2000. Influence of the testa on seed dormancy, germination, and longevity in Arabidopsis. *Plant Physiology* **122,** 403-413.

Debeaujon I, Lepiniec L, Pourcel, L, Routaboul J. 2007. Seed coat development and dormancy. In: *Annual Plant Reviews, Volume 27: Seed Development, Dormancy and Germination.* Bradford: 25-49.

Debeaujon I, Nesi N, Perez P, Devic M, Grandjean O, Caboche M, Lepiniec L. 2003. Proanthocyanidin-accumulating cells in Arabidopsis testa: Regulation of differentiation and role in seed development. *The Plant Cell* **15,** 2514-2531.

Debeaujon I, Peeters AJM, Léon-Kloosterziel KM, Koornneef M. 2001. The *TRANSPARENT TESTA12* gene of Arabidopsis encodes a multidrug secondary transporter-like protein required for flavonoid sequestration in vacuoles of the seed coat endothelium. *The Plant Cell* **13,** 853-872.

Delude C, Fouillen L, Bhar P, Cardinal MJ, Pascal S, Santos P, Kosma DK, Joubès J, Rowland O, Domergue F. 2016. Primary fatty alcohols are major components of suberized root tissues of arabidopsis in the form of alkyl hydroxycinnamates. *Plant Physiology* **171,** 1934-1950.

Doblas VG, Geldner N, Barberon M. 2017. The endodermis, a tightly controlled barrier for nutrients. *Current Opinion in Plant Biology* **39,**136–143.

Dolan L, Janmaat K, Willemsen V, Linstead P, Poethig S, Roberts K, Scheres B. 1993. Cellular organisation of the *Arabidopsis thaliana* root. *Development* **119,** 71-84.

Domergue F, Vishwanath SJ, Joubès J, Ono J, Lee JA, Bourdon M, Alhattab R, Lowe C, Pascal S, Lessire R, Rowland O. 2010. Three Arabidopsis fatty acyl-coenzyme A reductases, FAR1, FAR4 and FAR5 generate primary fatty alcohols associate with suberin deposition. *Plant Physiology* **153,** 1539-1554.

Gimeno-Garcia E, Andreu V, Boluda R. 1996. Heavy metals incidence in the application of inorganic fertilizers and pesticides to rice farming soils. *Environmental Pollution* **92,** 19-25.

Enstone DE, Peterson CA. 2005. Suberin lamella development in maize seedling roots grown in aerated and stagnant conditions. *Plant, Cell and Environment* **28,** 444-455.

Enstone DE, Peterson CA, Ma F. 2003. Root endodermis and exodermis: Structure, function, and responses to the environment. *Journal of Plant Growth Regulation* **21,** 335-351.

Esau K. 1977. Anatomy of seed plants. New York: John Wiley.

Fedi F, O'Neill, Carmel M, Menard G, Trick M, Dechirico S, Corbineau F, Bailly C, Eastmond PJ, Penfield S. 2017. Awake1, an ABC-Type transporter, reveals an essential role for suberin in the control of seed dormancy. *Plant Physiology* **174,** 276-283.

Fehling E, Mukherjee KG. 1991. Acyl-CoA elongase from a higher plant (*Lunaria annua*): Metabolic intermediates of very-longchain acyl-CoA products and substrate specificity. *Biochimica et Biophysica Acta* **1082,** 239-246.

Flowers TJ, Colmer TD. 2008. Salinity tolerance in halophytes.*The New Phytologist* **179,** 945-963.

Francoz E, Ranocha P, Burlat V, Dunand C. 2015. Arabidopsis seed mucilage secretory cells: regulation and dynamics. *Trends in Plant Science* **20,** 515-524.

Franke RB, Dombrink I, Schreiber L. 2012. Suberin goes genomics: use of a short living plant to investigate a long lasting polymer. *Frontiers in Plant Science* **3,** 4.

Franke R, Hofer R, Briesen I, Emsermann M, Efremova N, Yephremov A, Schreiber L. 2009. The *DAISY* gene from Arabidopsis encodes a fatty acid elongase condensing enzyme involved in the biosynthesis of aliphatic suberin in roots and the chalaza-micropyle region of seeds. *The Plant Journal* **57**, 80-95.

Franke R, Schreiber L. 2007. Suberin - A biopolyester forming apoplastic plant interfaces. *Current Opinion in Plant Biology* **10,** 252-259.

Franke R, Briesen I, Wojciechowski T, Faust A, Yephremov A, Nawrath C, Schreiber L. 2005. Apoplastic polyesters in Arabidopsis surface tissues – A typical suberin and a particular cutin. *Phytochemistry* **66,** 2643–2658.

Geldner N. 2013. The endodermis. *Annual Review of Plant Biology* **64,** 531–558.

Gibbs DJ, Voß U, Harding SA, Fannon J, Moody LA, Yamada E, Swarup K, Nibau C, Bassel GW, Choudhary A, Lavenus J, Bradshaw SJ, Stekel DJ, Bennett MJ, Coates JC 2014. AtMYB93 is a novel negative regulator of lateral root development in Arabidopsis. *New Phytologist* **203,** 1194-1207.

Graca J. 2015. Suberin: the biopolyester at the frontier of plants. *Frontiers in Chemistry* **3,** 62.

Gou M, Hou G, Yang H, Zhang X, Cai Y, Kai G, Liu CJ. 2017. The MYB107 transcription factor positively regulates suberin biosynthesis. *Plant Physiology* **173,** 1045–1058.

Graça J, Santos S. 2007. Suberin - A biopolyester of plants' skin. *Macromolecular Bioscience* **7,** 128-135.

Graça J, Pereira H. 1997. Cork suberin: A glyceryl based polyester. *Holzforschung* **51,** 225-234.

Graça J, Pereira H. 1998. Feruloyl esters of ω-hydroxyacids in cork suberin. *Journal of Wood Chemistry and Technology* **18,** 207-217.

Graça J, Pereira H. 1999. Glyceryl-acyl and aryl-acyl dimers in *Pseudotsuga menziesii* bark suberin. *Holzforschung* **53,** 397-402

Graça J, Pereira H. 2000a. Methanolysis of bark suberins: analysis of glycerol and acid monomers. *Phytochemical Analysis* **11,** 45-51.

Graça J, Pereira H. 2000b. Suberin structure in potato periderm: glycerol, long-chain monomers, and glyceryl and feruloyl dimers. *Journal of Agriculture and Food Chemistry* **48,** 5476-5483.

Graça J, Pereira H. 2000c. Diglycerol alkenedioates in suberin: Building units of a poly(acylglycerol) polyester. *Biomacromolecules* **1,** 519–522.

Griffith M, Huner NPA, Espelie KE, Kolattukudy PE. 1985. Lipid polymers accumulate in the epidermis and mestome sheath cell walls during low temperature development of winter rye leaves. *Protoplasma* **125,** 53-64.

Harpaz-Saad S, McFarlane HE, Xu S, Divi UK, Forward B, Western TL, Kieber, JJ. 2011. Cellulose synthesis via the FEI2 RLK/SOS5 pathway and CELLULOSE SYNTHASE 5 is required for the structure of seed coat mucilage in Arabidopsis. *The Plant Journal* **68,** 941-953.

Haughn G, Chaudhury A. 2005. Genetic analysis of seed coat development in Arabidopsis. *Trends in Plant Science* **10,** 472- 477.

Haughn GW, Western TL. 2012. Arabidopsis seed coat mucilage is a specialized cell wall that can be used as a model for genetic analysis of plant cell wall structure and function. *Frontiers in Plant Science* **3,** 64

Hayat S, Khalique G, Irfan M, Wani AS, Tripathi BN, Ahmad A. 2012. Physiological changes induced by chromium stress in plants: an overview. *Protoplasma* **249,** 599-611.

Hofer R, Briesen I, Beck M, Pinot F, Schreiber L, Franke R. 2008. The Arabidopsis cytochrome P450 CYP86A1 encodes a fatty acid ω-hydroxylase involved in suberin monomer biosynthesis. *Journal of Experimental Botany* **59,** 2347-2360.

Hose E, Clarkson DT, Steudle E, Schreiber L, Hartung W. 2001. The exodermis: A variable apoplastic barrier. *Journal of Experimental Botany* **52,** 2245-2264.

Hosmani PS, Kamiya T, Danku J, Naseer S, Geldner N, Guerinot ML, Salt DE. 2013. Dirigent domain-containing protein is part of the machinery required for formation of the lignin-based Casparian strip in the root. *Proceedings of the National Academy of Sciences USA* **110,** 14498-14503.

Hu B, Jia X, Hu J, Xu D, Xia F, Li Y. 2017. Assessment of heavy metal pollution and health risks in the soil-plant- human system in the Yangtze river delta, China. *International Journal of Environmental Research and Public Health* **14**, E0142

James RA, Blake C, Byrt CS, Munns R, 2011. Major genes for Na^+ exclusion, Nax1 and Nax2 (wheat HKT1; 4 and HKT1; 5), decrease Na^+ accumulation in bread wheat leaves under saline and waterlogged conditions. *Journal of Experimental Botany* **62,** 2939-2947.

Johansson I, Karlsson M, Johanson U, Larsson C, Kjellbom P. 2000. The role of aquaporins in cellular and whole plant water balance. *Biochimica et Biophysica Acta - Biomembranes* **1465,** 324-342.

Kolattukudy PE, Agrawal VP. 1974. Structure and composition of aliphatic constituents of potato tuber skin (suberin). *Lipids* **9,** 682–691.

Kolattukudy PE. 1981. Structure, biosynthesis and biodegradation of cutin and suberin. *Annual Review of Plant Physiology* **32,** 539-567.

Kolattukudy PE. 2001. Polyesters in higher plants. *Advances in Biochemical Engineering Biotechnology* **71,** 1-49.

Kolattukudy PE. 1984. Biochemistry and function of cutin and suberin. *Canadian Journal of Botany* **62,** 2918-2933.

Kosma DK, Molina I, Ohlrogge JB, Pollard M. 2012. Identification of an Arabidopsis fatty alcohol:caffeoyl-coenzyme A acyltransferaserequired for the synthesis of alkyl hydroxycinnamates in root waxes. *Plant Physiology* **160,** 237-248.

Kosma DK, Rice A, Pollard M. 2015. Analysis of aliphatic waxes associated with root periderm or exodermis from eleven plant species. *Phytochemistry* **117,** 351-362.

Kotula L, Ranathunge K, Schreiber L, Steudle E. 2009. Functional and chemical comparison of apoplastic barriers to radial oxygen loss in rice (*Oryza sativa* L.) grown in aerated or deoxygenated solution. *Journal of Experimental Botany* **60,** 2155-2167.

Kramer PJ. 1949. Plant and soil water relationships. University of Michigan: McGraw-Hill Book Co., Inc., New York. 189-211.

Kreszies T, Schreiber L, Ranathunge K. 2018. Suberized transport barriers in Arabidopsis, barley and rice roots: From the model plant to crop species. *Journal of Plant Physiology* **227,** 75-83.

Krishnamurthy P, Jyothi-Prakash PA, Qin L, He J, Lin Q, Loh CS, Kumar PP. 2014. Role of root hydrophobic barriers in salt exclusion of a mangrove plant *Avicennia officinalis*. *Plant, Cell and Environment* **37,** 1656-1671.

Krishnamurthy P, Ranathunge K, Franke R, Prakash HS, Schreiber L, Mathew MK. 2009. The role of root apoplastic transport barriers in salt tolerance of rice (*Oryza sativa* L.). *Planta* **230,** 119-134.

Krishnamurthy P, Ranathunge K, Nayak S, Schreiber L, Mathew MK. 2011. Root apoplastic barriers bolock Na^+ transport to shoots in rice (*Oryza sativa* L.). *Journal of Experimental Botany* **62,** 4215-4228.

Lashbrooke J, Cohen H, Levy-Samocha D, Tzfadia O, Panizel I, Zeisler V, Massalha H, Stern A, Trainotti L, Schreiber L, Costa F, Aharoni A. 2016. MYB107 and MYB9 homologs regulate suberin deposition in angiosperms. *The Plant Cell* **28,** 2097–2116.

Lee SB, Jung SJ, Go YS, Kim HU, Kim JK, Cho HJ, Park OK, Suh MC. 2009. Two Arabidopsis 3-ketoacyl CoA synthase genes, *KCS20* and *KCS2/DAISY*, are functionally redundant in cuticular wax and root suberin biosynthesis, but differentially controlled by osmotic stress. *The Plant Journal* **60,** 462-475.

Legay S, Guerriero G, André C, Guignard C, Cocco E, Charton S, Boutry M, Rowland O, Hausman JF. 2016. MdMyb93 is a regulator of suberin deposition in russeted apple fruit skins. *New Phytologist* **212,** 977-991.

Lens F, Tixier A, Cochard H, Sperry JS, Jansen S, Herbette S. 2013. Embolism resistance as a key mechanism to understand adaptive plant strategies. *Current Opinion in Plant Biology* **16,** 287-292.

Lévesque-Lemay M, Chabot D, Hubbard K, Chan JK, Miller S, Robert LS. 2016. Tapetal oleosins play an essential role in tapetosome formation and protein relocation to the pollen coat. *New Phytologist* **209,** 691-704.

Li B, Kamiya T, Kalmbach L, Yamagami M, Yamagichi K, Shigenobu S, Sawa S, Danku JMC, Salt DE, Geldner N, Fujiwara T. 2017. Role of *LOTR1* in nutrient transport through organization of spatial distribution of root endodermal barriers. *Current Biology* **27**, 758–765.

Li Y, Beisson F, Ohlrogge J, Pollard M. 2007. Monoacylglycerols are components of root waxes and can be produced in the aerial cuticle by ectopic expression of a suberin-associated acyltransferase. *Plant Physiology* **144,** 1267-1277.

Li Y, Li H, Li Y, Zhang S. 2017. Improving water-use efficiency by decreasing stomatal conductance and transpiration rate to maintain higher ear photosynthetic rate in drought resistant Wheat. *The Crop Journal* **5,** 231-239.

Lopez-Luna J, Gonzalez-C MC, Esparza-Garcia F, Rodriguez-Vazquez R. 2009. Toxicity assessment of soil amended with tannery sludge, trivalent chromium and hexavalent chromium, using wheat, oat and sorghum plants. *Journal of Hazardous Materials* **163,** 829-834.

Lukina A, Boutin C, Rowland O, Carpenter D. 2016. Evaluating trivalent chromium toxicity on wild terrestrial and wetland plants. *Chemosphere* **162,** 355-364.

Lulai EC, Corsini DL. 1998. Differential deposition of suberin phenolic and aliphatic domains and their roles in resistance to infection during potato tuber (*Solanum tuberosum* L.) wound-healing. *Physiological and Molecular Plant Pathology* **53,** 209-222.

Lulai EC, Freeman TP. 2001. The importance of phellogen cells and their structural characteristics in susceptibility and resistance to excoriation in immature and mature potato tuber (*Solanum tuberosum* L.) periderm. *Annals of Botany* **88,** 555-561.

Ma F, Peterson CA. 2003. Current insights into the development, structure, and chemistry of the endodermis and exodermis of roots. *Canadian Journal of Botany* **81,** 405-421.

Maia J, Dekkers BJW, Provart NJ, Ligterink W, Hilhorst HWM. 2011. The re-establishment of desiccation tolerance in germinated *Arabidopsis thaliana* seeds and its associated transcriptome. *PLoS ONE* **6,** e29123.

Marinova K, Pourcel L, Weder B, Schwarz MBD, Routaboul J, Debeaujon I, Kleina M. 2007. The Arabidopsis MATE transporter TT12 acts as a vacuolar flavonoid/H1-antiporter active in proanthocyanidin-accumulating cells of the seed coat. *The Plant Cell* **19,** 2023-2038.

Belmonte MF, Kirkbride RC, Stone SL, Pelletier JM, Bui AQ, Yeung EC, Hashimoto M, Fei J, Harada CM, Munoz MD, Le BH, Drews GN, Brady SM, Goldberg RB, Harada, JJ. 2013. Comprehensive developmental profiles of gene activity in regions and subregions of the Arabidopsis seed. *Proceedings of the National Academy of Sciences of the United States of America* **110,** E435-444.

Marques AV, Pereira H, Meier D, Faix O. 1994. Quantitative analysis of cork (*Quercus suber* L.) and milled cork lignin by FTIR spectroscopy, analytical pyrolysis, and total hydrolysis. *Holzforschung* **48,** 43-50.

Martinka M, Dolan L, Pernas M, Abe J, Lux A. 2012. Endodermal cell-cell contact is required for the spatial control of Casparian band development in Arabidopsis thaliana. *Annals of Botany* **110,** 361-371.

McFarlane HE, Gendre D, Western TL. 2014. Seed coat ruthenium red staining assay. *Bio-protocol* **4,** e1096.

Mendu V, Griffiths JS, Persson S, Stork J, Downie AB, Voiniciuc C, Haughn GW, DeBolt S. 2011. Subfunctionalization of cellulose synthases in seed coat epidermal cells mediates secondary radial wall synthesis and mucilage attachment. *Plant Physiology* **157,** 441- 453.

Mertz RA, Brutnell TP. 2014. Bundle sheath suberization in grass leaves: Multiple barriers to characterization. *Journal of Experimental Botany* **65,** 3371-3380.

Matzke K, Reiderer M. 1991. A comparative study into the chemical constitution of cutins and suberins from *Picea abies* (L.) Karst., *Quercus robur* L., and *Fagus sylvatica* L. *Planta* **185,** 233-245.

Millar AA, Kunst L. 1997. Very-long-chain fatty acid biosynthesis is controlled through the expression and specificity of the condensing enzyme. *The Plant Journal* **12,** 121-131.

Moire L, Schmutz A, Buchala A, Yan B, Stark RE, Ryser U. 1999. Glycerol is a suberin monomer: New experimental evidence for an old hypothesis. *Plant Physiology* **119,** 1137-1146.

Molina I, Bonaventure G, Ohlrogge J, Pollard M. 2006. The lipid polyester composition of *Arabidopsis thaliana* and *Brassica napus* seeds. *Phytochemistry* **67**, 2597-2610.

Molina I, Ohlrogge JB, Pollard M. 2008. Deposition and localization of lipid polyester in developing seeds of *Brassica napus* and *Arabidopsis thaliana*. *The Plant Journal* **53,** 437–449.

Molina I, Li-Beisson Y, Beisson F, Ohlrogge JB, Pollard M. 2009. Identification of an Arabidopsis feruloyl-coenzyme A transferase required for suberin synthesis. *Plant Physiology* **151,** 1317-1328.

Molina I. 2010. Biosynthesis of plant lipid polyesters. The AOCS Lipid Library, http://lipidlibrary.aocs.org/Biochemistry/content.cfm?ItemNumber=40311 Accessed March 2018.

Momoh E, Zhou W, Kristiansson B. 2002. Variation in the development of secondary dormancy in oilseed rape genotypes under conditions of stress. *Weed Research* **42,** 446-455.

Nawrath C, Schreiber L, Franke RB, Geldner N, Reina-Pinto, Kunst L. 2013. Apoplastic diffusion barriers in Arabidopsis. *The Arabidopsis Book* 11, e0167

Nawrath C. 2002. The Biopolymers Cutin and Suberin. *The Arabidopsis Book* **1,** e0021.

Naseer S, Lee Y, Lapierre C, Franke R, Nawrath C, Geldner N. 2012. Casparian strip diffusion barrier in Arabidopsis is made of a lignin polymer without suberin. *Proceedings of the National Academy of Sciences USA* **109,** 10101-10106.

Negrao S, Schmockel SM, Tester M. 2017. Evaluating physiological responses of plants to salinity stress. *Annals of Botany* **119,** 1-11.

North GB, Nobel PS. 1994.Changes in root hydraulic conductivity for two tropical epiphytic cacti as soil-moisture varies. *American Journal of Botany* **81,** 46-53.

North H, Baud S, Debeaujon I, Dubos C, Dubreucq B, Grappin P, Jullien M, Lepiniec L, Marion-Poll A, Miquel M, Rajjou L, Routaboul J, Caboche M. 2010. Arabidopsis seed secrets unravelled after a decade of genetic and omics-driven research. *The Plant Journal* **61,** 971-981.

Passardi F, Dobias J, Valerio L, Guimil S, Penel C, Dunand C. 2007. Morphological and physiological traits of three major *Arabidopsis thaliana* accessions. *Journal of Plant Physiology* **164,** 980-992.

Pereira A. 2016. Plant abiotic stress challenges from the changing environment. *Frontiers in Plant Science* **7,** 1123.

Peterson CA, Peterson RL, Robards AW. 1978. A correlated histochemical and ultrastructural study of the epidermis and hypodermis of onion roots. *Protoplasma* **96,** 1-21.

Peterson CA, Cholewa E. 1998. Structural modifications of the apoplast and their potential impact on ion uptake. *Journal of Plant Nutrition and Soil Science* **161,** 521-531.

Pollard M, Beisson F, Li Y, Ohlrogge J B. 2008. Building lipid barriers: biosynthesis of cutin and suberin. *Trends in Plant Science* **13,** 236-246.

Pourcel L, Routaboul J, Kerhoas L, Caboche M, Lepiniec L, Debeaujon I. 2005. *TRANSPARENT TESTA10* encodes a laccase-like enzyme involved in oxidative polymerization of flavonoids in Arabidopsis seed coat. *The Plant Cell* **17,** 2966-2980.

Rajjou L, Duval M, Gallardo K, Catusse J, Bally J, Job C, Job D. 2012. Seed germination and vigor. *Annual Review of Plant Biology* **63,** 507-533.

Ranathunge K, Thomas RH, Fang X, Peterson CA, Gijzen M, Bernards MA. 2008. Soybean root suberin and partial resistance to root rot caused by *Phytophthora sojae*. *Phytopathology* **98,** 1179-1189.

Ranathunge K, Schreiber L. 2011. Water and solute permeability of Arabidopsis roots in relation to the amount and composition of aliphatic suberin. *Journal of Experimental Botany* **62,** 1961-1974.

Ranathunge K, Schreiber L, Bi YM, Rothstein SJ. 2016. Ammonium-induced architectural and anatomical changes with altered suberin and lignin levels significantly change water and solute permeabilities of rice (*Oryza sativa* L.) roots. *Planta* **243,** 231-249.

Robbins II NE, Trontin C, Duan L, Dinneny JR. 2014. Beyond the barrier: Communication in the root through the endodermis. *Plant Physiology* **166,** 551-559.

Rodríguez MJA, De Arana C, Ramos-Miras JJ, Gil C, Boluda R. 2015. Impact of 70 years urban growth associated with heavy metal pollution. *Environmental Pollution* **196,** 156-63.

Rowland O, Domergue F. 2012. Plant fatty acyl reductases: Enzymes generating fatty alcohols for protective layers with potential for industrial applications. *Plant Science* **193-194,** 28-38.

Ryser P, Bernardi J, Merla A. 2008. Determination of leaf fresh mass after storage between moist paper towels: constraints and reliability of the method. *Journal of Experimental Botany* **59,** 2461-2467.

Salminen TA, Eklund DM, Joly V, Blomqvist K, Matton DP, Edqvist J. 2018. Deciphering the evolution and development of the cuticle by studying lipid transfer proteins in mosses and liverworts. *Plants* **7,** E6

Salas, J.J. and Ohlrogge, J.B. 2002 Characterization of substrate specificity of plant FatA and FatB acyl-ACP thioesterases. *Archives of Biochemistry and Biophysics* **403,** 25–34.

Schneitz K, Huilskamp M, Pruitt RE. 1995. Wild-type ovule development in *Arabidopsis thaliana*:a light microscope study of cleared whole-mount tissue. *The Plant Journal* **7,** 731-749.

Schreiber L, Franke R, Hartmann K. 2005a**.** Effects of NO_3 deficiency and NaCl stress on suberin deposition in rhizo-and hypodermal (RHCW) and endodermal cell walls (ECW) of castor bean (*Ricinus communis* L.) roots. *Plant and Soil* **269,** 333-339.

Schreiber L, Franke R, Hartmann K. 2005b. Wax and suberin development of native and wound periderm of potato (*Solanum tuberosum* L.) and its relation to peridermal transpiration. *Planta* **220,** 520-530.

Schreiber L, Franke R, Hartmann KD, Ranathunge K, Steudle E. 2005c. The chemical composition of suberin in apoplastic barriers affects radial hydraulic conductivity differently in the roots of rice (*Oryza sativa* L. cv. IR64) and corn (*Zea mays* L. cv. Helix). *Journal of Experimental Botany* **56,** 1427-1436.

Schreiber L, Hartmann K, Skrabs M, Zeier J. 1999. Apoplastic barriers in roots: chemical composition of endodermal and hypodermal cell walls. *Journal of Experimental Botany* **50,** 1267-1280.

Schreiber L, Franke RB. 2011. Endodermis and exodermis in roots. *eLS*. doi: 10.1002/9780470015902.a0002086.pub2

Schroeder JI, Kwak JM, Allen GJ. 2001. Guard cell abscisic acid signalling and engineering drought hardiness in plants. *Nature* **410**, 327-330.

Serra O, Hohn C, Franke R, Prat S, Molinas M, Figueras M. 2010. A feruloyl transferase involved in the biosynthesis of suberin and suberin-associated wax is required for maturation and sealing properties of potato periderm. *The Plant Journal* **62,** 277-290.

Shanker A, Cervantes C, Loza-Tavera H, Avudainayagam S. 2005. Chromium toxicity in plants. *Environment International* **31,** 739-753.

Shahid M, Pourrut B, Dumat C, Nadeem M, Aslam M, Pinelli E. 2014. Heavy-Metal-Induced Reactive Oxygen Species: Phytotoxicity and Physicochemical Changes in Plants. In: Whitacre D. (eds) *Reviews of Environmental Contamination and Toxicology* **232,** Springer, Cham. 1-44.

Siddiqui MM, Abbasi BH, Ahmad N, Ali M, Mahmood T. 2012. Toxic effects of heavy metals (Cd, Cr and Pb) on seed germination and growth and DPPH-scavenging activity in *Brassica rapa* var. turnip. *Toxicology and Industrial Health,* **30,** 238-249.

Silva SP, Sabino MA, Fernandes EM, Correlo VM, Boesel LF, Reis RL. 2005. Cork: properties, capabilities and application. *International Materials Review* **50,** 345–365.

Soliday C, Kolattukudy P, David R. 1979. Chemical and ultrastructural evidence that waxes associated with the suberin polymer constitute the major diffusion barrier to water vapor in Potato tuber (*Solanum tuberosum* L.). *Planta* **146**, 607-614.

Steudle E. 2000. Water uptake by roots: an integration of views. *Plant and Soil* **226,** 45-56.

Steudle E, Peterson C. 1998. How does water get through roots? *Journal of Experimental Botany* **49,** 775-788.

Sullivan S, Ralet M, Berger A, Diatloff E, Bischoff V, Gonneau M, Marion-Poll A, North HM. 2011. CESA5 is required for the synthesis of cellulose with a role in structuring the adherent mucilage of Arabidopsis seeds. *Plant Physiology* **156,** 1725-1739.

Taleisnik E, Peyrano G, Cordoba A, Arias C. 1999. Water retention capacity in root segments differing in the degree of exodermis development. *Annals of Botany* **83,** 19-27.

Thomas R, Fang X, Ranathunge K, Anderson TR, Peterson CA, Bernards MA. 2007. Soybean root suberin: Anatomical distribution, chemical composition, and relationship to partial resistance to *Phytophthora sojae*. *Plant Physiology* **144,** 299-311.

Verma P, Majee M. 2013. Seed germination and viability test in tetrazolium (TZ) assay. *Bio-Protocol* **3,** e884

Vishwanath SJ, Kosma DK, Pulsifer IP, Scandola S, Pascal S, Joubes J, Dittrich-Domergue F, Lessire R, Rowland O, Domergue F. 2013. Suberin-associated fatty alcohols in *Arabidopsis thaliana*: Distribution in roots and contributons to seed coat barrier properties. *Plant Physiology* **163,** 1118-1132.

Vishwanath SJ, Domergue F, Rowland O. 2014. Seed coat permeability test: Tetrazolium penetration assay. *Bio-Protocol* **4,** e1173.

Vishwanath SJ, Delude C, Domergue F, Rowland O. 2015. Suberin: biosynthesis, regulation, and polymer assembly of a protective extracellular barrier. *Plant Cell Reports* **34,** 573-586.

Watanabe K, Nishiuchi S, Kulichikhin K, Nakazono M. 2013. Does suberin accumulation in plant roots contribute to waterlogging tolerance? *Frontiers in Plant Science* **4,** 178

Weitbrecht K, Muller K, Leubner-Metzger G. 2011. First off the mark: early seed germination. *Journal of Experimental Botany* **62,** 3289-3309.

Western TL. 2012. The sticky tale of seed coat mucilages: production, genetics, and role in seed germination and dispersal. *Seed Science Research* **22,** 1-25.

Western TL, Burn J, Tan WL, Skinner DJ, Martin-McCaffrey L, Moffatt BA, Haughn GW. 2001. Isolation and characterization of mutants defective in seed coat mucilage secretory cell development in Arabidopsis. *Plant Physiology* **127,** 998-1011.

Western TL, Skinner D, Haughn G. 2000. Differentiation of mucilage secretory cells of the Arabidopsis seed coat. *Plant Physiology* **122,** 345-355.

Wu X, Lin J, Zhu J, Hu Y, Hartmann K, Schreiber L. 2003. Casparian strips in needles of *Pinus bungeana*: isolation and chemical characterization. *Physiologia Plantarum* **117,** 421-424.

Xiao F, Goodwin SM, Xiao Y, Sun Z, Baker D, Tang X, Jenks MA, Zhou JM. 2004. Arabidopsis CYP86A2 represses *Pseudomonas syringae* type III genes and is required for cuticle development. *The EMBO Journal* **23,** 2903-2913.

Xuan L, Wang Z, Jiang L. 2014. Vanillin assay of Arabidopsis seeds for proanthocyanidins. *Bio-Protocol***,** e1309.

Yadav V, Molina I, Ranathunge K, Castillo IQ, Rothstein SJ, Reeda JW. 2014. ABCG transporters are required for suberin and pollen wall extracellular barriers in Arabidopsis. *The Plant Cell* **26,** 3569-3588.

Yang W, Pollard M, Li-Beisson Y, Ohlrogge J. 2016. Quantitative analysis of glycerol in dicarboxylic acid-rich cutins provides insights into Arabidopsis cutin structure. *Phytochemistry* **130,** 159-169.

Yang WL, Bernards MA. 2007. Metabolite profiling of potato (*Solanum tuberosum* L.) tubers during wound-induced suberization. *Metabolomics* **3,** 147–159.

Yeats TH, Martin LBB, Viart HMF, Isaacson T, He Y, Zhao L, Matas AJ, Buda GJ, Domozych DS, Clausen MH, Rose JKC. 2012. The identification of cutin synthase: formation of the plant polyester cutin. *Nature Chemical Biology* **8,** 609-611.

Zayed AM, Terry N. 2003. Chromium in the environment: Factors affecting biological remediation. *Plant and Soil* **249,** 139-156.

Zeier J, Schreiber L. 1998. Comparative investigation of primary and tertiary endodermal cell walls isolated from the roots of five monocotyledoneous species: Chemical composition in relation to fine structure. *Planta* **206,** 349-361.

Appendix I:

Root staining method by fluorol yellow 088

A final concentration of 0.01% (w/v) fluorol yellow 088 was made by dissolving 0.01 g of fluorol yellow 088 in 50 ml of PEG 400 solution and heating at 90°C for 1 h (Brundrett *et al.,* 1991). An equal volume of 90% (v/v) glycerol solution was added to the PEG staining solution. Sections were counter stained with 0.5% aniline blue in distilled water for 30 min to quench auto-flourescense of aromatic suberin (Brundrett *et al.,* 1998) and then stained with the fluorol yellow 088 solution for 1 h at room temperature, The sections were then rinsed several times with distilled water, and observed under UV light for a bright yellow fluorescence (excitation filter 365nm, chromatic beam splitter Ft 395, emission filter LP 420nm) (Brundrett *et al.,* 1998). Unstained cell walls were also examined for autofluorescence as a test for the phenolic constituents of suberin.

Appendix II:

Primers used in PCR genotyping

Mutant	Publication	Locus and T-DNA insertion line	Primer Name and sequence (5'-3')
cyp86b1-1	Compagnon *et al.,* 2009	AT5G41040; SM_37066	LS 331(LP): TCCATCAGGAAATACGTCGTC
			LS 332(RP): CCTACTTGCGTGTGGAAGTTC
			LS 186(LB): TACGAATAAGAGCGTCCATTTTAGAGTGA
cyp86b1-2	Compagnon *et al.,* 2009	AT5G41040; SALK_130265	HS 101(LP): GGTTTAGCAGCCTCAACAGC
			HS 102 (RP): ATCTGGACCGAGACATCCTG
			HS 100 (LB): TGGTTCACGTAGTGGGCCATCG
far1-2	Domergue *et al.,* 2010	AT5G22500; SALK_149469	Far1-2(LP) : TGTTGCAATAAATGAAATGAACAG
			Far1-2(RP) : TACCTTGCACGACTATGTCCC
			LBb1 : GCGTGGACCGCTTGCTGCAACT
far4-1	Domergue *et al.,* 2010	AT3G44540; SALK_000229	Far4-1 (LP): TGTATTCATCAAACCAATTGATCC
			Far4-1 (RP): TTGCGATGGTGAACTACTTCC
			LBb1 : GCGTGGACCGCTTGCTGCAACT
far5-1	Domergue *et al.,* 2010	AT3G44550; SALK_152963	Far5-1 (LP) : TTCTTGCAACGTCCTTAGCTG
			Far5-1 (RP) : AAAGGTGGTATATAAAATTTCTTGTAGC
			LBb1 : GCGTGGACCGCTTGCTGCAACT
abcg2-1	Yadav *et al.,* 2014	AT2G37360; GABI_036B02	LP-GABI_036_B02: GAAGTTTAATCCCCTCGCTTG
			RP-GABI_036_B02: CCTTTTGGGGAATTGTCTAGG
			LBb1 : GCGTGGACCGCTTGCTGCAACT
abcg6-1	Yadav *et al.,*	At5G13580;	LP-salk_050113: GATGCTGGTGGTGACTACGAC

	2014	SALK_ 050113	RP-salk_050113: TCAGGACATAAAACCTGGTGG
			LBb1 : GCGTGGACCGCTTGCTGCAACT
abcg20-1	Yadav *et al.,*	At3G53510;	LP-Salk_011548C: GTTGGAAATCCAATTAACCCC
	2014	SALK_011548C	RP-Salk_011548C: TTGAAATCCGATTGGCTAATG
			LBb1 : GCGTGGACCGCTTGCTGCAACT
myb92-1	Murmu *et al.,*	AT5G10280	LP-SM_3_41690: GGGTAGGTTTTCTCTTTGAGTGG
	(unpublished)	SM_3_41690	RP-SM_3_41690: CAGTTAGTGGTTGTGAAGGAAGG
			Spm32_R(Lb): TACGAATAAGAGCGTCCATTTTAGAGTGA
myb93-1	Murmu *et al.,*	AT1G34670	LP-Salk_131752: TTTAAGAGGTTCATGGCATGG
	(unpublished)	SALK_131752	RP-Salk_131752: GGCTTCGTCGCTAGCTAGAAG
			LBb1 : GCGTGGACCGCTTGCTGCAACT

asft-1	Molina et al. 2009	AT5G41040; SALK_048898	ASFT-1-F1(LP): GTGCTGTTTTCTCCATTTGG ASFT-1-R1 (RP): GCCAGATATTTGTATTTTGTCG LBa1: TGGTTCACGTAGTGGGCCATCG
asft-2	Molina et al. 2009	AT5G41040; SALK_017725	ASFT-2-LP: GATCAGAAAACGAAGCTTCTCTTC ASFT-2-RP: ATTCTCTAATGGCTTCCTGTCAAG LB: TGGTTCACGTAGTGGGCCATCG
gpat5-1	Beisson et al. 2007	AT3G11430; SALK_018117	GPAT5-1 (Forward) :GCTATTTTTCCATTTGCAGATACGT GPAT5-1 (reverse) : ACATCTCGGATTCTTGTCAATC LBa1: TGGTTCACGTAGTGGGCCATCG
gpat5-2	Beisson et al. 2007	AT3G11430; SALK_142456	GPAT5-2(forward) : CTAAGGAGCATCTTAGAGCAGATGA GPAT5-2 (reverse): TCCAGCGAGAACCCTATACTTATCT LBa1: TGGTTCACGTAGTGGGCCATCG
myb107-2	Gou et al.2017	At3G02940; SALK_203615	LP-Salk_ 203615: AAATCCGATTTCTTAGCAAAAGTG RP-Salk_ 203615: AGGAAGAAGAGGTATTGTTGTTGC LBb1 : GCGTGGACCGCTTGCTGCAACT

Appendix III:

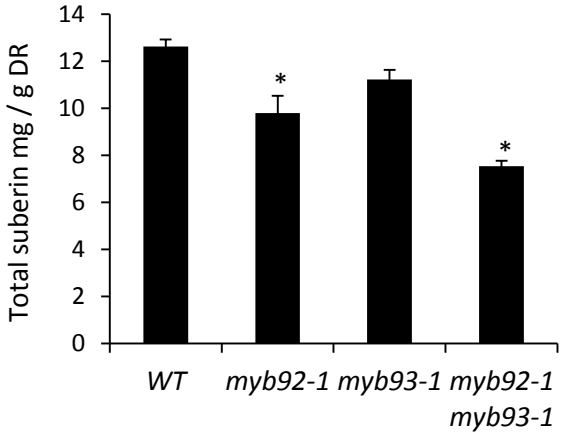

Comparison of total suberin content in WT and single mutants *myb92-1* and *myb93-1,* and double mutant *myb92-1 myb93-1.* Relative to WT, *myb92-1 myb93-1* had a 60% reduction in total root suberin content. Mean values are shown in milligrams per gram of delipidated dry mass. n=3-4 ± SE, asterisk indicates $p<0.05$ by student's t test comparing to wildtype plants.

Appendix IV:

Mutant collection

Genotype / allele	Locus and T-DNA insertion line	Reference
cesa5-2	AT5G09870; SALK_023353	Mendu *et al.,* 2011
cesa9-1	AT2G21770; SALK_107750C	Mendu *et al.,* 2011
cesa2-1 cesa5-1 cesa9-1		Mendu *et al.,* 2011
sos5-2	AT3G46550; SALK_125874	Xu *et al.,* 2008
fei2-1	AT1G31420; SALK_080073	Xu *et al.,* 2008
cobl2-1	AT3G29810; SALK_044883	Ben-Tov, 2015
cyp86b1-1	AT5G41040; SM_37066	Compagnon *et al.,* 2009
asft-1	AT5G41040; SALK_048898	Molina *et al.,* 2009
far1-2 far4-1 far5-1		Vishwanath *et al.,* 2013
gpat5-1	AT3G11430; SALK_018117	Beisson *et al*., 2007
abcg2-1 abcg6-1 abcg20-1		Yadav *et al.,* 2014
myb107-2	AT3G02940; SALK_203615	Gou *et al*., 2017
att1-1		Xiao *et al*. 2004
tds4-2	AT4G22880; CS_2105579	Appelhagen *et al.,* 2014
ban-5	AT1G61720 ; CS_2105581	Appelhagen *et al.,* 2014
tt10-7	AT5G48100; CS_2105588	Appelhagen *et al.,* 2014
aha10-6	AT4G22880; CS_2105579	Appelhagen *et al.,* 2014
tt3-1 (in Le*r* background)	AT5G42800; CS_84	Appelhagen *et al.,* 2014
tt8-6	AT4G09820; CS_302091	Appelhagen *et al.,* 2014
ttg1-22	AT5G24520; CS2_105596	Appelhagen *et al.,* 2014
tt12-2	AT3G59030; CS_2105586	Appelhagen *et al.,* 2014

Appendix V:

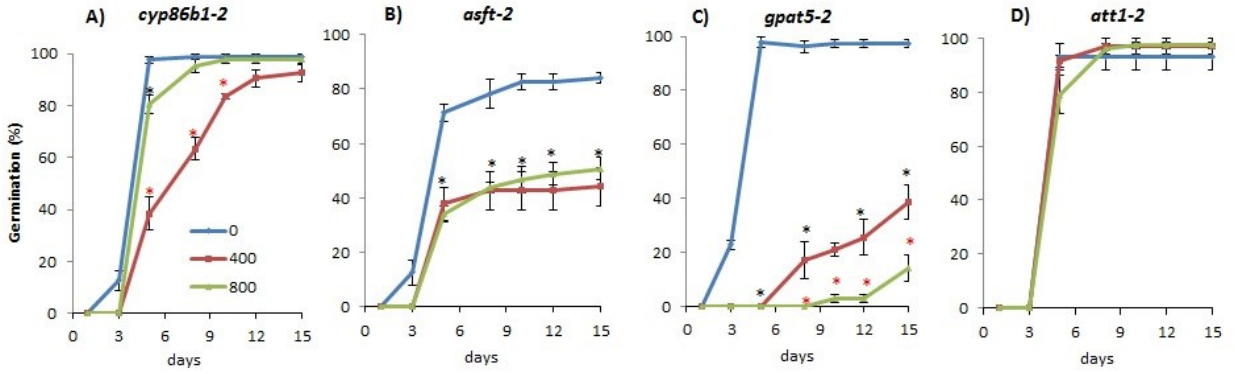

Time-course analysis of germination in mutants (alleles) not given under main results. These are suberin- (*cyp86b1-2*, *asft-2* and *gpat5-2*) and cutin-altered (*att1-2*) mutants at 0, 400 and 800 mg/L Cr^{3+} concentrations. Horizontal axes represent days after sowing. Values represent mean value ± standard error (SE). n=3, 25 seeds per replicate. Asterisks represent significant differences between [0] and [400] mg/L Cr^{3+} in black and between [400] and [800] mg/L Cr^{3+} in red by student t-test at $p<0.05$.

]